5G Programmable Infrastructure Converging disaggregated network and compUte Resources

D2.2 System architecture and preliminary evaluations

This project has received funding from the European Union's Framework Programme Horizon 2020 for research, technological development and demonstration

5G PPP Research and Validation of critical technologies and systems

Project Start Date: 1st June 2017

Duration: 30 months

Call: H2020-ICT-2016-2

Date of delivery: 31st July 2018

Topic: ICT-07-2017

Version 1.0

Project co-funded by the European Commission

Under the H2020 programme

Dissemination Level: **Public**

Grant Agreement Number:	762057
Project Name:	5G Programmable Infrastructure Converging disaggregated network and compUte REsources
Project Acronym:	5G-PICTURE
Document Number:	**D2.2**
Document Title:	System architecture and preliminary evaluations
Version:	1.0
Delivery Date:	31st May 2018 (31st July 2018)
Responsible:	University of Bristol (**UNIVBRIS-HPN**)
Editor(s):	Anna Tzanakaki (**UNIVBRIS-HPN**)
Authors:	Anna Tzanakaki (**UNIVBRIS-HPN**), Markos Anastasopoulos (**UNIVBRIS-HPN**), Andrea di Giglio (**TIM**), Alessandro Percelsi (**TIM**), Nicola Blefari Melazzi (**CNIT**), Salvatore Pontarelli (**CNIT**), Stefan Zimmermann (**ADVA**), Jens Bartelt (**AIR**), Jesús Gutiérrez (**IHP**), Daniel Camps-Mur (**I2CAT**), Kostas Katsalis (**HWDU**), Kostantinos Samdanis (**HWDU**), Chia-Yu Chang (**EUR**), Sevil Dräxler (**UPB**), Azahar Machwe (**ZEETTA**), Crispin Dent-Young (**ZEETTA**), Ioanna Mesogiti (**COS**), Elina Theodoropoulou (**COS**).
Keywords:	Flexible functional splits, Disaggregated RAN, hardware programmability, network softwarisation, Physical Network Functions, Virtual Network Functions, Performance Evaluation
Status:	Final
Dissemination Level	**Public**
Project URL:	http://www.5g-picture-project.eu/

Revision History

Rev. N	Description	Author	Date
0.0	Draft Table of Contents (ToC)	Anna Tzanakaki (UNIVBRIS-HPN)	19/04/2018
0.1	Section 3	Andrea di Giglio (TIM), Ioanna Mesogiti (COS)	20/04/2018
	Section 4	Vaia Kalokidou (UNIVBRIS-CSN)	20/04/2018
	Section 5.3	Azahar Machwe (ZEETTA)	23/04/2018
	Revision of Section 5.3 and 5.4	Sevil Dräxler (UPB)	25/04/2018
	Section 5.5	Sevil Dräxler (UPB), Azahar Machwe (ZEETTA)	25/04/2018
0.2	Section 5.2	Daniel Camps (I2CAT)	26/04/2018
	Section 5.1	Salvatore Pontarelli (CNIT)	27/04/2018
	Section 5.2.2	Jens Bartelt (AIR)	02/05/2018
	Section 4.1.2	Steinar Bjørnstad (TP)	03/05/2018
	Revised Section 3	Andrea di Giglio (TIM)	07/05/2018
	Section 5.2.1	Chia-Yu Chang (EUR), Daniel Camps (I2CAT)	07/05/2018
0.3	Revised Section 5.2.1.3.1 Revision of 5.3, 5.4, 5.5	Jens Bartelt (AIR), Sevil Dräxler (UPB), Azahar Machwe (ZEETTA)	09/05/2018
0.4	Added contributions to Wireless Technologies (Section 5.2.1)	Jesús Gutiérrez (IHP)	09/05/2018
	Revised Section 3	Andrea di Giglio (TIM)	11/05/2018
	Revised Section 5.5	Chia-Yu Chang (EUR)	14/05/2018
0.5	Revised Section 5.3 & 5.4	Ioanna Mesogiti (COS) Elina Theodoropoulou (COS)	21/5/2018
	Scalability of data and control plane, Section 6.2	Markos Anastasopoulos, Anna Tzanakaki (UNIVBRIS-HPN)	22/5/2018
	Multi-technology access, Section 6.4.2	Markos Anastasopoulos, Anna Tzanakaki (UNIVBRIS-HPN)	22/5/2018
	Control plane scalability Section 6.4.3	Markos Anastasopoulos, Anna Tzanakaki (UNIVBRIS-HPN)	22/5/2018
0.6	Revised and integrated draft version	Jesús Gutiérrez (IHP)	23/05/2018
0.65	Overall Technical Revision	Holger Karl (UPB), Giuseppe Bianchi (CNIT)	09/06/2018
	Updated content in Section 5, Overall technical revision	Markos Anastasopoulos Anna Tzanakaki (UNIVBRIS-HPN)	11/07/2018
0.7	Section Editors' Revisions	Salvatore Pontarelli (CNIT), Daniel Camps-Mur (I2CAT), Kostas Katsalis (HWDU) Azahar Machwe (ZEETTA), Sevil Dräxler (UPB)	23/07/2018
1.0	Last revision and submission of the document	Anna Tzanakaki (UNIVBRIS-HPN), Jesús Gutiérrez (IHP)	31/07/2018

Table of Contents

List of Figures

List of Tables

Executive Summary

5G-PICTURE focuses on the design and development of a converged fronthaul and backhaul infrastructure, integrating advanced wireless access and novel optical network solutions. To address the limitations of the traditional Distributed-Radio Access Network (D-RAN) and the recent Cloud-RAN (C-RAN) approaches, 5G-PICTURE adopts the concept of ***flexible functional splits*** for the baseband processing function chain. The suitable functional split is selected based on factors such as the transport network and service characteristics for resource and energy efficiency.

5G-PICTURE proposes a paradigm shift, from D-RAN and C-RAN to the "***Dis-Aggregated RAN"*** (DA-RAN) approach. DA-RAN "disaggregates" hardware (HW) and software (SW) components across wireless, optical and compute/storage domains. "Resource disaggregation" decouples HW and SW components creating a common "pool of resources" that can be independently selected and allocated on demand. These HW and SW components can be combined to compose any infrastructure service. Apart from increased flexibility, disaggregation offers enhanced scalability, upgradability, efficiency and sustainability. This is particularly relevant to 5G environments supporting a large variety of end-devices and services. To exploit the concept of disaggregation in RAN environments and the associated benefits, novel 5G technology solutions are needed. These will rely on i) ***hardware programmability***: allowing HW repurposing to enable dynamic, on-demand sharing of resources and ii) ***network softwarisation:*** enabling migration from the traditional closed networking model to open platforms, instantiating a variety of network functions on demand.

To support this architecture, 5G-PICTURE proposes a set of novel technology solutions as well as novel control and management platforms. These will allow service driven customisation enabled by enhanced network and compute HW and SW modularity that will improve overall density and energy efficiency. On demand allocation of resources from a common pool of network and compute/storage elements (flexible mix-and-match), will facilitate service composition and provisioning exploiting the notions of infrastructure softwarisation, HW programmability and the creation and deployment of programmable network functions. These will enable provisioning of any service without the prerequisite of owning or installing any specific HW or SW, adopting the concept of service chaining (SC). This networking approach will facilitate increased functionality and flexibility infrastructures, offering simplified management and advanced capabilities including slicing and virtualisation that allow the disaggregated resource pool to be shared and accessed remotely. Network slicing and service chaining will be facilitated through the adoption of SDN reference architecture and the ETSI Network Function Virtualization (NFV) standard. 5G-PICTURE will leverage control plane developments from the Phase 1 5G-PPP Project 5G-XHaul [1] and orchestrators from relevant Phase 1 5G-PPP Projects such as SONATA [2].

This document summarises the 5G Key Performance Indicators (KPIs) reported in detail in deliverable D2.1 [3] that the 5G-PICTURE solution needs to support, as defined by the relevant standardization bodies and communities. A description of a set of verticals that the generic 5G-PICTURE takes into account and aims to support is provided and their associated requirements are also discussed. These verticals include the Rail, the Smart City and a Stadium use case that the project is concentrating on in terms of demonstration activities. Additionally, Industry 4.0 is included in the discussion although no relevant demonstration activities are planned, as it is considered an important vertical that can be supported by 5G solutions and 5G-PICTURE aims to address from an architectural perspective.

This document also provides a high-level view of the 5G-PICTURE architecture, in terms of its functionalities, capabilities and features. The project's layered architecture is described and the details of the individual layers including the Programmable Data Plane, the Physical and Virtual Functions as well as the 5G-Operating System (5G OS) are discussed.

Finally, this document reports a preliminary evaluation of the 5G-PICTURE architecture, involving the description of purposely developed models and simulation tools as well as a set of initial use cases developed to analyse and benchmark the 5G-PICTURE solution. A set of relevant results are also presented and discussed highlighting the benefits of the proposed approach as well as associated trade-offs.

1 Introduction

The overall 5G vision is going far beyond the evolution of mobile broadband, becoming an enabler of the future digital world that will support the transformation of all economic sectors and the growing consumer market demand. An important aspiration of 5G is to offer services to new industrial stakeholders (referred to as vertical industries), and to support new business models and opportunities. This vision introduces the need to transform traditionally closed, static and inelastic network infrastructures into open, scalable and elastic ecosystems that can support a large variety of dynamically varying applications and services. In these environments, a heterogeneous set of air interfaces (i.e. 3G, 4G, Wi-Fi) is integrated with high-capacity wired network domains to provide ubiquitous access to a large pool of end-devices. At the same time, to further enhance spectral efficiency and throughput, small cells can be deployed either adopting the traditional Distributed Radio Access Network (D-RAN) paradigm, where Baseband Units (BBUs) and radio units are co-located; or the more recently proposed concept of Cloud Radio Access Network (C-RAN). In C-RAN, remote units (RUs) are connected to the Central Unit (CU), where the BBU pool is located, through high bandwidth transport links known as fronthaul (FH). Via its pooling and coordination gains, this approach can address the limitations of D-RAN at the cost of increased transport bandwidth requirements, low latency and strict synchronisation constraints.

Recognising the benefits of the C-RAN architecture and the associated challenges, equipment vendors try to address the intensive bandwidth requirements of FH networks by a variety of solutions and techniques. These include:

- the expansion of their mobile FH solutions, adopting more effective wireless technologies, i.e. operating in the Sub-6 GHz and 60 GHz frequency bands enhanced with advanced beam-tracking and Multiple-Input Multiple-Output (MIMO) techniques,
- the development of new versatile Wavelength Division Multiplexing (WDM) optical network platforms combining both active and passive optical elements [4], and
- the introduction of alternative architectures that can be used to relax the stringent FH requirements of C-RAN, while taking advantage of its pooling and coordination gains relying on flexible split of the baseband processing chain (Figure 1-1a)) [6]-[9]. The introduction of these splits allows dividing the baseband processing functions between the CU and the RUs. Through this approach, a set of processing functions can be performed at the RUs deploying local dedicated compute resources, whereas the remaining functions can be performed centrally, through shared compute resources. The required flexibility can be provided by programmable digital hardware, able to support flexible reconfiguration of hardware-accelerated (HWA) and software-realized baseband functions, which can be partitioned at different levels to serve different Key Performance Indicators (KPIs). These KPIs range from very high bandwidth (in the order of tens of Gb/s) and strict (less than 9 ns) jitter requirements when a Common Public Radio Interface (CPRI)-type of split option is adopted, to requirements characterized by low bandwidth (in the order of Mb/s) and less demanding synchronisation constraints.

However, the highly variable service requirements of this alternative RAN approach introduce the need to develop new solutions both at the transport network for the interconnection of the RUs with the BBUs and at the Data Centres (DCs) for the processing of BBU functions. Specifically, at the transport network segment, a solution must adapt to the highly variable bandwidth requirements of future RANs, offering at the same time high levels of flexibility, resource and energy efficiency. At the compute segment, given that workloads in future RAN environments will be characterized by a large number of signal processing tasks with small and moderate amounts of computing power requirements, a solution relying on a modular DC system integrating a large number of heterogeneous processing elements is expected to prevail.

5G-PICTURE focuses on the design and development of a converged FH and backhaul (BH) infrastructure integrating advanced wireless access and novel optical network solutions. To address the limitations of the current D-RAN and C-RAN approaches, 5G-PICTURE will adopt the concept of flexible functional splits selected based on factors such as the transport network and service characteristics for resource and energy efficiency.

More specifically, 5G-PICTURE proposes a paradigm shift, from the traditional RAN and recent C-RAN to the "***Dis-Aggregated RAN"*** (DA-RAN) approach. DA-RAN is a novel concept adopting the notion of "disaggregation" of HW and SW components across the wireless, optical and compute/storage domains. "Resource disaggregation" decouples HW and SW components, creating a common "pool of resources" that can be

independently selected and allocated on demand. These HW and SW components form the basic set of building blocks that, in principle, can be independently combined to compose any infrastructure service. Apart from increased flexibility, disaggregation, due to its modular approach, offers enhanced scalability, upgradability and sustainability potential. These features are particularly relevant to 5G environments, when supporting enormous and continuously growing number of end-devices and services, as well as novel features such as the concept of flexible functional splits for the baseband processing function chain. To exploit the concept of disaggregation in RAN environments, novel 5G technology solutions are needed to increase the density and power efficiency of the "pool of resources", supporting at the same time high bandwidth connectivity between them. These will rely on i) ***hardware programmability***: allowing HW repurposing to enable dynamic on demand sharing of resources and ii) ***network softwarisation:*** enabling migration from the traditional closed networking model, focusing on network entities, to an open reference platform instantiating a variety of network functions.

To support this architecture, 5G-PICTURE proposes a set of novel technology solutions as well as novel control and management platforms. These will allow service driven customisation enabled by enhanced network and compute HW and SW modularity that will improve overall density and power efficiency. The pool of network and compute/storage elements can be considered jointly to support dynamic on demand allocation of resources (flexible mix-and-match) for service provisioning enabled through infrastructure softwarisation to facilitate HW programmability and the creation and deployment of programmable network functions. Such novel networking approaches facilitate increased functionality and flexibility infrastructures, offering simplified management and advanced capabilities including slicing and virtualisation that allow the disaggregated resource pool to be shared and accessed remotely. On-demand selection and allocation of these resources and will enable provisioning of any service without the prerequisite of owning and installing any specific HW or SW, through the notion of service chaining (SC). Network slicing and SC will be facilitated adopting architectural models such as the SDN reference architecture and the ETSI NFV standard. 5G-PICTURE will leverage control plane developments from Phase-1 5G-PPP project 5G-XHaul [1], and orchestrators from the 5G-PPP Project SONATA [2].

This will involve the deployment of a hierarchical compute and storage structure supported by the corresponding network hierarchy, exploiting an integrated wireless and optical network infrastructure for access and transport (Figure 1-1a). The transport network will adopt programmable wireless technologies at the edge and a hybrid passive/active optical network solution. The active optical network technology can allocate both spectral and time slots of variable size, thus supporting services with continuous channel allocation at various bit rates (i.e. heavy and light CPRI), and services with sub-wavelength time-slot allocation (Ethernet flows). At the same time, the necessary processing power to execute BBU functions is provided by a modular compute platform comprising a heterogeneous set of general and specific-purpose processors (GPP and SPP, respectively). This platform acts as "*a pool of resources*" allowing its construction elements to be independently selected and allocated on demand to provide any infrastructure service. In theory this approach allows functions with different computational features to be assigned to the suitable type and number of processing units, reducing the overall processing latency and improving energy efficiency. By jointly considering elastic optical networks and modular DC platforms in future RAN environments, significant benefits are expected.

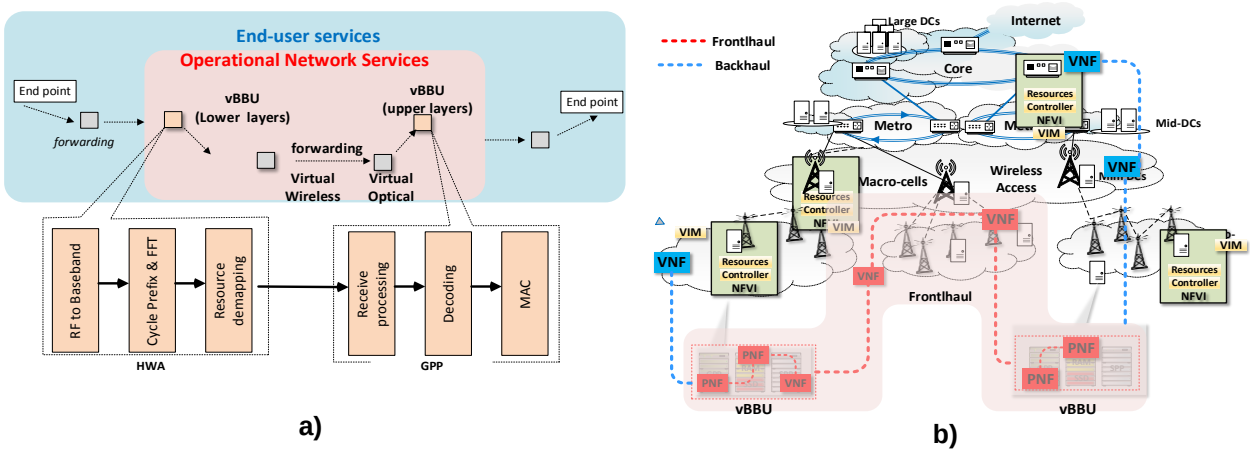

Figure 1-1: a) Service chaining over DA-RAN b) DA-RAN in support of converged FH and BH functions.

Organisation of the document

This document comprises six sections. Following the Executive Summary and Introduction sections, Section 2 summarises the 5G KPIs that the 5G-PICTURE solution needs to support, as defined by the relevant standardisation bodies and communities. A description of some verticals and their associated requirements is also included. Section 3 provides a high-level view of the 5G-PICTURE architecture, in terms of its functionality, capabilities and features and an overview of the project layered architecture structure and individual layers. Section 4 focuses on the evaluation of the proposed architecture, involving the description of purposely developed models and simulation tools as well as a set of initial use cases used to analyse and benchmark the 5G-PICTURE solution. A set of relevant results are also presented and discussed. Finally, a conclusions section is included.

2 Requirements and KPIs

This section summarises the 5G Key Performance Indicators (KPIs) discussed in detail in deliverable D2.1 [3], as defined by standardisation bodies (ITU-R) and important scientific communities (NGNM, 5G-PPP), highlighting the extremely challenging context of 5G. It includes as well a description of some relevant verticals (rail, smart city and Internet of Things (IoT), stadium and mega event, and Industry 4.0), reporting their specific requirements.

In D2.1 [3], we reported also Industry 4.0 requirements. In fact, even if 5G-PICTURE does not consider any demonstration based on Industry 4.0, we consider this vertical as a cornerstone of 5G applications and it is important to demonstrate that the general architecture, DA-RAN, basis of 5G-PICTURE investigation, is able to support traffic compatible with Industry 4.0 requirements.

2.1 5G KPIs

The wireless research community is on the way to create the technologies of tomorrow that will deliver important improvements in network capacity, enhancements in spectral efficiency, reduced end-to-end latency, increased reliability and more. These improvements are driven by key performance requirements defined by the International Telecommunications Union (ITU). Figure 2-1 summarizes the performance improvements for the International Mobile Telecommunications IMT-2020 (target for 5G) over IMT-Advanced (current situation represented by 4G advanced). The required improvements are significant, with a 20x increase in peak data rate, from 1 Gb/s to 20 Gb/s, a user-experienced data rate that increases 10x, from 10 Mb/s to 100 Mb/s, while latency is reduced by a factor of 10, from 10 ms down to 1 ms.

Contrary to the legacy network technologies, including 4G, for which all the activities related to development and commercialisation (comprising requirements and specifications definition, design, standardisation and deployment activities) were based on an abstract, application/service-agnostic definition of the network Quality of Service (QoS) requirements, the respective 5G development activities are based on a more stakeholder/application/service requirements-aware approach.

With respect to IMT-advanced, 5G targets the following numbers as new network characteristics:

- 100 times higher mobile data volume per geographical area.
- 10 times more connected devices.
- 10 times to 100 times higher typical user data rate.
- 100 times lower energy consumption.
- 1 ms end-to-end latency.
- Ubiquitous 5G access including low-density areas.

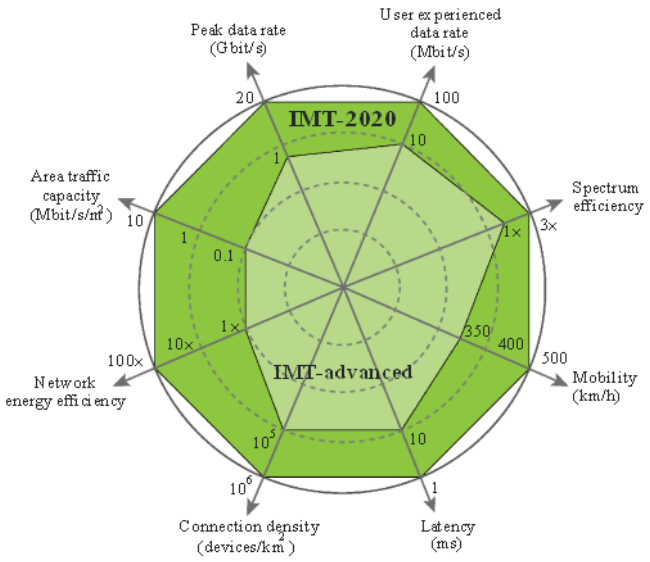

- **Figure 2-1: Radar diagram reporting 5G requirements (source ITU-R [5]).**

Together with performance KPIs, the 5G community (NGNM, ITU-R, 5G-PPP) identified business and societal objectives. In particular, business KPIs are related to the involvement of small medium enterprises in the research (funding greater than 20% of the total) and to reach a global market share for 5G equipment & services delivered by European headquartered ICT companies at, or above, the reported 2011 level of 43% global market share in communication infrastructure.

On the other hand, five KPIs related to societal aspects have been identified:

- Enabling advanced user controlled privacy.
- Reduction of energy consumption per service up to 90% (as compared to 2010).
- European availability of a competitive industrial offer for 5G systems and technologies.
- Stimulation of new economically-viable services of high societal value like U-HDTV and M2M applications.
- Establishment and availability of 5G skills development curricula.

2.2 5G Vertical requirements

Besides the general technical QoS KPIs and target values for 5G technologies, the 5G network deployments and operation will be tailored to support the requirements of a range of stakeholders and services in a holistic manner. For this purpose, technical activities around 5G are tightly coupled with activities related to the analysis of stakeholders and their service requirements, in order to map them to 5G network capabilities, functionalities, deployment strategies, etc.

For this purpose, 5G-related activities are converging to address the following major Vertical industries:

- Automotive, focusing on services provided in high mobility scenarios, IoT applications/services, etc.
- eHealth, especially focusing on remotely provided health services with high latency and reliability requirements,
- energy, especially focusing on IoT based energy monitoring, management and network control scenarios,
- media & Entertainment, especially focusing on next generation applications/services provisioning such as UHD content, Crowdsourced/multi-user created content, highly interactive services, etc., and
- factories of the future, referring to Industry 4.0 setups.

It becomes evident that these vertical industries involve large service groups, which can be provided by various business stakeholders depending on the specific market/social environment, and can include various applications/services.

On top of these verticals, existing ICT services and business/stakeholder requirements are considered during all steps of 5G technology development, including among others:

- Provisioning of 5G emergency communication services to individuals, first responders, etc.
- Efficient utilization of ICT infrastructure and minimization of its deployment and operational cost.
- Effective support of multiple tenants over a single infrastructure.

Following the top-down approach, the vertical use cases can be broken down to services falling in the 5G (3GPP, ITU) identified categories: enhanced Mobile Broadband (eMBB), massive Machine Type Communications (mMTC), Ultra-Reliable and Low Latency Communications (URLLC) and Network Operation services, as depicted in Figure 2-2.

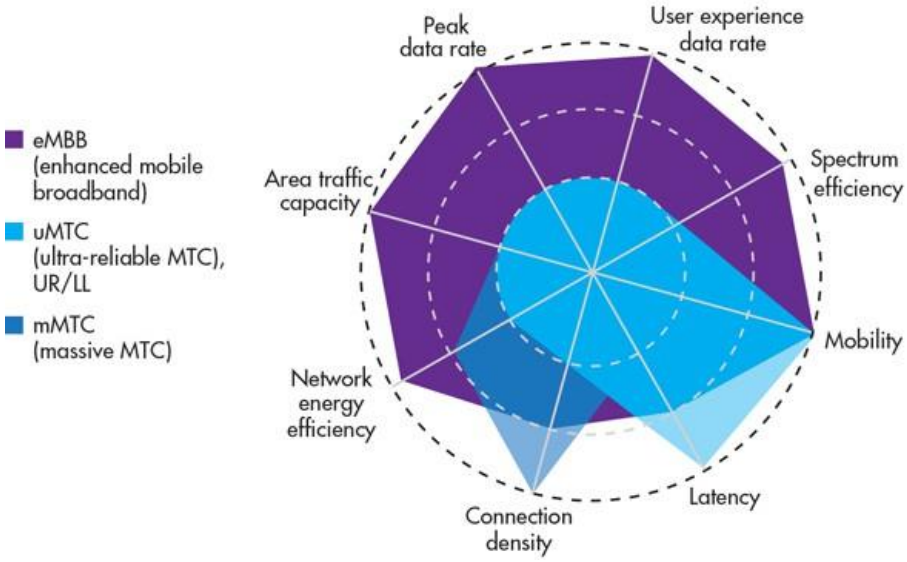

Figure 2-2: 5G use cases defined by the ITU Vision for 2020.

- **eMBB (enhanced Mobile BroadBand)**: including bandwidth intensive services/applications ,i.e., with (very) high data speed requirements such as streaming, video conferencing and virtual reality. The bandwidth requirements of this type of services are expected to be about 100 Mb/s per user, while in some cases it can be in the order of some Gb/s, reaching even 10 Gb/s.
- **mMTC (massive Machine-Type Communications)**: extending LTE IoT capabilities – for example, Narrow Band-IoT – to support huge numbers of devices with lower costs, enhanced coverage and long battery life. This type of services implies the provisioning of connectivity to thousands of end-devices.
- **URLLC (Ultra-Reliable, Low-Latency Communications)**: also named uMTC (ultra-reliable MTC), referred to as "mission-critical" communications, including latency-sensitive ones, i.e. services with extremely short network traversal time requirements, such as applications/services enabling industrial automation, drone control, new medical applications and autonomous vehicles. The latency requirements for this type of services are expected to range between 1 ms and 2 ms for the user plane and less than 10 ms for the control plane.

In parallel, 3GPP's work on 5G services and their requirements has resulted in an almost identical classification corresponding to enhanced Mobile Broadband (studied in 3GPP TR 22.863), massive Internet of Things (studied in 3GPP TR 22.861) and Critical Communications (studied in 3GPP TR 22.862) services. On top of this, Network Operation Services (studied in 3GPP TR 22.864) are distinguished as a separate class with a number of functional requirements such as multi-tenancy, energy efficiency, etc. 3GPP has already started consolidating the four Technical Reports into a single Technical Specification (TS 22.261 [11]), where specific system requirements are reported.

Last but not least, towards addressing the automotive vertical requirements, 5G will consider also the provisioning of services in very high mobility environments up to 500 km/h with acceptable QoS – corresponding to high speed trains.

2.3 5G-PICTURE verticals requirements

The 5G-PICTURE Verticals reflect those in the 5G ecosystem. They also address all the main 5G services categories. More specifically:

- The Rail Vertical represents the "Automotive", and includes eMBB, URLLC and mMTC services.
- The Smart City & IoT Vertical represents the "Energy", "e-Health" and "Automotive" ones and will focus primarily on mMTC services.
- The Stadium Vertical represents basically the "Media and Entertainment", and include eMBB, mMTC and URLLC.
- The Industry 4.0 Vertical represents the "Factories of the Future", and focuses on URLLC, mMTC and eMBB services.

Network Operation Services, such as slicing and multi-tenancy, are relevant to all 5G-PICTURE Verticals as they facilitate the provision of the differentiated services required by each Vertical.

The 5G-PICTURE Verticals and the addressed use cases/applications are described in detail in the following sections. It should be noted that 5G-PICTURE has planned to demonstrate a set of use cases associated with the rail, the smart city and the stadium verticals. However, for Industry 4.0, although it has been identified as an important Vertical that needs to be considered in the overall 5G-PICTURE architecture in terms of requirements, no relevant demonstration plans are included during the project lifetime.

2.3.1 Rail

The Rail Vertical includes communication based services that can be classified according to the following use cases, as described in deliverable D2.1 [3]:

- Rail operation critical support services, covering all the mission-critical and safety related aspects needed for proper operation of rail transport service.
- Rail operation non-critical support services, i.e., passenger information services, location operation services, security services and maintenance infrastructure services.
- Enhanced passenger's experience, which are services typically provided by telecommunication operators focused on passengers' mobile activities, with no safety consequences.

Figure 2-3 provides a visual representation of the Railway requirements for the three applications described above, considering the most probable Train Communication Network (TCN) scenario, in which only the highest TCN level, i.e. the Ethernet Train Backbone level (ETB), is served through a radio system.

Thus, the most significant requirement for rail is mobility, which reaches the peak requirements marked by the external hexagon. All the on-board services in the three categories described above are affected by this requirement.

Within the first group, the different Automatic Train Control (ATC) systems (CCBTC or ERMTS) are classified as URLLC (Ultra-Reliable, Low-Latency Communications); they constitute "mission-critical" communications, including latency-sensitive, i.e. services requiring extremely short network traversal times. The latency requirements for this type of services are specified for 1 ms or less for the user plane and less than 10 ms for the control plane.

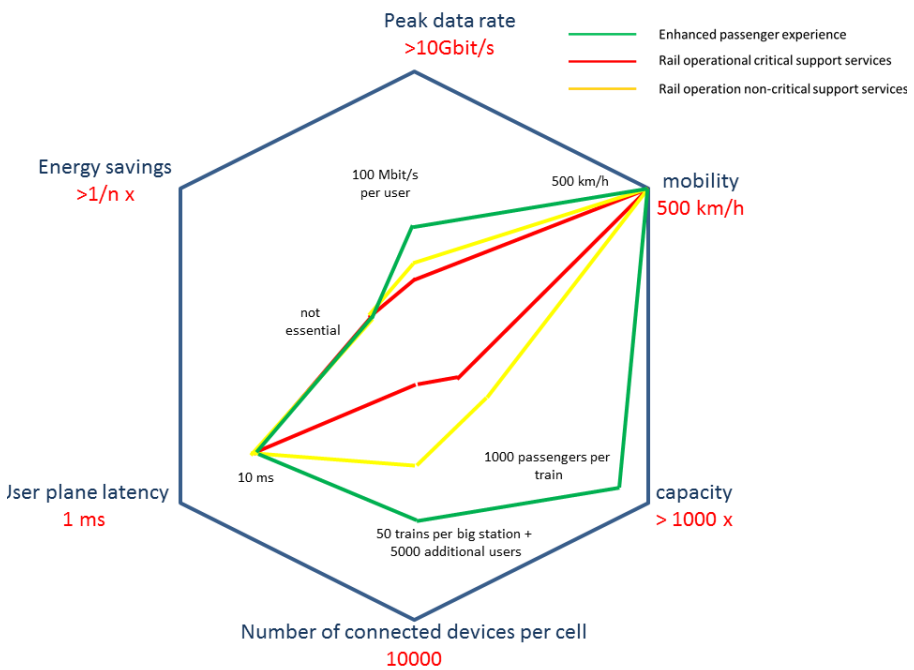

Figure 2-3: Pictorial view of the requirements for Railway applications, following ITU-R.

Passengers and operational CCTV-based services are classified as eMBB (enhanced Mobile Broadband): bandwidth-intensive services/applications. Considering several assumptions (including statistical gain, train length and maximum number of vehicles, maximum number of users per train), a throughput close to 2 Gb/s will be required for this group of services. Note that this number is on a per-train basis; then, the capacity and number of devices are strongly influenced by the fact that several trains can be found in a big station at the same time. Non-passengers' resources must also be allocated for station visitors, but the numbers for a unique train (even two, crossing in opposite direction) and the trackside are different. For this reason, the green line seems to contain the yellow one (critical support services), but this is true only in some situations, for example a central station at peak hour.

In general, there a lot of arguments showing that the network must be pervasive, sufficient data rate with the appropriate level of redundancy and service availability.

2.3.2 Smart city and IoT

In a smart city, data from multiple domains (transportation, public administration, emergency services, weather sensing, etc.) are brought together within the IT systems to facilitate better planning and faster responses to changing situations. IoT and the related communication infrastructure are therefore critical aspects for smart cities.

Smart city applications are extremely diverse, including transportation, energy, facilities management, health care, public safety, etc. Based on the requirements placed on the network, smart-city applications can largely be classified into the following four families, as described in deliverable D2.1 [3]:

- Machine-type Communications, mainly characterised by huge volumes of end-points and connections, using low-cost devices and modules like sensors;
- Mission-critical Applications, mainly characterized by real-time monitoring and control;
- Disaster Monitoring and Public Safety Services, mainly characterized by reliable communication even when disaster conditions occur such as during earthquake, tsunami, flood, hurricane, etc.
- Tactile Internet, characterized by real-time control of remote objects and systems.

Figure 2-4 summarises the network requirements of smart city and IoT applications. Notice that the curves for these applications reach the peak requirements, marked by the external hexagon, apart from the peak data rate and capacity. Thus, smart city and IoT applications are characterised by relatively low data requirements. In addition, the area of the hexagon covered by the different curves is high. This shows that the diversity of the smart city and IoT applications' requirements is high and that overall the network requirements for this vertical are quite stringent.

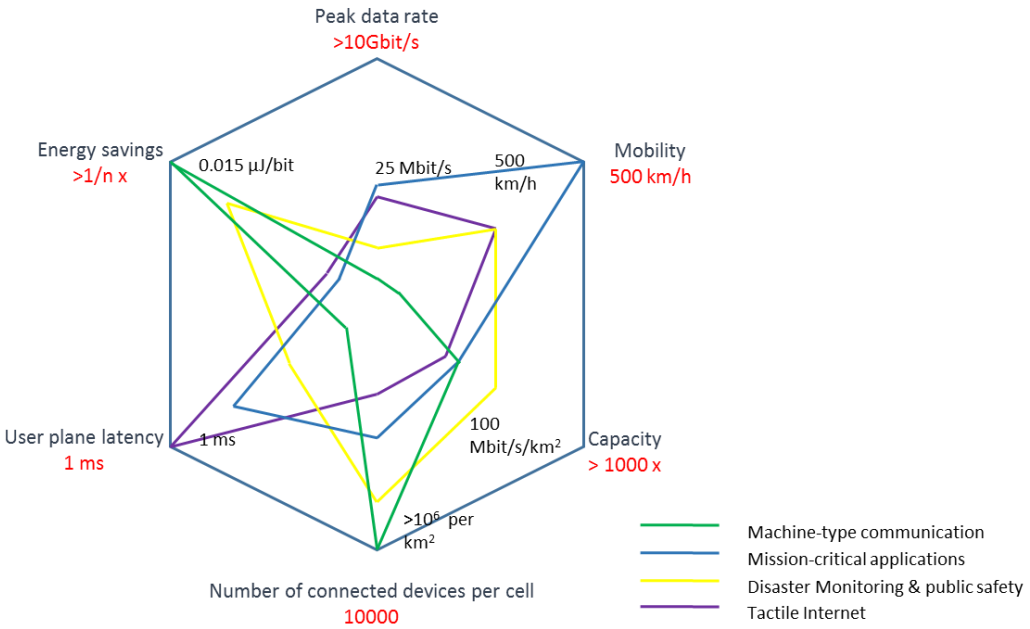

Figure 2-4: Pictorial view of the requirements for Smart City and IoT applications, following ITU-R.

We now discuss each curve in Figure 2-4. The green curve denotes the requirements for machine-type communications. This application requires high energy efficiency and the network must support a large number of devices. The blue curve represents the requirements for mission-critical applications. These applications require low latency and the network must be capable of supporting high user mobility. Furthermore, they require high reliability and availability. The yellow curve denotes the requirements for disaster monitoring and public safety applications. Its requirements are not extreme in general. The key requirement is energy savings as batteries might have to last for several days to weeks in case of an emergency. Lastly, the purple curve represents the requirements for tactile internet. This application is characterized by extremely low latency, high availability and reliability. Although the other requirements are not critical, achieving user plane latencies as low as one millisecond is quite challenging.

2.3.3 Stadium and mega events

One of the major 5G challenges is the support of the envisaged huge traffic/service demands with extremely irregular and seasonal characteristics at ultra-dense hotspots, such as a large stadium. The “Stadium and mega events” vertical has different services with very diverse requirements that involve a high number of stakeholders (service providers, tenants, subscribers, etc.). These services are principally qualified by huge traffic demands generated in precise time windows (during events) with specific QoS performance requirements, together with business-related support systems (security/surveillance, energy management, new services, etc.) besides the usual low traffic needs for daily operations.

For this vertical, the following use-cases have been considered (see deliverable D2.1 [3]):

- High Speed Wireless Access, mainly characterised by high variation of traffic/services requirements due to seasonality (from daily operations to big-events support);
- URLLC/Critical Communications, mainly characterised by very low network traversal latency, with automatic network (re)configuration capability to provide priority access to certain types of end-users/tenants/applications (e.g. Security and Operational Staff) in case of emergency situations;
- Wireless Access Connectivity for Private/Local Events, mainly characterised by a user-friendly, ad hoc provisioning of the required connectivity;
- IoT Services (Asset tracking, Power Management), mainly characterised by a large number of connections handled by the network;
- Next Generation Applications, such as Crowdsourced Video, mainly characterised by hundreds or even thousands of network connected users which create and upload live video streams using a smartphone application;
- UHD Broadcasting Services, mainly characterised by lossless ultra-high definition (UHD) (e.g. 4K) video streams to support immersive experience services – e.g. Virtual Reality (VR) – during mega-events and matches.

Figure 2-5 summarises the critical requirements for Stadium and Mega Events use-cases. The main ones of interest are:

1. Peak Data Rate: this is a cross cutting requirement across all the use-cases. This especially impacts High-Speed Wireless Access, UHD Broadcasting Services and Next Generation Applications.
2. User Plane Latency: this is especially critical for use-cases with strict QoS requirements such as UHD Broadcasting Services, URLLC/Critical Communications and High-Speed Wireless Access.
3. Number of Connected Devices: this is important for use-cases such as URLLC/Critical Communication, High Speed Wireless Access and Next Generation Applications. Here a point to be noted is that there is a requirement not just to handle large number of devices but also the large variety of devices such as (but not limited to): smart phones, drones, IoT sensors, cameras and smart displays.
4. Capacity: this is another cross-cutting concern especially important for High Speed Wireless Access, Next Generation Applications and UHD Broadcasting Services.

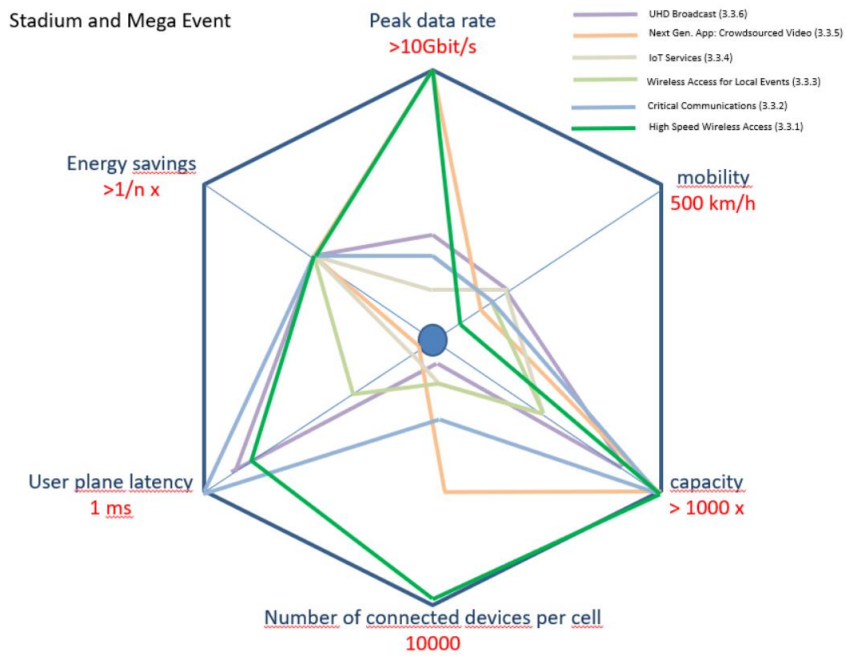

Figure 2-5: Pictorial view of the requirements for Stadium and mega events applications, following ITU-R.

The one requirement that is also highlighted in Figure 2-5 but not part of the ITU-R framework is the requirement for rapid scaling up/down of resources without affecting any services. Typically, in a given year a large venue like a Stadium will host 10-15 events out of which a very small percentage would be categorised as 'mega-events'. Over provisioning of resources and infrastructure to meet 'peak' demand is not possible on a permanent basis, therefore, the requirement for resource scaling without impacting any services. This also ties in with the Energy Savings aspect from the ITU-R framework.

2.3.4 Industry 4.0

The term Industry 4.0 indicates a trend of industrial automation that integrates some new production technologies to improve working conditions and increase productivity and production quality of the plants.

The described Industry 4.0 vertical refers to a factory in the automotive field where the size of the factory is about 1 km^2 and some hundreds robots are working in it. The total number of sensors is some thousands.

Due to the high complexity of the scenario, it is important to note that, from a network requirement point of view, the Industry 4.0 vertical can be split to different services or applications, presenting different requirements.

In brief, the "applications" to be considered within the Industry 4.0 umbrella are:

- Communication network for robot arms controllers – Ultra-Reliable Low Latency Communication (URLLC) 5G service category.
- Automated guided vehicles (AGVs) inside the factory, to transport manufacturing (URLLC 5G service category).
- Video-surveillance (Ultra Mobile Broad Broadband UMBB 5G service category[1]).
- Quality check video / images (UMBB 5G service category).
- Augmented reality (UMBB 5G service category).

[1] Normally, video-surveillance would not be included in Ultra Mobile BroadBand services but, in case of massive adoption of safety-oriented or enhanced security applications like facial-recognition, it is worth including it.

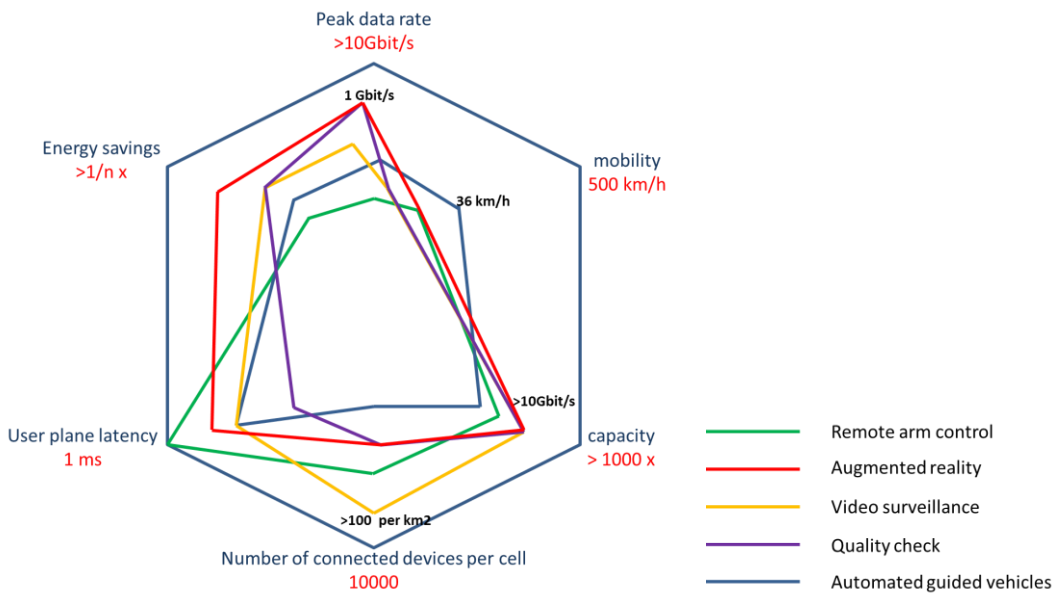

Figure 2-6: Pictorial view of Industry 4.0 requirements, following ITU-R.

The requirements for Industry 4.0 use cases are reported in Figure 2-6. In more detail, the robotics arms control (green line) shows that the most stringent requirement is the user plane latency of 1 ms, while the other parameters are not so critical.

There is not a specific parameter that has stringent value influencing the AGV (light blue line). The unique aspect that influences the AVG service is mobility, in fact vehicles can reach speeds of some tens of kilometers per hour. The control and management of signals that interact with sensors network have to be accurate, considering that they are moving vehicles, but it does not imply critical constraints because of low peak speeds.

About the video-surveillance use-case requirements (yellow line), it seems that this application is not impacting heavily the network requirements: only latency and capacity can become a bit challenging, depending on how much the innovative services are deployed with respect to the traditional approach only focused on security. The hexagon reporting the quality-check video application shows immediately that the requirements are not really challenging.

On the other hand, the area of the red hexagon representing augmented reality is quite big, i.e., this means that some requirements are challenging. The high data rate required for this application (augmented reality), even in a quite low number of devices, implies a huge total capacity of the network. Mobility is not important but energy saving is mandatory.

2.3.5 Network requirements

The derived vertical requirements, which refer to the overall network performance (see Table 2-1), cover the most challenging KPI figures envisaged by 5G community. This demonstrates that the verticals studied and/or demonstrated in 5G-PICTURE will give a complete set of scenarios to test the network architecture and functionalities envisaged by the project.

For this purpose a crucial activity, that is going to give some preliminary results, is the translation of the verticals specific performance requirements into 5G-PICTURE network architecture and technologies selection targeting to a future 5G network deployment. This work does not include only performance requirements, but also network capabilities and functionalities, as well as operational (non-functional) aspects.

Table 2-1: Summary of the Verticals' requirements.

	Latency	Peak data rate	mobility	number of connected devices
Rail	1 ms	> 10 Gb/s	500 km/h	5000
Smart city and IoT	1 ms	25 Mb/s	500 km/h	> 10^6
Stadium and mega events	1 ms	> 10 Gb/s	some km/h	10^5
Industry 4.0	1 ms	1 Gb/s	36 km/h	100
Whole 5G	1 ms	> 10 Gb/s	500 km/h	10^6

To satisfy such challenging requirements, WP2 identified some network characteristics and it considered them as fundamental. The main idea is that, since verticals requirements are both challenging and interesting for different network aspects, a network that has the ambition to collect and carry the traffic generated by all these verticals, should be as most flexible as possible. The first idea, discussed by previous H2020 projects (i.e. 5G-XHaul and 5G-Crosshaul) is that the RRH/BBU processing could have a variable splitting option that can be also application dependent. The result of this flexible splitting option is the requirement for variable fronthauling and backhauling endpoints: fronthauling can be very short if some functionalities should be taken close to the user, or longer if the goal is to centralise the processing of the associated functions; as a consequence, the network should be able to carry fronthauling and backhauling traffic together. In order to exploit at best variable splitting options, 5G-PICTURE adopts the novel concept of DA-RAN, i.e., "disaggregation" of HW and SW components across wireless, optical, compute and storage domains, creating a common "pool of resources" supporting different functional splits for different services and at different network levels, in order to overcome the scaling problems due to CPRI available in previous C-RAN solutions.

All these needs of flexibility and dynamicity bring, as direct consequence, the necessity to implement hardware programmability and programmable distribution of network resources. The former is essential to address the dynamic change of role that a piece of hardware can have, while the latter is indispensable to support different access and transport technologies and to deliver high QoS network connectivity. An example of the outcome of hardware programmability is BBU virtualisation (vBBU), really useful to assist in complying with different latency and jitter requirements. In general, programmable distributed pools of compute and network resources based on the SDN and NFV paradigms and controlled by a Management & Orchestration platform essential for the DA-RAN deployment.

Form the technological point of view, the functional requirements include different, concurrent solutions, on which also novel synchronisation approaches will be considered:

- Dynamically programmable, low latency Radio transmission at high frequency – millimetre wave (mmWave), Sub-6 GHz – and high bandwidth (order of GHz) utilizing massive MIMO techniques in various modes.
- A common data plane frame to efficiently encapsulate, monitor and control the traffic, based on Multi-protocol, Multi-PHY interfaces (MPIs) and fast packet/flow process through Open Packet Processors (OPPs) with X-Ethernet (PCS at L1.5) fast forwarding function and Flex-E as interface technology in order to support MAC rates different form PHY rates.
- A high capacity elastic optical solution, based on hybrid passive-active WDM PON and Time Shared Optical Network (TSON), with multidimensional Bandwidth Variable Transponders (BVTs) and advanced Bandwidth Variable (BV) cross-connects, offering elastic and fine granular bandwidth allocation (with variable size spectral/time slots), for the support of various access nodes' functional splits and services with sub-wavelength time-slot allocation.

Granularity at Ethernet and optical levels are essential to guarantee multi-tenancy and slicing, allowing multiple virtual networks customised to meet the specific needs of applications, services, devices, customers or operators, created on top of a common shared physical infrastructure. Security and isolation between tenants must be guaranteed, as well as QoS.

Finally, other non-functional requirements, that are critical to satisfy the requirements of emerging verticals, include HW and SW modularity, extensibility/upgradability, maintainability and interoperability with legacy networks (both 3G/4G/Wi-Fi and access technologies).

3 5G-PICTURE Architecture

In accordance with the 5G vision and the requirements and KPIs described in section 2, 5G-PICTURE will design and develop a next-generation converged infrastructure **integrating a variety of wireless network technologies with optical and packet transport network solutions**. This infrastructure will interconnect a large number of "disaggregated" compute/storage and network elements and **deploy the concepts of hardware programmability and network softwarisation** to facilitate the DA-RAN approach. These technologies combined and connected will enable the provisioning of any service across the infrastructure by flexibly and efficiently mixing-and-matching network, compute and storage resources. To achieve this, 5G-PICTURE relies on a set of hardware and software innovations covering both the data and the control plane. The overall 5G-PICTURE layered architecture is building on the 5G-XHaul architecture reported in [21] [4], and it is shown in Figure 3-1. The extensions 5G-PICTURE bring into the 5G-XHaul architecture and development work are indicated as white boxes.

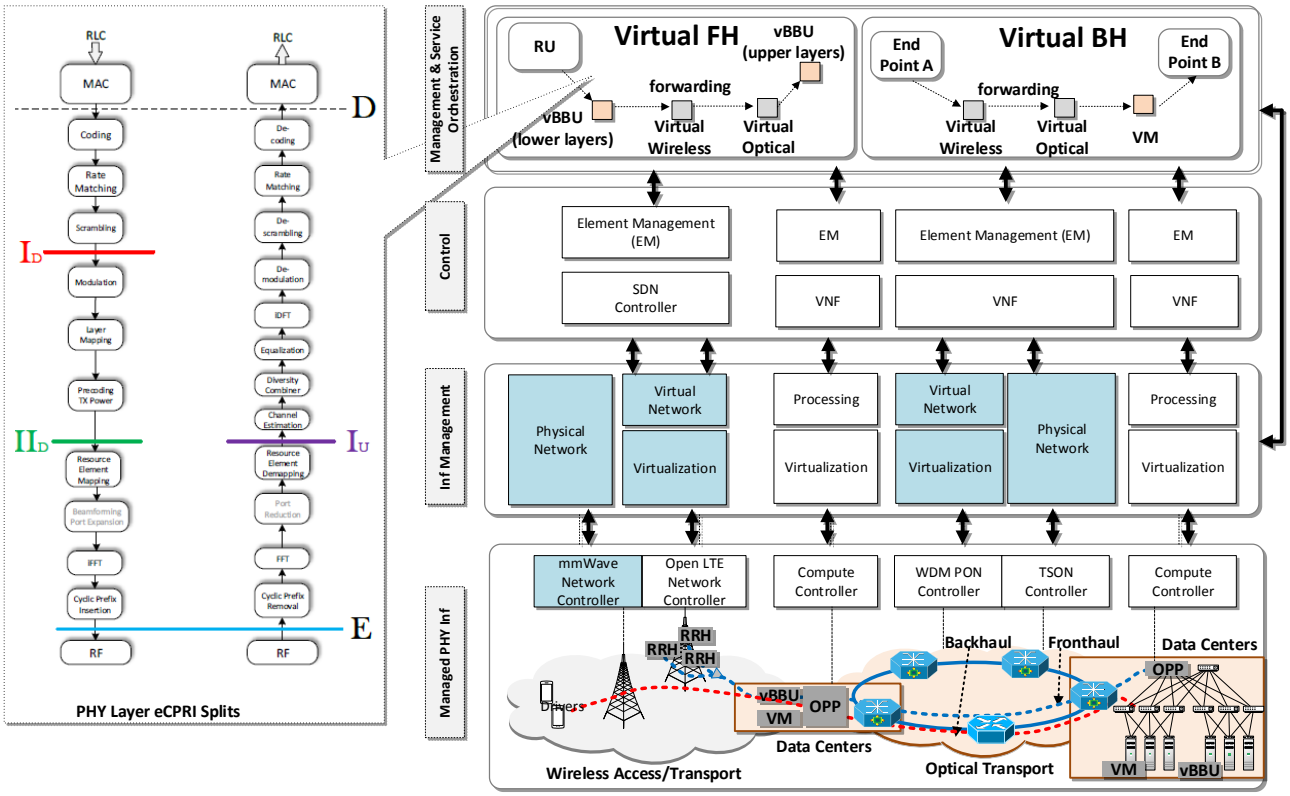

Figure 3-1: 5G-PICTURE leveraging and extending the 5G-XHaul infrastructure.

The 5G-XHaul data plane considered an integrated optical and wireless network infrastructure for transport and access. The wireless domain comprises small cells complemented by macro cells. Backhauling can be supported through mmWave and Sub-6 wireless technologies or using a hybrid optical network platform combining both passive and active optical technologies. In 5G-PICTURE the data plane is extended with the following capabilities:

a) a packet-based transport network segment,
b) the details of compute resources required for both BH and FH services, and
c) enhanced functionality through novel programmability features.

To address the challenge of managing and operating this type of complex heterogeneous infrastructure in an efficient manner, 5G-XHaul proposed the adoption of SDN and NFV [17] reference models. In this context, the **Infrastructure Management Layer (IML)** is responsible for the management of the different technology domains and the creation of virtual infrastructure slices, comprising heterogeneous resources. These slices enable multi-tenancy operator models providing both FH and BH services. This layer communicates with the various network and compute controllers that are responsible for retrieving information and communicating with the individual domains. Once the information has been collected, the resources are abstracted and

virtualised. Management of traditional non-virtualised physical infrastructures is also supported. Cross-domain orchestration of the virtual and physical infrastructures, created and exposed by the IML to the higher layers, is carried out by the **Control Layer**. This layer has a holistic view of all network segments and technology domains and implements converged control and management procedures for dynamic and automated provisioning of end-to-end connectivity services (i.e. service chaining), according to specific QoS considerations. However, it should be noted that no computation related functions were included in the 5G-XHaul framework. These considerations are being addressed by 5G-PICTURE. Finally, 5G-XHaul identified a **Management and Service Orchestration Layer**, which is responsible of orchestrating computation and network services, but no relevant work was carried out.

In accordance to the generic architectural vision of 5G-XHaul, 5G-PICTURE also proposes to merge the SDN and NFV approaches to address function programmability. This will take advantage of SDN's clean separation of control and data plane via open interfaces, exploiting limited reconfigurability of high-performing switching HW; and NFV's full programmability of network functions via SW on commodity platforms that, in general, does not rely on open programming interfaces. To support this functionality, 5G-PICTURE adopts a similar layered architecture. However, the architecture proposed by 5G-PICTURE utilises a programmable data plane (which will be described in the following sections) and relies on the creation of functions needed for the required service compositions. These functions are then exposed to the higher layers through suitable interfaces. Functions can then be selected and combined together in the form of service chains by the orchestration capabilities offered through the 5G OS developed in the framework of the project.

A schematic representation of the proposed architecture and the mapping of the associated work to the relevant project activities is shown in Figure 3-2. This figure also aims to indicate the 5G-XHaul activities that are leveraged by 5G-PICTURE as well as the clear new extensions that 5G-PICTURE is bringing in. A more detailed discussion on the functionality of the individual 5G-PICTURE architectural layers is provided in this section.

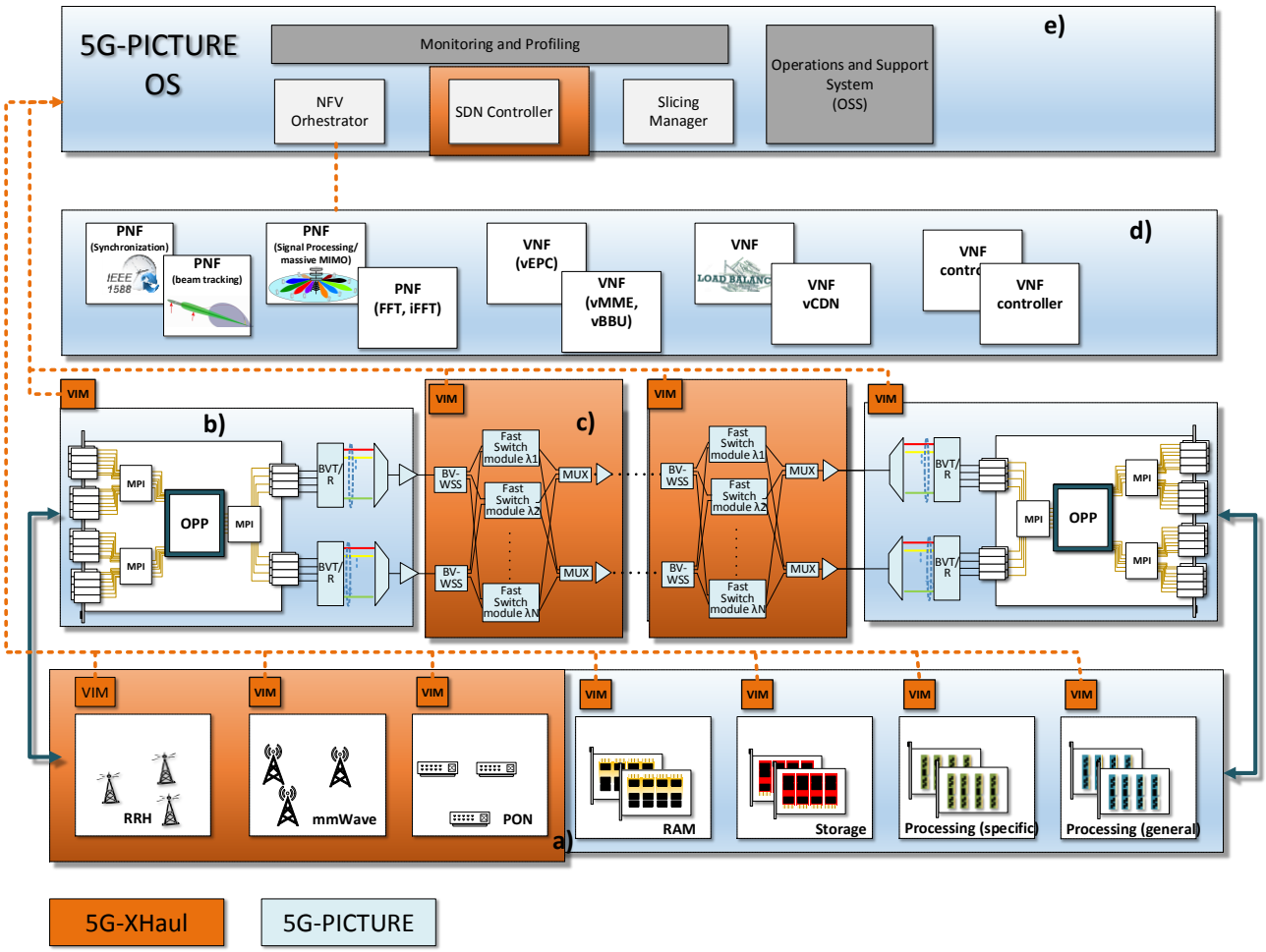

Figure 3-2: The 5G-PICTURE architecture and project activities mapping.

3.1 Programmable Data Plane

As already discussed, in 5G-PICTURE the data plane considers a set of highly configurable wired/wireless infrastructures and interfaces, integrated in a single transport solution supporting both 5G ICT and vertical operational services. At the wired segment, 5G-PICTURE adopts a hybrid network solution deploying passive and high capacity elastic optical networks as well as packet/Ethernet based networks. At the wireless segments, 5G-PICTURE combines mmWave and massive MIMO technologies to improve data rates, reliability and energy efficiency. To further enhance spectral efficiency, a dense layer of small cells operating in the frequency range of 100 MHz-100 GHz is also considered. A high-level view of the data plane transport network technologies supported in the 5G-PICTURE project along with the physical layer interfaces is provided in Figure 3-3.

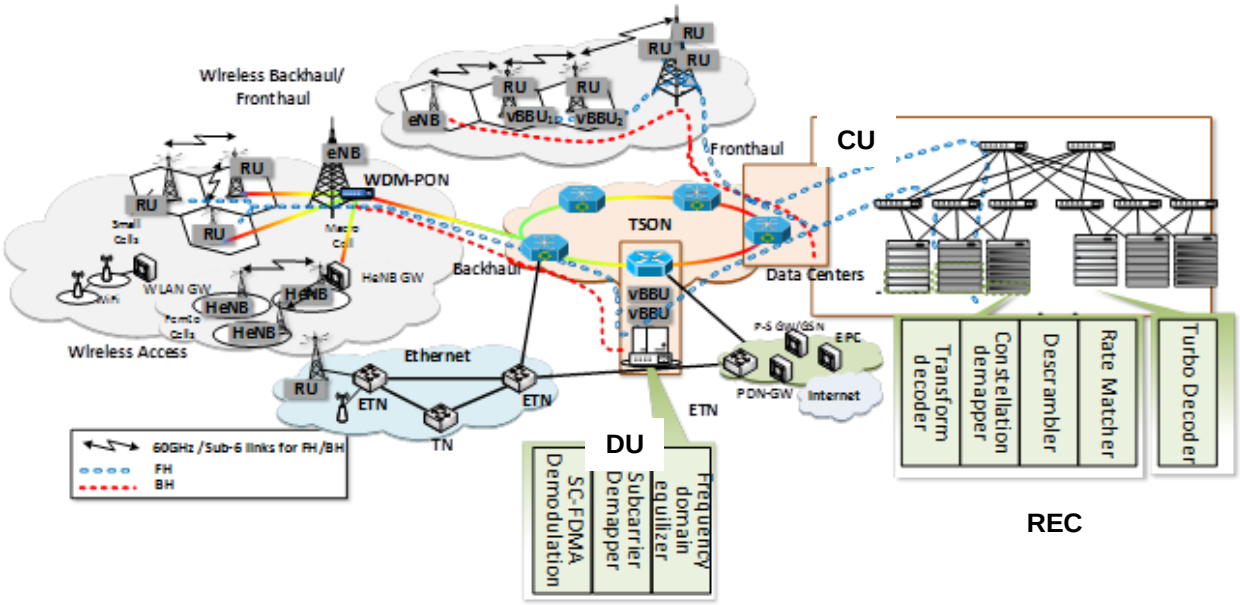

Figure 3-3: 5G-PICTURE data plane technologies.

As the transport network technologies considered in 5G-PICTURE have very different characteristics, including rates of operation spanning from few Mb/s up to several Gb/s, and adopt a wide range of protocols and technology solutions, we rely on high-speed programmable multi-Protocol/PHY interfaces to enable mapping of traffic across infrastructure domains. The interface solutions utilise state-of-the-art Field Programmable Gate Array (FPGA)-based HW to perform a wide range of functionalities including traffic adaptation, protocol mapping, etc. To support these activities, the elastic optical network, equipped with HW programmability features at the edge nodes, will be tightly integrated with the 5G-PICTURE Open Packet Processor (OPP) and will be equipped with programmable multidimensional optical Bandwidth Variable Transponder (BVTs). A variety of multi-protocol/PHY interfaces will be supported, which allow mapping of very different traffic streams coming from the wireless access domain to optical frames/streams, capitalising on a number of HW programmable building blocks, including OPPs.

In addition to traffic adaptation, 5G-PICTURE develops solutions for programmability of data plane functionalities offering HW acceleration for high performance and low latency processing. The lower part of Figure 3-3 shows an example of the capability of the 5G-PICTURE solution to enable the concept of functional splits by: *i)* dynamically allocate physical resources, *ii)* map traffic flows with different service characteristics from one domain to another, and *iii)* rely on HW accelerators for the processing of computational intensive tasks. As discussed in the following subsections, flexible functional splits [8] can decrease the data rate demands between the RUs and the Radio Equipment Control (REC), limiting at the same time the complexity of the RU.

Data plane programmability has been advocated as the perfect solution to manage the heterogeneity of the 5G network as well as to provide fast and easy network function deployment. The development of programmable data planes requires both the design of high-speed, highly flexible hardware architectures and the identification and development of suitable programmable abstractions – domain-specific languages,

Application Programming Interfaces (APIs), hardware abstractions, etc. These programmable abstractions are used to simplify the design of network functions that the programmable data plane must execute.

In the following, a high-level description of the programmable data plane that is under development during the 5G-PICTURE project is described. However, to realize this concept one of the biggest challenges that 5G-PICTURE needs to address is to allow physical and network functions to be appropriately combined and deployed on top of any compute and/or network element. Joint consideration of network softwarisation and HW programmability will allow a variety of tasks to be dynamically allocated between centralized and distributed elements. E.g., programmable optical network functions can be either placed locally at the network nodes (suitable for low-latency applications), or at a remote server (no strict latency constraints). For example, from Figure 3-3 we can observe that the 5G C-RAN BBU can be divided between the CU and the Distributed Unit (DU). Accordingly, the FH domain splits into two parts: the first part covering the network segment between the RU and the DU hosted at Mobile Edge Computing (MEC) servers, and the second part addressing the network segment from the DU to the CU. The first part (from the RU to the MEC) provides connectivity for lower-layer functional splits having high data rate, stringent delay and synchronisation requirements. The second part provides the suitable network and compute resources for higher layer functional splits which have lower data rate, less stringent delay and relaxed synchronisation requirements.

3.1.1 Optical Transport

For the optical transport, we consider a high-capacity WDM-PON solution that allows to interconnect the RUs with the TSON edge nodes and the BBUs. The block diagram of the key components of an indicative WDM-PON solution is provided in Figure 3-4 d). In the uplink, traffic generated from RUs is multiplexed at the ingress Optical Network Units (ONUs)' buffers through the creation of Virtual Output Queues (VOQs) transmitted at the suitable frame. At the same time, ONUs are equipped with wavelength-tunable lasers that can select, at every time instance, a suitable wavelength. This configuration achieves significant statistical multiplexing gains, especially in highly dynamic traffic scenarios. Once the wavelengths have been selected, uplink traffic passes through the Remote Nodes (RNs) before it reaches the Optical Line Terminals (OLTs). RNs offer add-drop capabilities in the downlink and multiplexers for the reverse operation in the uplink. More specifically, in the uplink, the egress traffic from the ONU is forwarded to the ingress port of the RN. In the downlink, traffic is redirected to the ONU receivers. The OLT is equipped with tunable receivers and transmitters which are shared by the ONUs. OLTs are also equipped with VOQs, allowing downlink traffic to be stored and multiplexed before it is placed to the suitable timeslot for further transmission into the network.

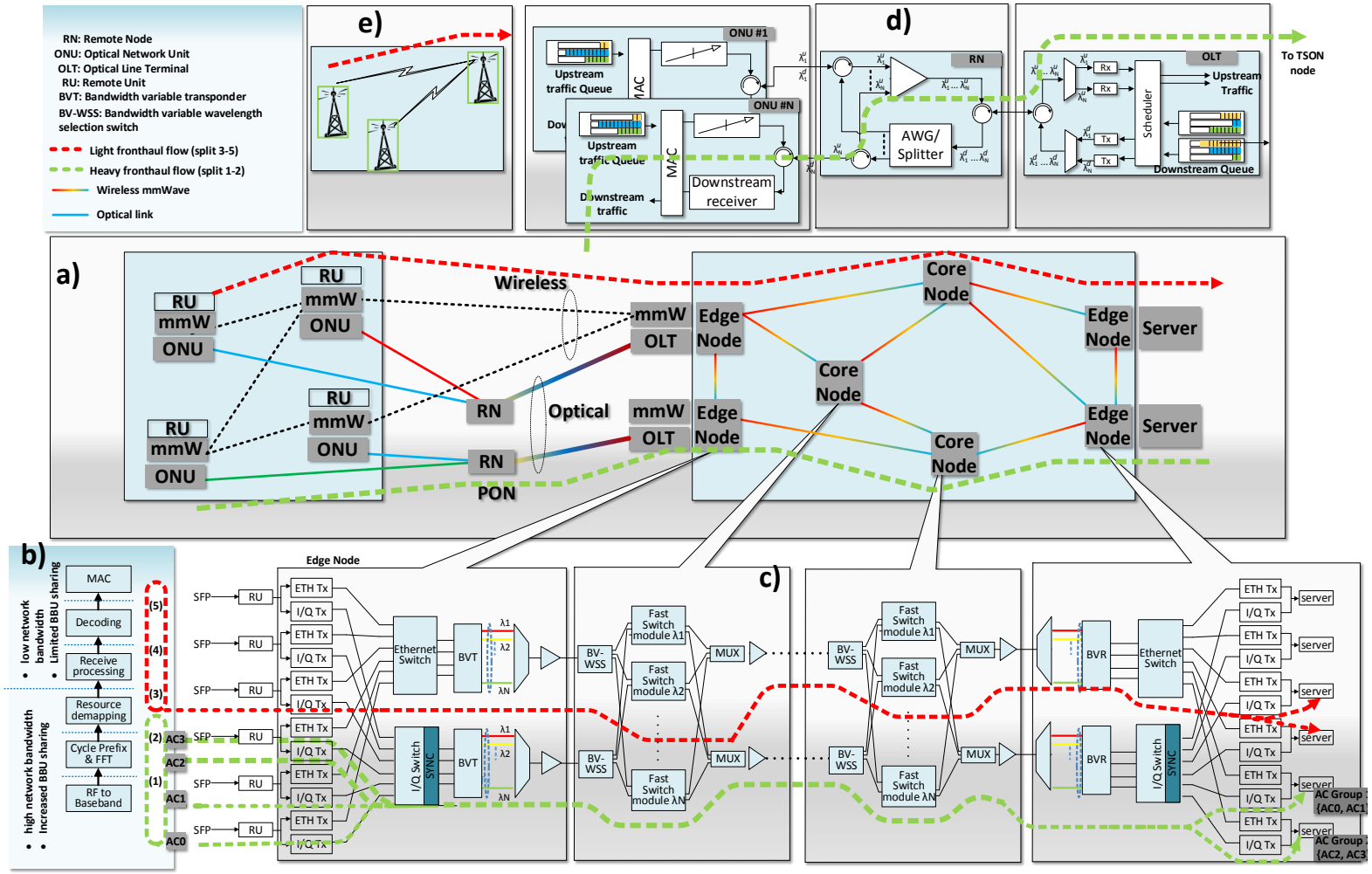

Figure 3-4: a) Integrated optical transport network technologies: a) Multi-technology network infrastructure, b) BBU processing chain and functional split [6], c) Data path interfaces, AxC data stream generation (upper part) and multiplexing (middle) over TSON, d) WDM-PON components, f) microwave BH network.

For the active optical network, we consider TSON in Figure 3-4 c), a frame-based optical network solution offering sub-wavelength switching granularity [70]. TSON edge nodes receive the incoming traffic, aggregate it into optical frames, which are then assigned to suitable time slots and wavelengths for further transmission. At the egress point the reverse function takes place. The optical edge node is also equipped with elastic bandwidth allocation capabilities supported through the deployment of BVTs. The objective of TSON is to provide connectivity for a number of RUs and end-users with a set of general purpose servers. The use of general purpose servers enables the concept of virtual BBUs (vBBUs), facilitating efficient sharing of compute resources. This joint functionality is facilitated by the edge nodes that comprise a hybrid subsystem able to handle continues (I/Q streams) and packetised flows (Ethernet traffic). The operation of this system is supported by a synchronisation block that manages the synchronisation signals between the end points.

To send and receive data, each TSON edge node uses four SFP+ transceivers, two 1310 nm 10 km reach for end-point server traffic and control, and DWDM transceivers operating at the at 1550 nm window. The 1310 nm interfaces can be used to support both data and control traffic either separately or combined depending on whether out-off band or in-band control is adopted.

When the ingress part of the edge node receives traffic the FPGA waits to finish the processing of the current frame, and then starts to transmit time-slices of optical bandwidth. The optical bandwidth which is allocated to the different services is not fixed but can be elastically defined based on the requirements of each service. Therefore, TSON can support elastic time and optical bandwidth allocation. As an example, when the input traffic comprises Ethernet frames at the ingress part of the edge node, the Ethernet frames received at the 10 Gb/s receiver (RX) are passed to the 10GE Medium Access Control (MAC). The MAC then discards the preambles and Frame Check Sequence (FCS), transmits the data to the Receiver (RX) in a first in, first out (FIFO) manner and indicates whether the packet is good or not; The RX FIFO receives the data, waits for the good/bad indication from MAC, sends it to the DEMUX block if there are any valid data. The DEMUX analyses the Ethernet frame information (i.e. Destination MAC address, Source MAC address, etc.), and puts them in a different FIFO. After that, the FIFO does not send any data until the AGGREGATION gives a command. The register file of AGGREGATION, which contains the Time-slice Allocation information, is updated by the Lookup Table (LUT) (this table stores information related to time-slice Allocation and the fast optical switch that is incorporated in the edge TSON node). The AGGREGATION module waits until the burst-length Ethernet frames are ready in the FIFO and the time-slice allocation is available, to then transmit the bursts with a suitable wavelength through the TX FIFO. For the egress part of the edge TSON node, when the 10 Gb/s RX receives a burst (time-slice), it drops the burst in the RX FIFO Lamda0/Lamda1. After the burst is completely received, the SEGREGATION block segregates the burst to Ethernet frames and transmits them to a TX FIFO. Every time the TX FIFO receives a complete Ethernet frame it sends it to the 10GE MAC. Finally, MAC passes the data to the 10 Gb/s transmitter and transmits them out (see Figure 3-5).

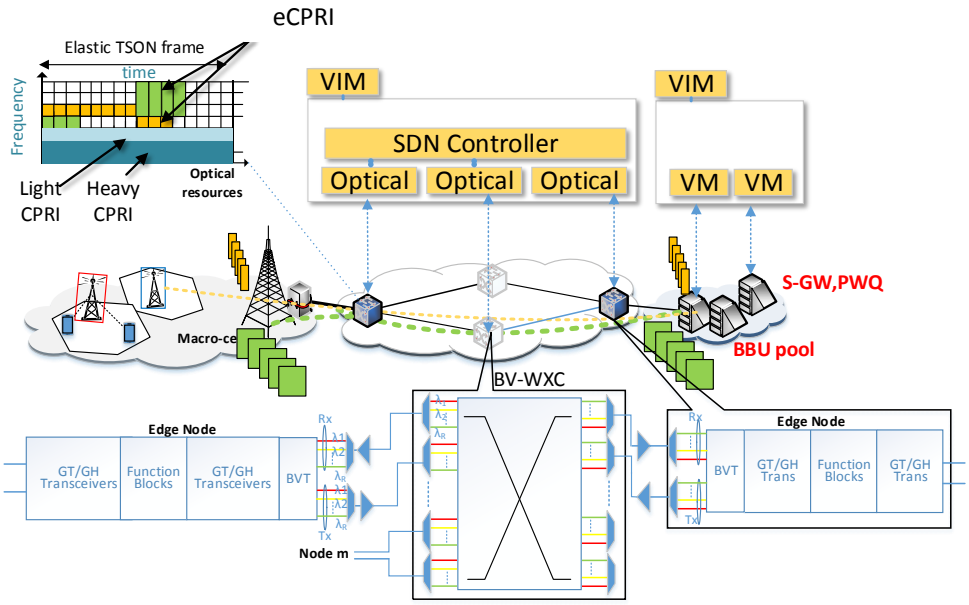

Figure 3-5: TSON architecture.

The TSON core nodes do not carry out any data processing, but need to switch the traffic optically. Therefore, the FPGA-based TSON core node controls the fast optical switches to setup the path with a client's request. These nodes switch transparently the optical frames to the appropriate output port utilising the fast optical switching which in the core node (as happens also in the edge node case). The TSON core nodes adopt the wavelength selective architecture and, as such, they require one switch per wavelength to direct the incoming optical time-sliced signals towards the appropriate output ports, as defined by the control plane. The dimension of the space switch is defined by the number of fibres that are interconnected through the node. The TSON core node uses the same type of high performance FPGA boards for the control of the fast switch. The FPGA LUTs are filled in by the control plane through customised Ethernet communication carrying PLZT switching information. This enables changing the switch state per time-slice on the PLZT switches with the aim to establish and maintain optical paths across the TSON domain. The basic functions for the operation of TSON domains have been implemented in internal modules within the SDN controller, which cooperates for the on-demand provisioning of connectivity between TSON core and edge nodes.

The latest TSON implementation is based on a Xilinx Virtex7 board (156.25 MHz clock frequency), supporting multiple 10 Gb/s (for control and transport) DWDM SFP+ transceivers. Nevertheless, the architecture can support beyond 10 Gb/s (i.e. 25, 40, 100 Gb/s). For the optical layer, TSON relies on fast optical switches [74] having 10 ns switching speed as well as a set of active and passive components including Erbium Doped Fibre Amplifiers (EDFAs), MUX/DEMUXes, etc.

Natively, TSON allows handling of Ethernet frames and, therefore, it is fully compliant with the eCPRI protocol. In addition to this, TSON can support a broad range of framing structures and communication protocols including CPRI [75], either natively or through their packetized versions. To achieve this, TSON relies on a generic and flexible resource allocation framework adopting a hierarchy of three levels of resource granularity including *Connections*, *frames*, and *time-slices* (Figure 3-6). Connection refers to a sub-wavelength light path establishment between any two end points in the TSON domain. To improve statistical multiplexing of data units, each connection lasts for number of frames with minimum size of 1 ms. Each frame is divided into time-slices as the smallest units of network resource, i.e. the actual sub-lambda resources. The frame length and the number of time-slices inside a frame define the minimum granularity achievable by the TSON network [74]. The TSON framework offers a very flexible optical platform that supports sub-wavelength switching, frame lengths varying from 64 ns to 25.6 μs, and variable bit rates spanning from of 30 Mb/s up to several Gb/s, with 30 Mb/s step.

Taking advantage of its flexible resource allocation structure, TSON currently supports CPRI [71] and will be also extended to support eCPRI. The CPRI frame structure can be encapsulated into the TSON frame structure and transmitted after the establishment of a Constant Bit Rate (CBR) connection, as shown in Figure 3-7.

The eCPRI protocol can be supported in a similar fashion by encapsulating the eCPRI frames into the TSON framing structure as shown in Figure 3-8.

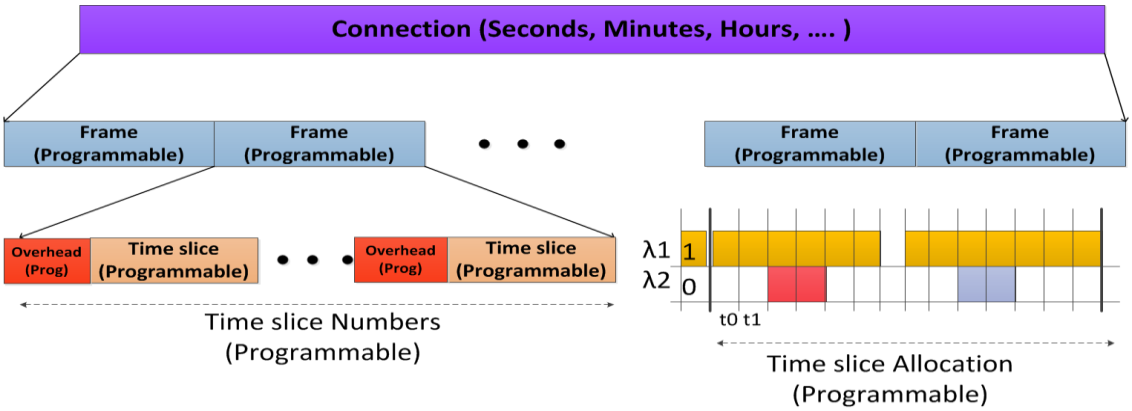

Figure 3-6: Structure of connection, frame and burst [71].

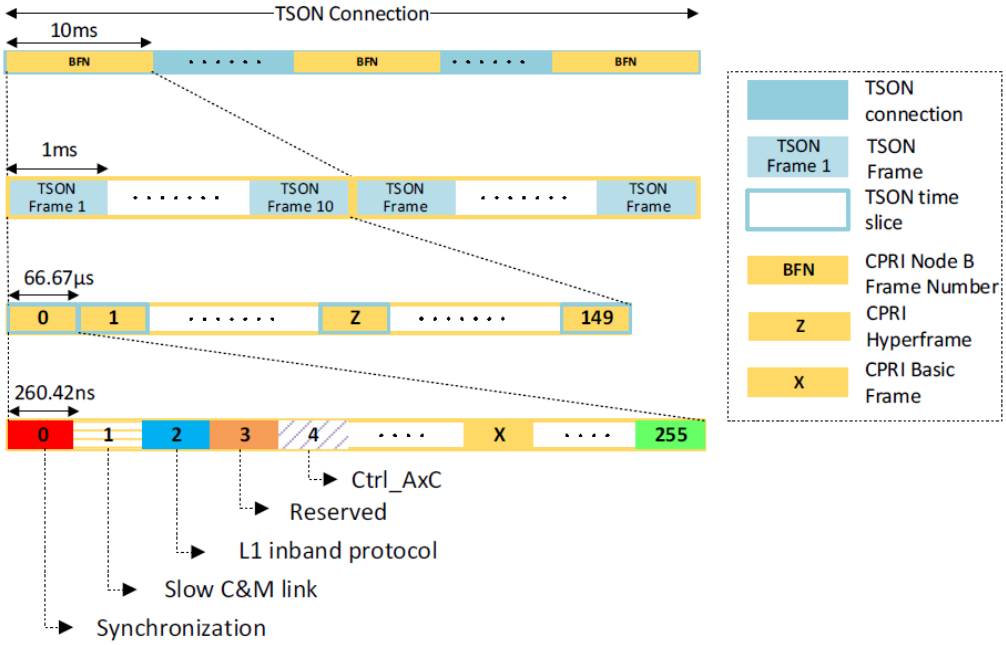

Figure 3-7: CPRI frame structure over TSON.

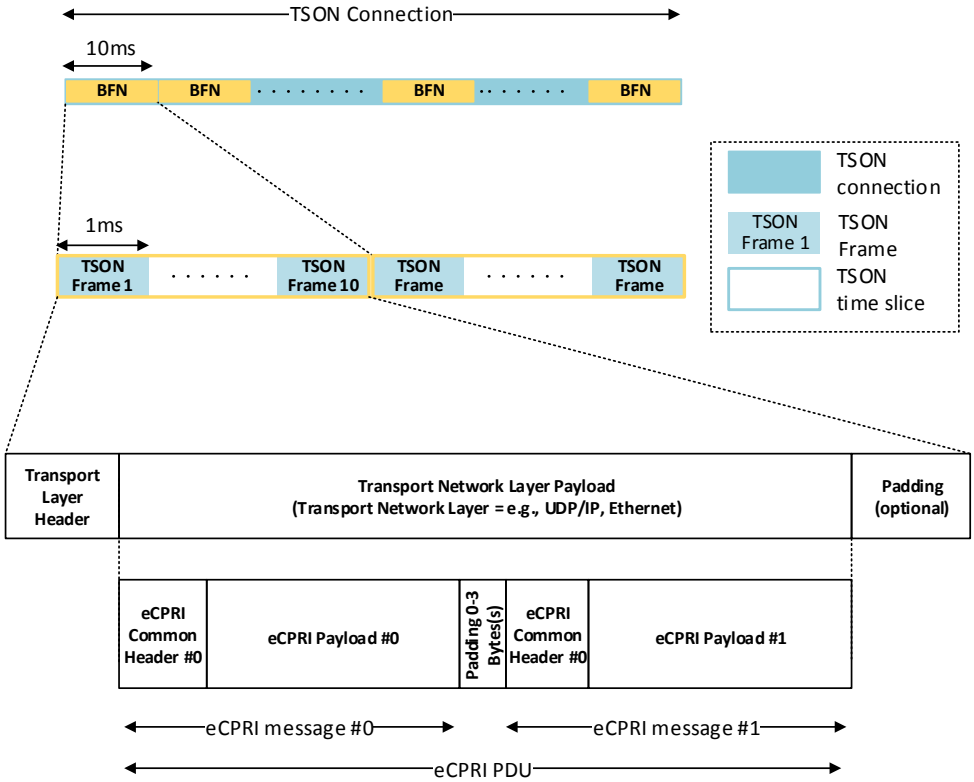

Figure 3-8: eCPRI over TSON.

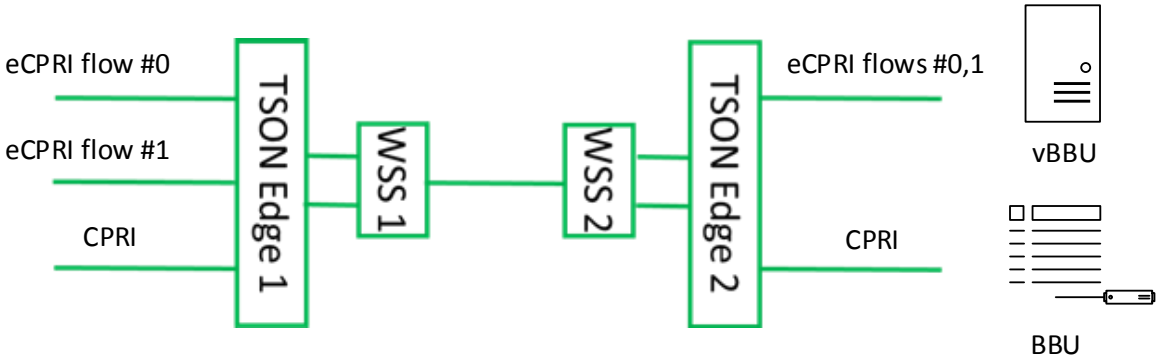

Figure 3-9: Multiplexing of eCPRI and legacy CPRI over TSON.

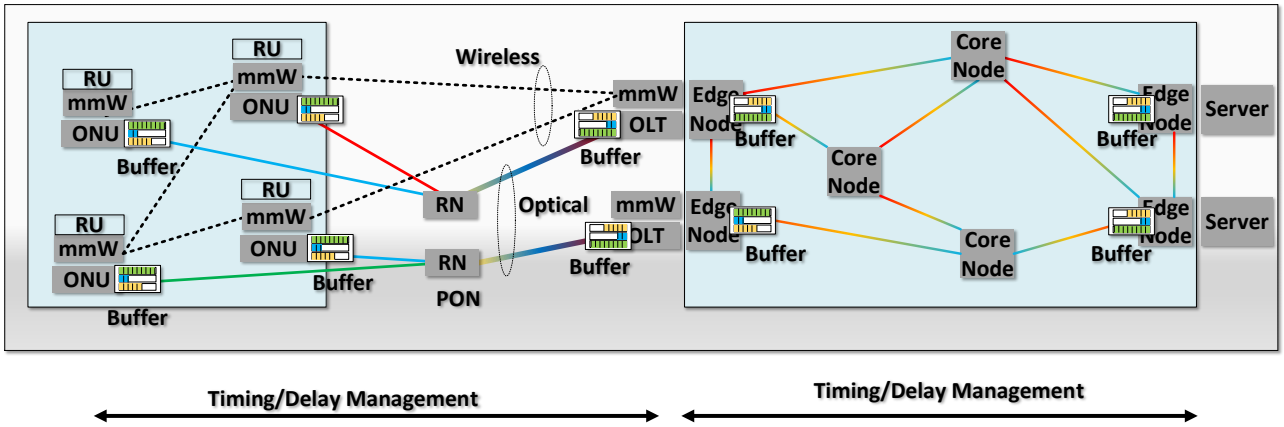

Figure 3-10: Delay Managements.

TSON also gives the ability to multiplex eCPRI and CPRI traffic by appropriately assigning the suitable resources (wavelengths, timeslots) and setting different priorities for different traffic flows depending on the needed QoS.

An example of this process is shown in Figure 3-9 where two Ethernet-based eCPRI flows aggregate into one flow and are then multiplexed together with the CPRI flow, assigning a different wavelength to each of them. These two wavelengths are then fed into a Wavelength Selective Switch 1 (WSS 1). Then, WSS 1 multiplexes eCPRI and CPRI packets over a single fibre and sends them to WSS 2. The WSS 2 receives the upstream flows and demultiplexes them into eCPRI and CPRI packet flows based on their wavelength. The TSON Edge 2 node receives the packets from the Ethernet and CPRI ports and passes them individually to their clients. In the downstream scenario, the reverse operation is performed.

TSON edge nodes can interface multiple technology domains (e.g., wireless, PON and DCs) providing long-reach coverage. A typical example is shown in Figure 3-10, where a WDM-PON provides flexible FH connections between RUs at the antenna side and BBUs at the central office (CO), where the key component for a feasible low-cost implementation is the tuneable laser at the remote interface.

To address synchronisation requirements of the CPRI and eCPRI protocols, the 5G-PICTURE architecture solution takes advantage of the IEEE-1588 v2 protocol [76] and is able to provide a common timestamp across all technology domains. Timestamping can be performed using both in-band and out-of-band information exchange. To enhance the accuracy of the system the time stamper unit is located between the MAC and PCS/ Physical Medium Attachment (PMA) IP cores, uses the Timer Sync clock and follows the IEEE 1588 protocol. In addition, the time stamper considers the link delays for stamping.

Furthermore, the edge nodes have buffers to absorb the fluctuation of transport network delay as well as the variation of processing time which depends on the traffic and processing load. The goal of delay management is to avoid overflow/underflow of buffer memories and to decrease the overall delay, the necessary size of buffer memories, etc. at the same time. Additionally, a sort of traffic shaping may be necessary at the transmitter side to avoid unnecessary traffic congestion [27].

3.1.2 Wireless Technologies

Network heterogeneity in 5G involves the integration of advanced wireless systems, allowing the interconnection of a large variety of end-devices. The wireless transport and access network, shown in Figure 3-11, will be based on mmWave technologies, Sub-6 technologies and massive MIMO techniques using much greater numbers of antennas at the base stations (BSs) to improve data rates, reliability as well as energy efficiency. These will coexist with legacy (2-3G), Long Term Evolution LTE (4G) and Wi-Fi technologies to allow broader coverage and availability, higher network density and increased mobility.

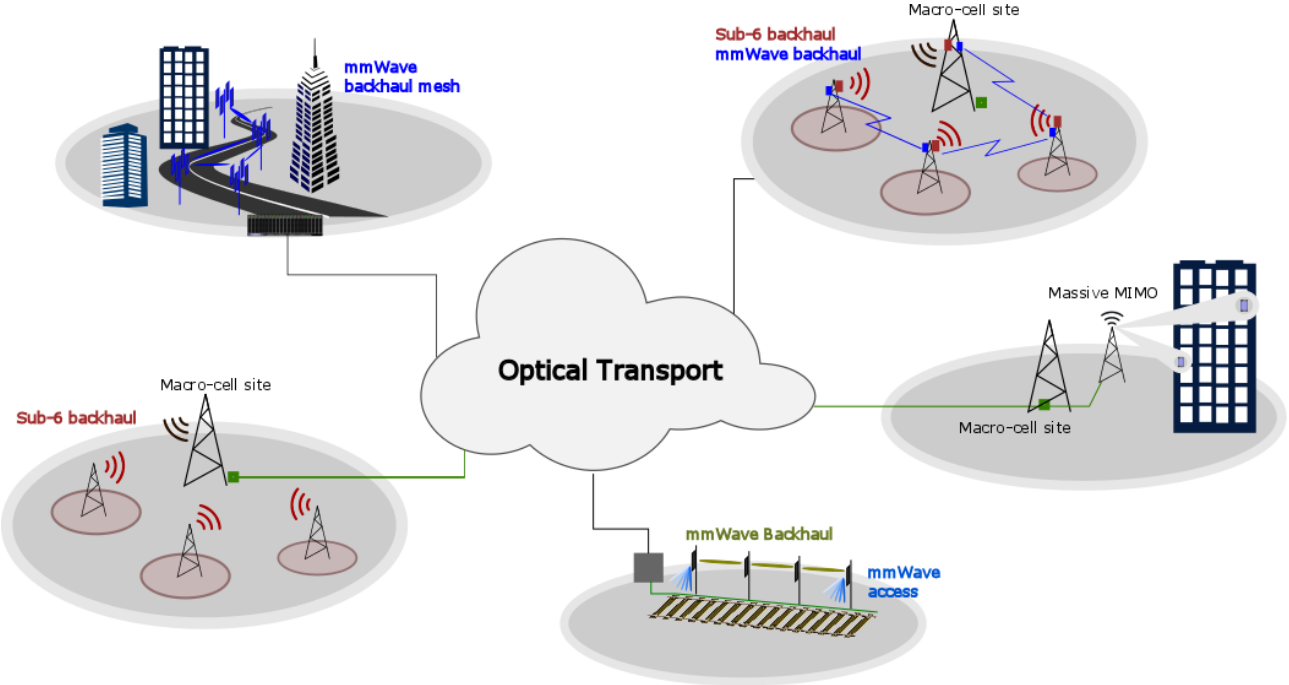

Figure 3-11: 5G-PICTURE wireless technologies.

3.1.2.1 High speed RAN featuring programmable Massive MIMO

Massive MIMO is seen as a key technology to achieve large capacity gains both in 4G and 5G networks. It exploits large arrays of antenna elements to form narrow beams towards users.

However, different approaches to forming these beams exist. While in some scenarios (e.g., for slow moving users), the beams can be calculated dynamically from channel state information (CSI), in other scenarios (e.g. fast moving users), it is more suitable to use semi-static beams to form many “virtual” cells. At the same time, many different frequency band allocations and channel configurations exist, depending on the region or network operator. The number of possible combinations will increase with the upcoming allocation of 5G spectrum. Furthermore, 5G New Radio (NR) spaces subcarriers more flexibly, which could also depend on scenario or the allocated bandwidth. Finally, different functional splits might be desired by network operators depending on available FH capacity in their network.

In light of these different combinations, it is desired to include some programmability/configurability into the radio access network (RAN), in order to serve different scenarios with the same hardware platform. However, BSs need to perform complex signal processing which usually call for dedicated ASICs or at least FPGA implementations for lower-layer processing. For specific frequency band and different carrier configurations, even analog hardware in the form of mixers, band and channel filters are required. This limits conventional BS architectures in terms of configurability and programmability on the lower layers compared to the higher layers, where GPPs can more conveniently be employed. 5G-PICTURE is now investigating programmable massive MIMO by innovative new approaches [20]. With a combination of FPGA-based baseband processing with GPP co-processors and a direct-conversion RF architecture, 5G-PICTURE will introduce an unpreceded degree of flexibility in 5G RAN architecture.

While massive MIMO is often connected to mmWave technology due to the smaller antenna elements, 5G-PICTURE will also focus on Sub-6 GHz technology as this is still the dominant frequency for 4G and early 5G deployments. Millimetre wave technology will be discussed in the next section.

3.1.2.2 Millimetre Wave (60 GHz) & Sub-6

From a wireless technology perspective, 5G-PICTURE considers a dense layer of small cells operating in the frequency range of 100 MHz – 100 GHz. Seamless integration of mmWave BH technology with Sub-6 Non-Line-of-Sight (NLoS) technology is generally recognised as the technology providing the ideal combination of capacity and coverage by operators deploying wireless BH, particularly in complex urban deployments [24].

In Figure 3-11, the macro cell is connected to the optical metro network via fibre, which provides connectivity to the CN elements, typically deployed in a Data Centre (DC). In practice, the different wireless nodes, either Sub-6 or mmWave, may also have a direct connection to the optical transport network.

We identified a necessary building block for densification of mmWave wireless backhaul links: multi-gigabit meshed BH technologies based on WiGig (IEEE 802.11ad) operating in the V-band at 60 GHz, making use of beam-steering algorithms to establish different configurations. The nodes will support beam-tracking and, at a later stage, MIMO techniques. This technology will be enhanced with programmable network processors to allow network functions to be easily configured/modified or controlled by an SDN controller. An accurate channel modelling analysis, applicable to realistic environments extracted from the vertical use cases, will be carried out between Sub-6 GHz and mmWave frequencies. In the context of Sub-6 GHz and mmWave, the merits of MIMO and appropriate beamforming [20] will be investigated by system-level analysis for the railway vertical user case that will be demonstrated in WP6. Nodes with mmWave capabilities will be utilised to convey functional splits.

Millimetre wave technologies will be complemented with Sub-6 GHz technologies [20]. Sub-6 solutions allow NLoS operation and can complement mmWave nodes in situations where mmWave nodes face NLoS conditions. Sub-6 technologies will be provided with self-backhauling capabilities.

3.1.3 Ethernet Transport

Network architectures compliant with the SDN design paradigm are expected to provide extreme flexibility for service-orientation and to allow efficient use of network resources. Nevertheless, radical reconsidering and removal of boundaries set out when studying multi-domain communications are required, in order to unleash the hidden potential of SDN and provide a “holistic” network view.

Key objectives for both SDN and carrier Ethernet are to reduce overall costs and improve operation efficiency. On the transport network “all IP, the all Ethernet” technology is aiming to provide the underpinning over which the mobile network operators (MNOs) will build their future programmable SDN-based and network slice ready networks. On the radio side efforts concentrate around eCPRI and Radio over Ethernet (RoE). For the transport network the main activities are around Ethernet over Multi-Protocol Label Switching (EoMPLS), Ethernet over SONET/SDH, Ethernet over DWDM and Ethernet over OTN. Recently approaches focus also on Flex-E and X-Ethernet technologies for higher capacities and to handle load dynamicity and provide performance guarantees.

Flex-E technology is introduced as a thin layer (called Flex-Shim) between Ethernet MAC and Physical Coding Sublayer (PCS) and is able to support multiple MAC clients over multiple PHY layers. The idea is that through Flex-E, the MAC layer speed of a client can be decoupled from the actual PHY layer speed. The Flex-E functionality is based on a time-division multiplexing mechanism that is able to drive the asynchronous Ethernet flows over a synchronous schedule over multiple PHY layers.

Furthermore, Time Sensitive Networking (TSN) Ethernet mechanisms have recently been proposed for enabling low latency in Ethernet combined with statistical multiplexing. The TSN initiatives includes both standardization work within the IEEE 802.1 and the FUSION networking mechanisms from TransPacket. Both synchronized slotted approaches and asynchronous approaches are proposed. In addition to low-latency transport, FUSION includes a Guaranteed Service Transport (GST) class with ultra-low Packet Delay Variation (PDV). This enables high accuracy synchronisation by timing transparent transport of IEEE 1588 PTP packets. In Figure 3-12 an Ethernet TSN network for aggregation, transport and de-aggregation in FH is illustrated, while Figure 3-13 shows how the Ethernet TSN may be further combined with WDM aggregation enabling a scalable FH transport.

In 5G-PICTURE, in order to manage, control and efficiently operate this type of complex infrastructures in an efficient manner, SDN and programmable Ethernet transport networks are investigated in and within the scope of an overall programmable data plane framework, where the relevant control systems are managed by an integrated 5G OS orchestration and management solution.

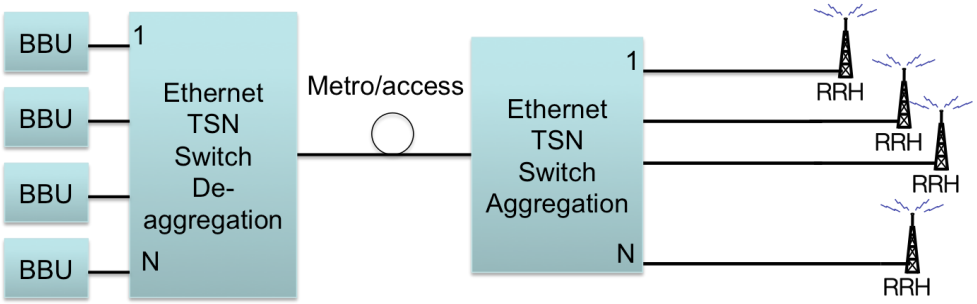

Figure 3-12: Ethernet TSN network for aggregation, transport and de-aggregation in FH.

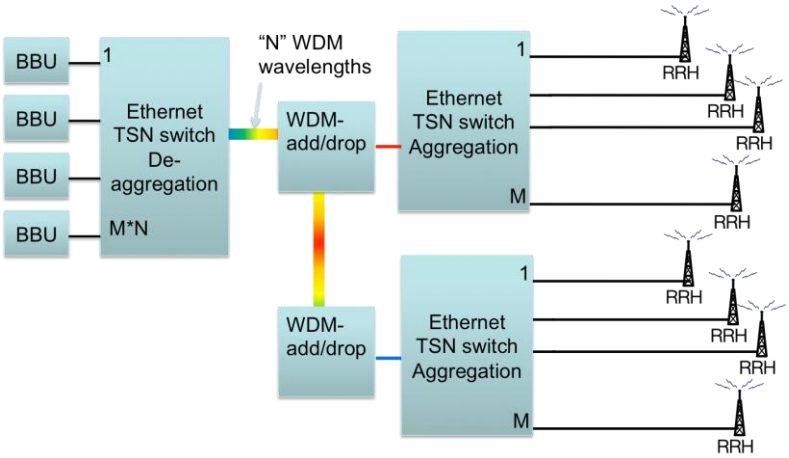

Figure 3-13: Combination of Ethernet TSN with WDM aggregation enabling a scalable FH transport.

Furthermore, a programmable Ethernet functionality is useful for adapting the required functionality to the requirements of the variable functional split options. The different types of FH functional splits define different requirements with regards to latency, bitrate and traffic pattern. For example, a CPRI over Ethernet mapping will produce a CBR stream of data at a high bitrate compared to the offered user data-rate. The eCPRI splits, on the other hand, allow statistical multiplexing and lower bitrates for the same offered user data-rate while latency requirements remain as strict as the ones for CPRI. The latter are further relaxed for higher level splits. Hence, a programmable Ethernet transport may accommodate an adaption of functionality needed for meeting the different requirements from the different functional splits and also a flexible architecture combining integrated transport of different functional splits within a single network.

3.1.4 Programmable Packet Processors

The programmable data plane will be able to provide protocol independence, thus managing programmable parsing of the protocol stack for generic field extraction and packet encapsulation/decapsulation. The programmability of the data plane will be extended both in terms of switch matching capabilities and in terms of actions to apply to the processed packets using programmable pipelines of match/action stages. Finally, the programmable packet processors will offload several monitoring/management tasks directly to the data plane using per-flow stateful primitives. The 5G-PICTURE project is developing several technologies that are directly related to the programmability of the data plane at the packet/flow level. In particular, three technologies are under development: i) a VLIW (Very Long Instruction Word) processor called V-PMP tailored for packet manipulation task; ii) OPP, a programmable data plane focused on the implementation of stateful per-flow functionalities; and iii) a P4 compiler to configure high speed Mellanox Ethernet switches.

The first technology for programmable packet processors focuses on the programmability of the actions to apply to the packet travelling into the network. While in the past these actions were very limited, in particular on the network switches, now the number and also the complexity of these actions is constantly growing. And the programmability of these action is arising as a key element to provide protocol independence and to match the different protocols utilised by different networks. The encapsulation/decapsulation of VxLAN tags used in

large cloud computing deployments or the management of GPRS Tunnelling Protocol (GTP) termination used for tunnelling in the mobile edge are examples of possible applications for a flexible and programmable engine focused on the extrapolation/manipulation of packet headers.

The second technology, namely OPP, focuses on the design of stateful per-flow functionalities. One of the bigger limitations in the current programmable data planes is the absence of a clear per-flow stateful model for storing directly in the data plane the information gathered on the different flows under analysis. There are two types of stateful elements in programmable data planes: tables and counters/registers. Nowadays tables can be controller only from the control plane (insertion/update/delete operation can be executed only using specific control-plane commands). Registers/counters array can be updated directly in the data plane, but it is hard to map a row of the array to a specific flow. The mapping between the flow and the array elements can be also realized using a matching table, but the use of this approach prevent the data plane update of the table (e.g. when a new flow arrive or a flow expires. OPP solves these issues providing some specific tables that can be updatable directly in the data plane. Design an efficient data plane updatable table while retaining wire speed is a challenging engineering task, as discussed in deliverable 3.1 [20]. From the programmability point of view this enables the in-data plane management of several per-flow network functions, spanning from configurable Network Address Translation (NAT) services to flow monitoring, from QoS policies up to the deployment of data-driven routing/forwarding mechanisms.

Finally, the third element for the packet programmable processor is the development of a P4 compiler to configure the Ethernet switches used in the 5G-PICTURE architecture. The 5G-PICTURE project will leverage the programmability of the current generation of the Mellanox Switch ASIC (Spectrum™) using this chip as the target of the P4 compiler.

3.1.4.1 Leveraging PPP for flexible functional split

Dataplane programmability is an important enabler for the deployment of complex but efficient functional splits. In fact, the actual deployment of an efficient functional split requires to transmit the data collected from the access points towards the computing resources across several heterogeneous network nodes. Thus, it requires to perform several complex encapsulation/decapsulation (at packet level) or tunneling (at flow level) tasks. Examples of these tasks are the VxLAN tags used in large cloud computing deployments or the GTP termination used in MEC. Even if this is a conceptually simple task the performance of these operations is critical to realize an efficient (in terms of latency, throughput and also energy saving) functional split. The V-PMP is an excellent candidate to efficiently (both in terms of throughput and latency) execute complex tunneling tasks. Moreover, the high programmability of V-PMP will permit both to reuse the same component across different network nodes and also to enable modification of the various packet transmission standards since the support of a new standard will not require architectural modifications.

Similar considerations can be done for the OPP technology as an enabler for flexible functional splits. The data plane level stateful per-flow functionalities permit to avoid the latency overhead and throughput bottleneck for the network function primitives used to provide the functional split. An example of network functionalities on top of OPP of the 5G-PICTURE project is the development of a routing algorithm for DCs able to dynamically estimate the best path in terms of latency/throughput. This will allow to take routing decisions depending on the flow requirements, i.e. forwarding latency critical flows using the low latency paths.

Finally, it is true that the resource disaggregation concept allows efficient provisioning of the hardware and software resources that are available in the network. However, the actual use of these resources requires having some functionalities (that can be at least roughly identified as network functions) to be independently deployed and executed in different heterogeneous computing resources. In principle, the same function could be realized in a fixed functionality ASIC chip in a highly specialised processor (DSP for signal processing or in a network processor for packet level operations), in an FPGA, in a GPU or in an off the shelf x86 host. All these resources have different programming languages and different interfaces with the external world. The obvious solution for designing the same functions in all possible platforms on which the function can be executed is not scalable. This is due to the large number of platforms and to the very different programming models that need to be applied. To solve this issue, we can take advantage of the fact that the set of functionalities we need to realise is actually restricted with respect to the general purpose computing supported by the FPGA/GPU/CPU architecture. To this aim, 5G-PICTURE is developing “code once run anywhere” network functionalities for the dataplane using domain specific languages or portable intermediate languages and abstraction. For the domain specific languages 5G-PICTURE is leveraging the increased interest in P4 for the dataplane programmability and the use of portable intermediate languages such as eBPF (that currently can be executed on Linux kernel and on some smartNICs). The same OPP model is an example of a portable

abstraction, since both an efficient software implementation and a HW-based implementation are available. At the transport level, 5G-PICTURE plans to develop an ad-hoc domain specific language able to seamlessly execute transport protocol in different platforms. Similar considerations can be done for the functions executing signal processing tasks, where the adoption of OpenCL could help to reuse the same code to deploy the function in different type of computing resources.

3.2 Physical and Virtual Functions

5G-PICTURE considers the development of physical and virtual functions in three main domains:

1. Physical and virtual functions implementing RAN, i.e. BS components.
2. Functions to enable programmable slicing capabilities in heterogeneous transport networks, including wireless, packet and optical transport.
3. Functions able to provide synchronisation on-demand to distributed RAN and transport functions.

Figure 3-14 describes the operational framework that ties together these different types of functions.

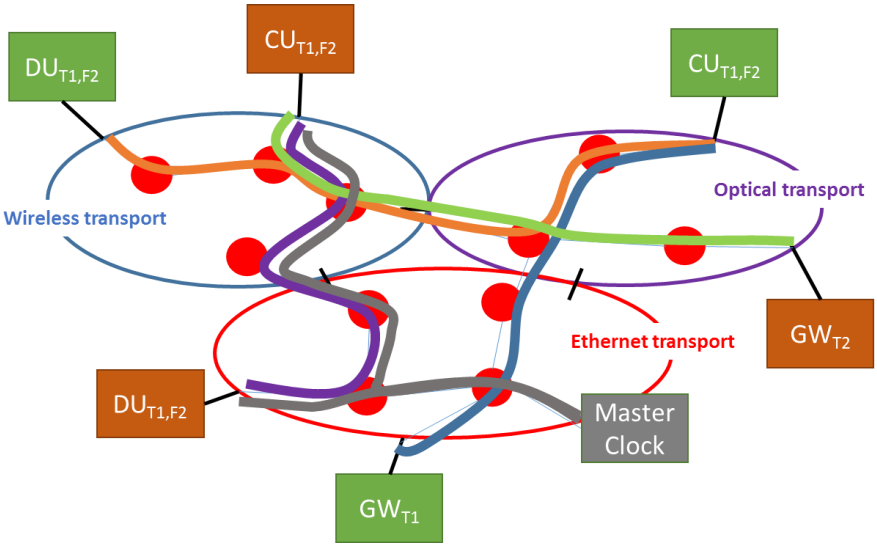

Figure 3-14: Interaction between functional elements considered in WP4. DU$_{Ti,Fj}$ and CU$_{Ti,Fj}$ represent respectively a distributed and centralized unit using technology i, and functional split j.

Figure 3-14 illustrates how the different 5G-PICTURE functional elements relate to each other [25]. The development of the relevant Virtual Network Functions (VNFs) and Physical Network Functions (PNFs) will be carried out in the context of WP4 activities. In particular, we can see a heterogeneous transport infrastructure consisting of a wireless domain, an optical domain, and a packet (native Ethernet) domain. The 5G-PICTURE slice-enabled transport network is used to provide the necessary connectivity for different tenants' RAN functions, namely DU, CU, with packet Gateways over the shared transport infrastructure. Tenants may use different technologies and RAN functional splits.

We can see in Figure 3-14 that tenant's DUs and CUs functions belonging to a network slice (same colour) are connected using transport tunnels that span various technology domains. Furthermore, CUs and packet gateways belonging to the same technology may also be connected using different transport tunnels. As we can also observe in the figure a Master Clock needs to be connected to the network and provide the necessary synchronisation services to one of the DU/CU pairs.

The synchronisation requirements between each DU/CU pair may vary depending on the technology and functional split being implemented. It is worth noting how the separate multicast tunnel is used to transport clock related information.

Next, we provide a summary of the actual functions that will be developed under each category. The interested reader can refer to deliverable D4.1 [25] for a detailed description and initial function design.

3.2.1 Physical and virtual RAN functions

3.2.1.1 RAN functional split

To represent the segmented RAN processing among disaggregated RAN nodes (i.e., RU/DU/CU), several functional split options are proposed by 3GPP [26] and eCPRI [27] as discussed in section 2. These functional split options correspond to how baseband processing functions as well as corresponding network functions are distributed and chained. The chosen functional split will highly impact the FH throughput and characteristics of the transported samples over the Fronthaul (FH) interface. In Figure 3-15, several functional split options provided by 3GPP and eCPRI are shown. Functional splits that are far away from the radio frequency part, i.e., the left side of the figure, have the most relaxed latency and throughput requirements over the FH interface; however, they offer a few centralisation gain, i.e., only centralised Radio Resource Control (RRC) in 3GPP option 1. Among all splits, current standardisation efforts focus on the Option 2 split between CU and DU, i.e., the Packet Data Convergence Protocol (PDCP) processing and above are at CU while the Radio Link Control (RLC) processing with below layers are at DU. The communication interface between PDCP and RLC is taking place through the F1 Application Protocol (F1AP), as indicated in the 3GPP standards for the NG-RAN interface in [33] and [34]. Note that the functional splits for Downlink (DL) and Uplink (UL) directions are not necessarily the same; hence, more flexibilities are enabled via deploying network functions of different directions independently. More state-of-the-art on the comparisons and measurements of different functional splits are provided in Section 3.1 of deliverable D4.1 [25].

Based on the functional split, the specific RAN network functions (either virtual or physical) will be leveraged to compose the whole processing chain. Moreover, as the network functions can be either customised or shared, the functional split can be both *horizontal* (e.g., between CU/DU/RU) and *vertical* (e.g., dedicated or shared network functions). More specifically, the vertical splits aim to provide customised network functions if requested by some services, while shared network functions can be utilised by services that do not request such customisation and can enhance statistical resource multiplexing gain. An example is shown in Figure 3-16 with three different slices, in which slice 1, 2 and 3 have different portions of function customisation. Such characteristic can be enabled through the forwarding engine in each disaggregated RAN node.

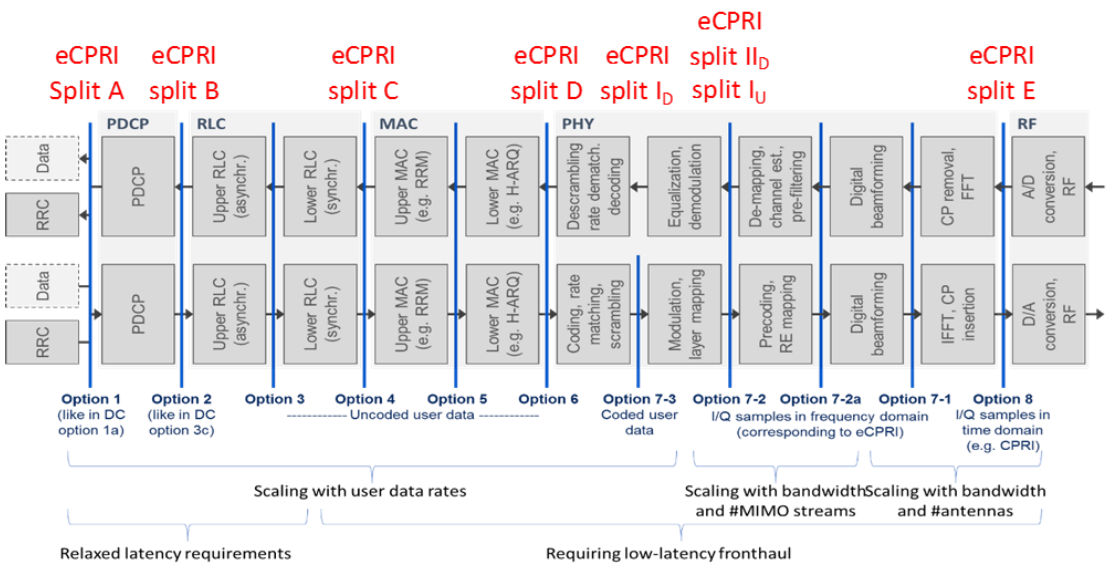

Figure 3-15: Main functional split options provided by 3GPP (bottom) and eCPRI (top) for 5G RAN.

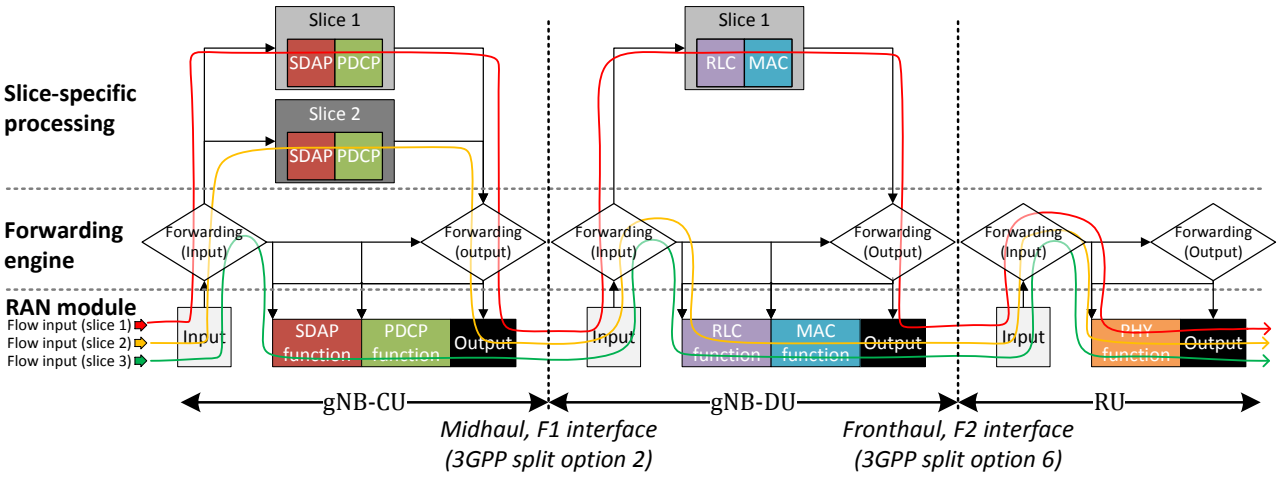

Figure 3-16: Chaining of customised (above) and shared (bottom) network functions in three-level disaggregated RAN.

Based on the aforementioned functional splits for RAN network functions, the development of RAN network functions in 5G-PICTURE will be provided through the following technical components introduced from Section 3.2.1.2 to Section 3.2.1.5. These four sections correspond to four keys of the network function design at the RAN domain: feasibility, optimality, dynamicity and extendibility.

3.2.1.2 Requirements of different network functions

In this paragraph, we analyse each network function in terms of the processing cost and processing time. These results provide an initial understanding of the management of these network functions and show their deployment feasibility.

3.2.1.2.1 Processing requirements of different network functions

Each functional split has specific processing and network bandwidth requirements, e.g. in the case of 3GPP split option 8 RF to baseband conversion is performed at the RU; whereas all other functions (i.e. Cycle Prefix and Fast Fourier Transform (FFT), resource de-mapping, modulation-equalization and forward error correction (FEC), MAC, as well as RLC) are performed at the DU/CU. In this case, the required FH bandwidth is proportional to the number of antennas and the sampling rate; it also depends on the bit resolution per I/Q sample. For example, a 2x2 antenna system with 20 MHz bandwidth requires 2.47 Gb/s line rate. These requirements can be relaxed if additional functions are processed at the RUs. The exact evaluation of these requirements can be found in [6]; a numerical example for a 2x2 MIMO system with 20 MHz bandwidth is provided in the left part of Figure 3-17. In addition to network requirements, each function of the processing chain has also specific processing requirements. To identify the instructions per second (IPS) and the associated running times for each function, we rely on the open-source implementation provided in [87]. The plot in the right part of Figure 3-17 provides an overview of the relative processing cost per functional split at the centralised DU/CU taking as a baseline split option E. The total processing workload for functional splits 8, 7-1 and 7-2 at the DU/CU is very high due to the very high processing requirements of the “FEC Encoder” function.

In the relevant study, we assume that the processing requirements of the DU/CU chain are accommodated through a resource pool comprising both GPPs and SPPs hosted at regional or mobile edge DCs. Therefore, in addition to the optimal split selection, mapping of FH functions to suitable GPPs/SPPs within the DC is part of the optimisation process.

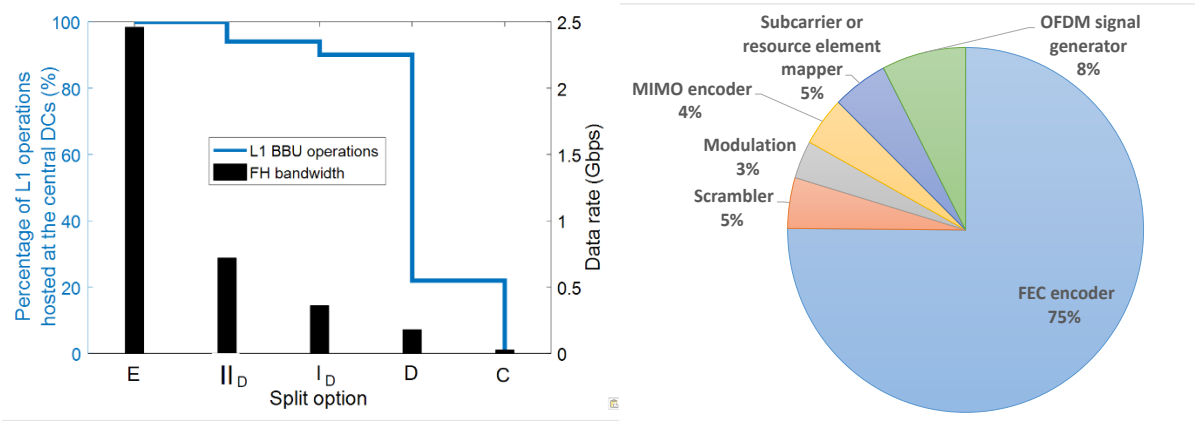

Figure 3-17: (left) Network and processing requirements of the various functional splits for a 2x2 MIMO system with 20 MHz bandwidth and (right) Relative processing cost per function in the DU/CU service chain.

3.2.1.2.2 Processing time of different network functions

The processing time needs to be taken into account to properly place the function. For instance, the Hybrid Automatic Repeat reQuest (HARQ) timing constraint in the uplink direction is shown in Figure 3-18. This constraint imposes the requirement that every received MAC protocol data unit (PDU) should be acknowledged (ACK'ed) or non-acknowledged (NACK'ed) within a specific time duration. In FDD LTE case, the HARQ round trip time (T_{HARQ}) is 8 ms, and each MAC PDU sent at the Nth subframe is propagated (T_{prop}), acquired (T_{acq}), and processed both in the reception ($T_{Rx,eNB}$) and transmission ($T_{Tx,eNB}$) chains for the ACK/NACK response. Then, this response is received at the $(N + 4)^{th}$ subframe by the user and the re-transmission starts at the $(N+8)^{th}$ subframe. Hence, the maximum allowed time for eNB reception and transmission is within 3 ms as shown in [88], which includes the delay due to processing, transportation and packetisation.

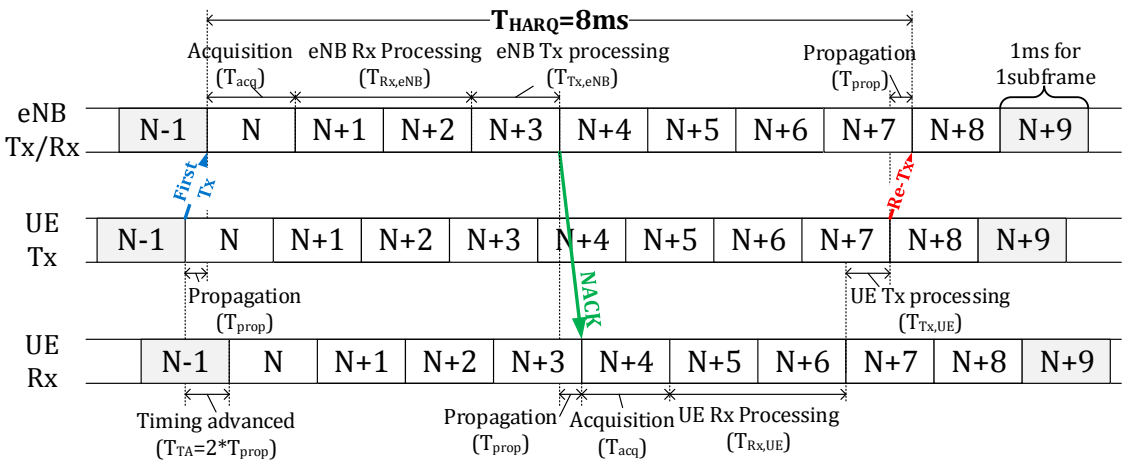

Figure 3-18: Uplink HARQ timing of an LTE system.

In the following, we measure the execution time of the LTE protocol stack using the OpenAirInterface (OAI) platform with a single commercial user equipment (UE) and 5 MHz radio bandwidth. Such UE can achieve 16 Mb/s throughput in DL direction and 7 Mb/s in UL direction. The results are shown in Figure 3-19 for both UP and DL directions. We can observe that the most time-consuming processing corresponds to L1_High, which includes the UE-specific L1 signal processing and channel (de-)coding. In contrast, L1_Low only includes the cell-common processing such as FFT/IFFT, L2_Low includes the MAC and RLC processing, and L2_High comprises the PDCP and Service Data Adaptation Protocol (SDAP) processing. Further, the L1_High functions of the UL direction require longer execution times than the L1_High equivalent in the DL direction. The reason is that the decoding process requires several iterations to successfully decode the receiving data from the UE side.

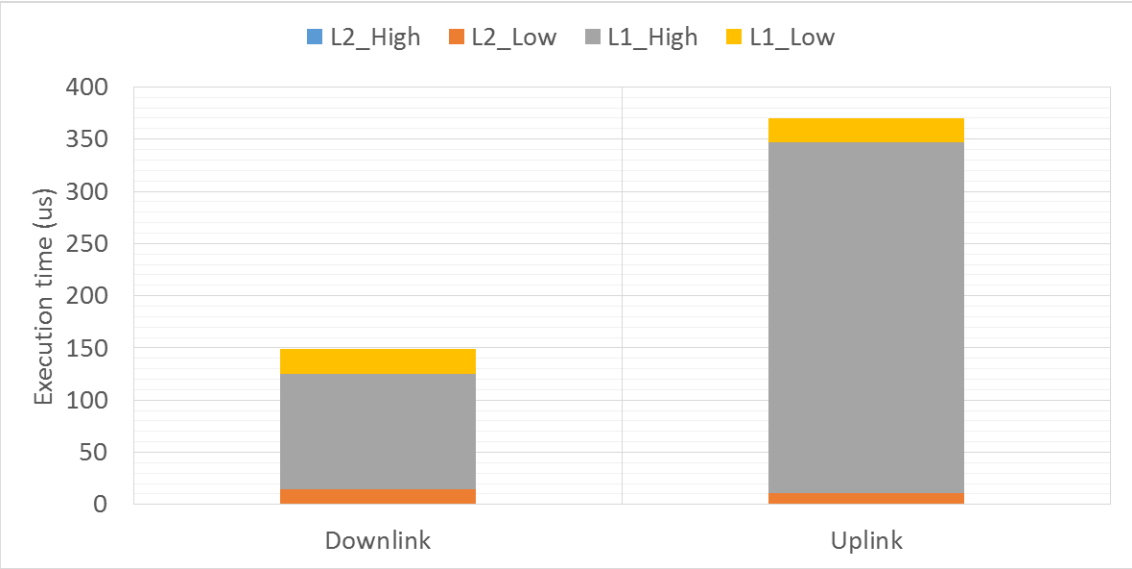

Figure 3-19: Execution time of different processing for both DL/UL directions.

3.2.1.3 Derivation of optimal functional splits

Different functional splits have different characteristics in terms of the level of collaborative processing and different FH requirements in terms of capacity and latency. Our goal is to explore the trade-off between centralisation gains and transport network requirements, and to identify the most suitable functional split for specific scenarios considering the various constraints and requirements. In that sense, the optimal functional split depends on the target service (e.g., low-latency traffic), scenario (e.g., massive MIMO) to be provided towards the end-users and on the FH network conditions (e.g. ideal or non-ideal). Hence, we focus our investigation on deriving optimal functional splits for two particular scenarios: (a) Massive MIMO and (b) Densely-deployed radio access network. Such technology component aims to provide the intelligence to be applied at the RAN-domain controller to apply the most suitable split based on different objectives and constraints. Note that the aim of this section is to derive the optimal functional split in terms of the "utilisation efficiency", e.g. spectral efficiency and power efficiency, and it is based on the feasibility investigation of the processing cost and processing time in Section 3.2.1.2.2.

3.2.1.3.1 Functional Splits for Massive MIMO (Options 7-2, 7-2a, and 7-A)

In massive MIMO, Remote Units (RUs) are equipped with several tens or hundreds of antenna elements. This enables massive MIMO to achieve high spectral and energy efficiencies via array gains since it generates highly directional, narrow beams and spatial multiplexing gains. However, providing FH connectivity to massive MIMO is a challenge. In Option 8 (CPRI), quantized I/Q samples for each antenna element are transported over FH since beamforming is done at CU. Thus, the FH data rates for these splits increase linearly with the number of antenna elements and are not suitable for massive MIMO. For example, forty 10G CPRI lanes are required to transport 200 MHz bandwidth signal for a 64 x 64 antenna configuration with Option 8 [27]. At the same time, processing requirements increase dramatically according to the higher number of antenna and data streams. Therefore, a special focus needs to be put on the investigation of massive MIMO for the 5G-PICTURE architecture.

To limit the increase in FH data rate with the number of antenna ports, beamforming is moved fully or partially to the RU. This leads to different intra-PHY functional splits. However, certain splits are more suitable for massive MIMO integration and are hence separately discussed in the following. Also, a non-standard split noted Split 7-A is discussed.

The different options for massive MIMO functional splits are again highlighted in Figure 3-20.

1. *Option 7-2:* As per this option, functional split occurs between layer mapping and resource element blocks as shown in Figure 3-20. Since quantized frequency domain I/Q samples for different spatial streams are transported over FH, the required FH capacity does not scale with the number of antenna elements. For example, this split requires only five 10G CPRI lanes to transport 200 MHz bandwidth signal for a 64 x 64 antenna configuration. In addition, only utilized Physical Resource Blocks (PRBs)

are transported on the FH, hence the FH rate also scales with cell load. However, more hardware resources compared to Split 8 (CPRI) are required at the RU as computational complexity increases linearly with the number of antenna elements and streams. Furthermore, coordinated beamforming across multiple cells is no longer possible. However, Coordinated Multi-Point (CoMP) gains can still be realised by coordinated scheduling and power control.

2. *Option 7-2a:* This option moves the resource element mapper to the CU compared to split 7-2. While this option has the disadvantage of the FH rate no longer scaling with the cell load, it simplifies the interface, as simply all subcarriers can be transmitted instead of having to also forward information on the exact mapping of occupied subcarriers. Although this split was not specified by 3GPP [29] it is of particular interest for 5G-PICTURE and the industry as a whole, as it was selected by the xRAN Forum, where it is called 7-2x. The xRAN Alliance is an industry group "formed to develop, standardise and promote a software-based, extensible Radio Access Network" [30]. Recently, xRAN merged with the C-RAN Alliance into the ORAN Alliance, to "form a world-wide, carrier-led effort to drive new levels of openness in the radio access network of next-generation wireless systems" [31] As such, it can be expected to gain significant traction for 5G networks.
3. *Option 7-A [2]:* This split is similar to Option 8 (CPRI) except that time-domain beamforming is performed at the DU, and before the Digital-to-Analogue Converter (DAC). A similar beamforming model is considered in Rel. 14 of LTE [32]. This split option retains the advantages of the stream-dependent data rate but with lower computational requirements at the RU. However, it requires higher FH capacity as time-domain I/Q samples are transported over FH. As noted in [20], it has several advantages such as more flexibility and independence since beamforming is done after the 3GPP PHY layer processing and requires lower inter-connect data rates. However, per-subband beamforming is not possible anymore.

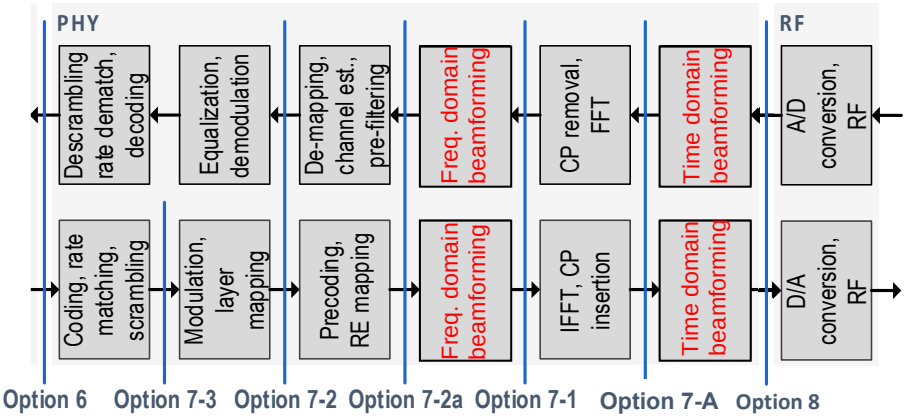

Figure 3-20: Functional splits for massive MIMO.

3.2.1.3.2 Functional Splits for clustering RUs in densely-deployed RAN

In this scenario, we aim to group RUs into disjoint RU clusters for joint processing based on the applied functional splits within the formed clusters to reduce the interference within each cluster. Such RU clustering can boost the area spectral efficiency (i.e., bps/Hz/m^2) via coordinated processing among RUs within the cluster, e.g. joint processing or joint scheduling. Moreover, the RUs within a cluster shall apply the same functional split and shall be anchored to the same processing pool (i.e., same DU/CU processing).

However, as abovementioned, the trade-off between the degree of centralisation and FH bandwidth/latency shall be taken into consideration when forming an RU cluster. More specifically, we focus on the low-level functional split in the PHY part, i.e. split option 8, 7-1, 7-2, 7-3 and 6, as they can bring more significant trade-offs than high-level functional splits.

3.2.1.4 Development and demonstration of flexible functional splits

Based on the three-level RAN disaggregation mentioned above there are two functional splits in between: (1) RU-DU split and (2) CU-DU split. For the former RU-DU split, our implementation targets to investigate split option 8, 7-1 and 6 on the OAI platform with proper sample compression scheme to reduce the required FH throughput (e.g., A-law compression). As for the latter CU-DU split, we aim to investigate the split option 2, also on the OAI platform, termed as F1AP interface (i.e. F1-C and F1-U) by 3GPP standards. Moreover, we

also aim to examine the feasibility of utilising different RATs between CU and DU, e.g., a single CU connects to 4G/5G/Wi-Fi DUs. More initial surveys and design details can be found in deliverable D4.1 [25].

Additionally, aforementioned implemented function splits shall be designed to support a flexible functional split change to enable our derived optimal functional split in Section 3.2.1.3. Such technical component is focusing on the RAN service continuity in a dynamic split change, since it might take some time to reconfigure the RAN service chain during a functional split change. Specifically, we consider the functional split reconfiguration time (ms) as the interested KPIs. It is note that such reconfiguration time is dependent on platform, infrastructure and source/target split. Hence, our initial consideration focuses on the low-level RU-DU split running on the OAI platform under Intel x86 machines and USRP software-defined radio (SDR). More design details and the control mechanism can also be found in deliverable D4.1 [25].

3.2.1.5 Interactions between functional splits and transport technologies

Beyond the description of the aforementioned components, here we extend the view on validating how SDN-enabled wireless transport technologies address the requirements of different RAN functional splits, like the ones introduced in the previous sections. More specifically, we assume a heterogeneous wireless transport network, where network devices are SDN enabled. The considered wireless technologies comprise: (i) Typhoon 60 GHz modules, and (ii) IEEE 802.11ac-based wireless devices. Wireless devices are controlled through an SDN controller developed in the 5G-XHaul project [1]. These technologies will be leveraged to understand how wireless transport may impact the performance of different RAN architectures. The insights obtained in the aforementioned components will be used to pre-select the functional splits that are more likely to function properly over a wireless transport. The considered functional splits will be instantiated using the OAI platform. The findings of this investigation will be fed back to the RAN control function that dynamically configures RAN functional splits, to be able to account for the impacts introduced by wireless transport technologies. In order to evaluate the impact of wireless transport on RAN functional splits we will consider both transport level KPIs (delay and jitter) and access level KPIs (e.g., user throughput), as detailed in deliverable D4.1 [25].

3.2.2 Functions related to transport slicing

When looking at transport slicing, 5G-PICTURE adopts the three main attributes for the new transport network as defined in the Third Network vision and strategy launched by the Metro Ethernet Forum (MEF) [36]:

- Agile: the service providers' operational environment needs to be agile to achieve accelerated time-to-market for new service introduction.
- Assured: the network as a service has to assure security and consistent performance.
- Orchestrated: dynamically and automatically manage the entire lifecycle of connectivity services.

Thus, 5G-PICTURE will pursue solutions that enable the MEF vision of Agility/Assurance/Orchestration in three transport domains, namely Optical, Packet and Wireless.

These three domains have been chosen for the following reason. There is a clear industry trend to consolidate services around packet-based transport solutions based on Ethernet. Hence, 5G-PICTURE cannot ignore developments in this domain. On the other hand, placing orchestration and slicing capabilities directly at the optical layer holds the potential to maximise efficiency and performance, hence we also investigate in this domain. We see the packet and optical domains as complementary, with packet-based solutions taking the role of evolutionary technologies, which can be easily deployed in the field, and the intelligent optical technologies taking the role of a more revolutionary, thus longer-term solution. Finally, wireless transport is a key enabler of massive deployments of Small Cells, which are required to reach the area capacities promised by 5G, and hence also required from intelligence and slicing capabilities.

The technical approaches 5G-PICTURE pursues in each transport domain are the following:

- Optical Transport Network Slicing: In 5G-PICTURE TSON is implemented on FPGA platforms described in deliverable D3.1 [20] with advanced optical components to enable high performance transparent networking. Each TSON node provides interfaces for the different resource domains such as wireless, PON, and DC. A TSON node is controlled by an SDN controller which is associated with an OpenFlow agent able to program it. In addition, the TSON node is able to classify the data traffic according to a VLAN tag, allowing network slicing. As a result, the SDN controller programs the TSON node to provide end to end network traffic slicing.

  Figure 3-21 shows the TSON system configured with the FPGA platform and the applications that can control the communication with the SDN controller and orchestrator. The SDN agent application running on the server operating system controls the TSON hardware by receiving and sending extended

OpenFlow protocol messages to the SDN controller. The received instructions from the controller are translated and are sent to the TSON hardware. The extension of the OpenFlow protocol is necessary to allow the controller the support the TSON features. The TSON hardware implemented on the FPGA platform receives and sends the configuration parameters and status by using Programmed input/output (PIO) interfaces over the PCIE bus. The agent running on top of the TSON hardware can communicate with the controller through the network interface on the Network Interface Card (NIC) installed on the TSON system server.

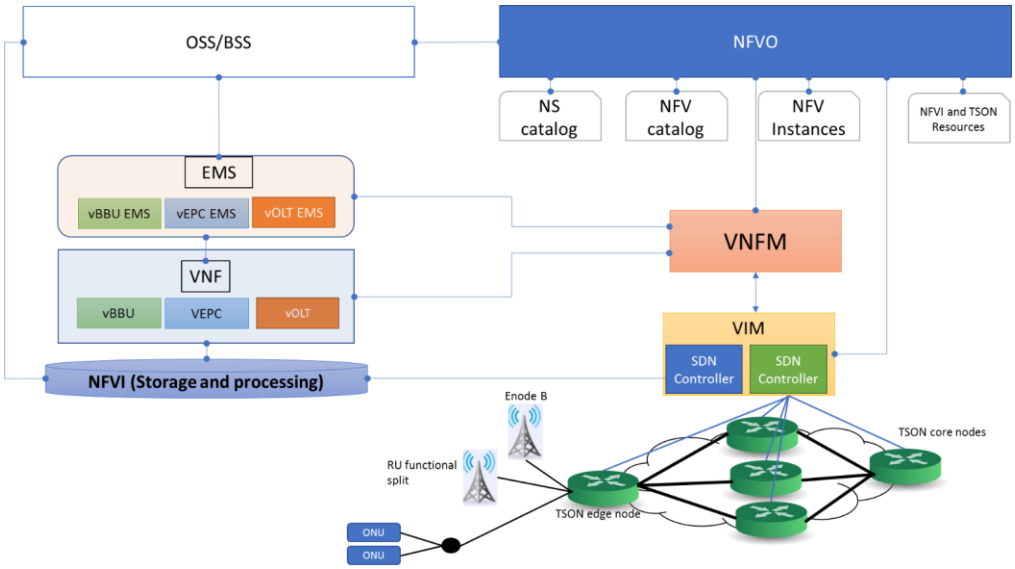

Figure 3-21: TSON Technical approach based on ETSI NFV and SDN.

TSON offers a hierarchy of three levels of resource granularity: connections, frames, and time-slices. The TSON nodes also adopt the wavelength selective architecture to direct the incoming optical time-sliced stream towards the destination output port, as defined by the controller. TSON can increase its flexibility and scalability by making programmable the frames, the number of time slots, the time slot duration, the time slot allocation, the time slot interface mapping, and wavelength. Network slicing in the optical transport via TSON is handled by classifying the traffic data according to the VLAN tag. In this case, each slice of the network should be encapsulated in the VLAN tag. For example, in the 5G-XHaul project, this encapsulation is handled by an orchestrator running on the top of the SDN controller of each area. This orchestrator has knowledge of the end-to-end topology and the right VLAN tags that need to be to set before the data traffic is transported within a specific area.

- Ethernet transport networks: The technical approach we are considering combines the notion of Interface Slicing (hard slicing) together with Logical Network Slicing (soft slicing):

Interface Slicing: In 5G-PICTURE, we will thoroughly investigate through testbed experimentation the Flex-E and the X-Ethernet technologies as a means to realize interface slicing and fast switching respectively. Flex-E will be studied and evaluated as a key technology that is able to split a physical interface into isolated sub-channels, decouple MAC rate from PHY rate and achieve “hard” bandwidth isolation. X-Ethernet technology introduces Ethernet PCS switching, eliminates table lookup and buffer queuing and will be investigated as a fast switching mechanism that is exploiting PCS layer relay. Furthermore, Ethernet TSN FUSION technology will be investigated as a layer-2 technology for achieving “hard” slicing and QoS isolation in Ethernet networks. Aggregation of lower bitrate Ethernet client channels (i.e. slices) into a common Ethernet line-side channel (i.e. interface), as well as switching of these, will be investigated. Furthermore, statistical multiplexing of dynamic bandwidth channels of lower priority (soft slicing) with the “hard” slice channels within the same Ethernet interface will be investigated.

Logical Network Slice: Customised logical networks (VPN-based) can be created based on the demand of service/tenant. Computation of network topology and the required resources for network slice needs to be allocated by the orchestration/management and control systems. These are also responsible to allocate sliced network resources from the network infrastructure, and to associate dedicated resources with the logical network slice.

- Multi-tenant Small Cells with integrated Access and Backhaul (IAB): 5G-PICTURE aims to develop novel technologies that support the massive deployment of outdoor small cells required to fulfil the 5G promises on capacity. In this regard, 5G-PICTURE puts forward the concept of multi-tenant small cells with IAB support. The proposed technology will allow a 5G-PICTURE operator that manages a small cell deployment in an urban scenario, to dynamically instantiate virtual networks on behalf of its tenants (i.e. MNOs). The MNO's customers will be able to discover the virtual access network, connect to it without the intervention of the 5G-PICTURE operator, execute handovers between the tenant's virtual small cells, and have their traffic transported until the tenant's home network, where appropriate billing and services can be applied.

The interested reader is referred to section 4 of deliverable D4.1 [25] for a description of the technology components that will be designed to pursue the previous technical approaches:

3.2.3 Synchronisation functions

Figure 3-22 depicts the vision of 5G-PICTURE towards an integrated multi-domain synchronisation. The approach adopted relies on the concept of a synchronisation harmonizer in the control plane, namely an entity that has views on the different synchronisation domains, such as the one proposed in [37].

Timing support needs to be available in all transport nodes along the network, but with different error contributions. The harmonizer ensures that the path (highlighted) introducing the minimum total node processing error is used. The architecture requires the specification of the communication interfaces between the harmonizer and the nodes, especially in the way the existing IEEE 1588 management interface is exploited.

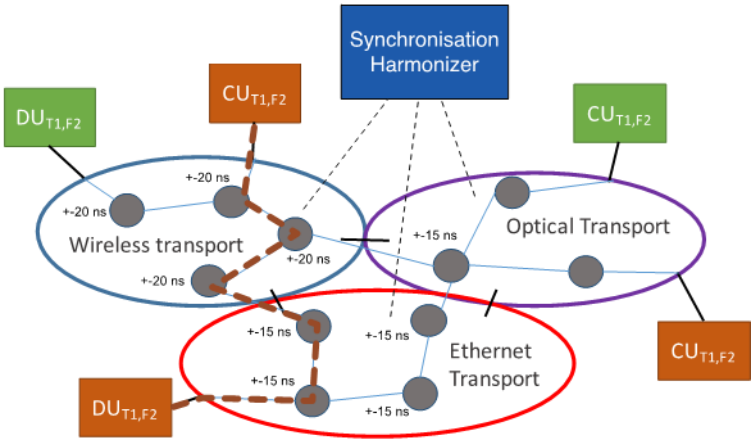

Figure 3-22. Harmonizer with knowledge of synchronisation features along the 5G-PICTURE network.

The following technical approaches will be pursued to bring about the previous vision:

- A framework for Synchronisation "as a Service": In the context of 5G-PICTURE networks, where heterogeneity and flexibility are key aspects, it is attractive to rely on a synchronisation harmonizer in the control plane which can therefore choose the best path and devices to rely synchronisation messages.
- Synchronisation over 5G-PICTURE transport technologies: The given control plane infrastructure automates the provision of synchronisation services in the context of a highly-heterogeneous and dynamic network, such as the 5G-PICTURE transport network. Building on this infrastructure, a further objective is to develop the necessary mechanisms for end-to-end multi-domain synchronisation support for transport networks within specific technology domains that have not been traditionally used for this purpose. For example, the Precision Time Protocol (PTP) messages exchange and relevant optimizations over 60 GHz (IEEE 802.11ad) mesh nodes, Sub-6 GHz wireless (IEEE 802.11ac) nodes and Flex-E are investigated.

The interested reader is referred to section 5 of deliverable D4.1 [25] for a description of the technology components that will be designed to pursue the previous technical approaches.

3.3 5G Operating System Concept

The 5G PICTURE project proposes a programmable network to fulfill the KPIs and requirements of the 5G vision described in detail in Section 2. Some of the building blocks required to implement a programmable network have already been presented in Section 3, namely:

1) Programmable Data Plane.
2) VNFs/PNFs.

This section describes the remaining important components of a programmable network:

1) components that perform control and orchestration of these resources so that they can be shared between service users,
2) have ability to supporting multiple function splits and being able to choose between them,
3) a set of consistent APIs that provide access to underlying shared heterogeneous resources via the above components, and
4) patterns of interaction between components via APIs to translate a 'service' request (for example as defined by ITU-T: Massive Machine-Type Communication, Ultra Reliable Low Latency Communication and Enhanced Mobile Broadband) into provisioned resources.

A 5G infrastructure consists of heterogeneous physical and virtual resources. Resources include network as well as compute and storage resources, supporting different technologies, e.g. optical network, MPLS, etc. Service providers and their end users benefit from the large-scale heterogeneous resources but should not have to deal with the complexities of managing and operating them. 5G-PICTURE Operators and infrastructure providers also need appropriate tools for efficient management of their resources and handling the requests from their customers. Moreover, well-defined interfaces required to deal with different types of resources are needed to unify the distributed, heterogeneous resources into a common 5G infrastructure that can host different services.

This arrangement closely resembles a computer OS where device drivers implement a specified API. These drivers are provided by the manufacturer to access virtual and physical resources (such as network interfaces, storage and graphics). Above these drivers, we have a layer of OS components that interface with the device drivers (via southbound OS-specific API) and provide aggregated, easier-to-use, vendor-agnostic northbound APIs for the OS and third-party programs. Virtual machines (VMs) further extend this concept by providing a standard environment to a program, irrespective of the underlying OS being used (write once, run anywhere) [10][12].

To abstract the complexities of the underlying 5G infrastructure and to provide the common functionalities required for efficient and flexible service and slice management and orchestration, we propose the 5G OS. In short, 5G OS will **abstract** and **manage resources** of a 5G system – in complete analogy to an ordinary OS. The 5G-PICTURE architecture includes 5G OS at its core. The same set of functional abstractions are present in 5G OS as described for a computer OS. Figure 3-23 provides a mapping between a computer OS and 5G OS.

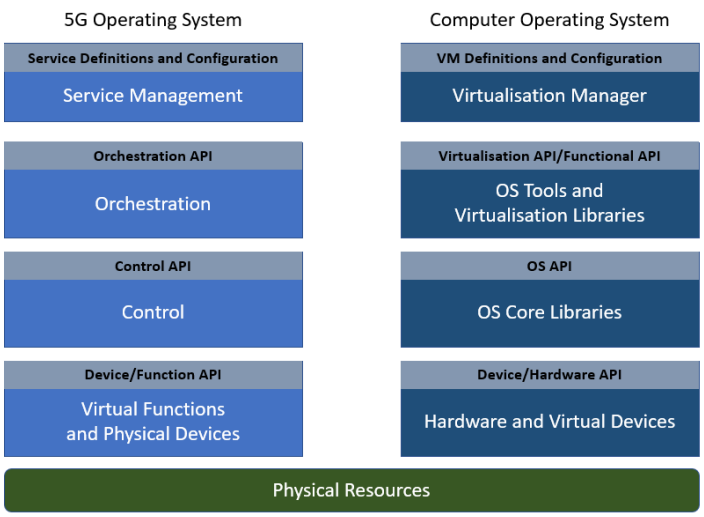

Figure 3-23: Comparison between layers of a computer OS and 5G OS.

Programmable Data Plane components, VNF providers, and PNF providers offer APIs using standard interfaces such as OpenFlow, NETCONF, RESTCONF, SNMP and OVSDB. These interfaces provide access to the underlying resources such as flow tables, ports, as well as QoS and device data such as configuration, monitoring, statistics, and management.

The layer of controllers sits above this and is equivalent to the OS core libraries that provide easy-to-use access to underlying resources. They also abstract any differences. For example, installing flows on an OpenFlow switch could vary from vendor to vendor, depending on things like OpenFlow version, coverage and hardware limitations. But the well-defined interface provided by the controllers can minimize the impact of this variance by providing generic and device/vendor-specific data models.

Similarly, for VNFs the providers use standard packaging and descriptors so that these can be deployed on third-party infrastructures (e.g., by using the virtual machine concept). This makes the VNFs controllable and manageable via a well-defined interface irrespective of the vendor of the VNF.

Once there is a standard mechanism to access and request for resources, orchestration components can be layered on top. These represent OS programs, tools, utilities and virtualization libraries that work on top of the control layer and use or provide access to underlying resources employing abstract components. For example, a virtual machine library provides access to underlying vendor-specific hardware in terms of abstract components such as vCPUs, memory and storage. For the network, abstract components could be at the node level, such as “OpenFlow Switch” and “Router” or at the function level, such as “Mux/Dmux” and “Flow Table”. The Device/Function API layer also takes important decisions regarding placement of abstract components and resource guarantees that can be provided. An example from a virtual machine is when a user asks for 10GB of storage and there are multiple disks available including a mix of technologies like solid-state and mechanical. Several decisions need to be taken, e.g., what is the optimal mapping? How does this change when another user requires specific guarantees with respect to minimum read/write times?

At the highest level, a service management component is required to provide information on the types of available services, tools for requesting services, deploying custom services, or extending existing services. Such a component is analogous to a virtual machine manager/web interface in a computer OS.

Each of these 5G OS components are discussed in detail in the following sections, after an overview of the definitions and the assumptions used for describing 5G OS.

3.3.1 Definitions

3.3.1.1 Domains

Given the versatility of resources in a 5G environment and the multiplicity of stakeholders processing, operating, or consuming these resources, the term “domain” may mean different things, subject to the specific 5G deployment. NGMN [13] and subsequently 5G Americas [56] have defined various types of domains in terms of *technology* (wired/wireless network/cloud infrastructure domain), *administration rights* (administrative domain, operator domain, resource management domain), *network section* (access network and core network domains), etc.; the term *administrative domain* has also been used by 3GPP [15] to define a set of resources managed by a single operator.

Taking into account existing work and terminology while considering the 5G-PICTURE architecture, in the context of 5G-PICTURE, we refer to a group of resources having the same technological specifications as a *technological domain*; i.e. RAN, transport, core network, cloud setup can be considered as different technological domains. Moreover, different resources may be subject to different usage and operational rules and policies; i.e. administrative policies. We refer to a group of resources under the same administrative policies as an *administrative domain*; e.g., a cluster of wireless access resources administered by a single operator or provided to tenants/end-users under a common policy can constitute a wireless access administrative domain).

3.3.1.2 Network Slicing

The standard abstraction of functions used in 5G OS at the user level is that of a network slice. The following description from NGMN provides a good definition of a “network slice instance” [13]: *a set of network functions, and resources to run these network functions, forming a complete instantiated logical network to meet certain network characteristics required by the Service Instance(s)*.

- A network slice instance may be fully or partly, logically and/or physically, isolated from another network slice instance.
- Resources comprise both physical and logical resources.

- A Network Slice Instance may be composed of sub-network Instances, which as a special case may be shared by multiple network slice instances.
- The Network Slice Instance is defined by a Network Slice Blueprint.
- Instance-specific policies and configurations are required when creating a Network Slice Instance.
- Examples for network characteristics are ultra-low latency, ultra-high reliability, etc.

A Network Slice instance may also be classified based on the capabilities/rights the 5G-PICTURE Operator (i.e. the Slice Provider) provides to the 5G-PICTURE Tenant (i.e. the Slice Consumer) who requests the slice. The Tenant may or may not be the End User of the services provided by the Network Slice. 3GPP provides such a classification of capabilities [15]:

1. Monitoring only. The Slice Provider offers only means to monitor the slice KPIs as agreed in the contract. Network slice configuration is chosen from a catalogue of ready-made slice templates. Accesses via dashboard-like web service and/or northbound interfaces provided by the Slice Provider.
2. Limited control to Slice Consumer to perform design and composition of network slice. Slice Consumer can change configuration of deployed network functions and/or onboard own certified network functions into Slice Provider's repository using interfaces provided by the Slice Provider.
3. Extended Control. In this case the Slice Consumer deploys and operates the network slice using its own MANO stack and Network Management System (NMS). The Slice consumer has tight control over its own network functions and services while has limited control over MANO network functions.

The Monitoring Only version is a 'degenerate' slice and represents a Network Service. Extended Control version is the other end of the spectrum and provides a fully controllable slice. Extended Control will allow the Tenant to further slice their network slice instance to provide to their End Users.

Each network slice instance is based on a Network Slice Definition. The Network Slice Definition provides the following pieces of information (depending on what type of slice instance is required):

1. Topology definition (Nodes, Links and Ports).
2. Specifications for Nodes, Links and Ports which includes implementing VNFs, binding information and constraints (e.g. link latency and bandwidth).
3. Required resources (abstract definition).
4. Other slice definitions that it depends upon.

Network Slice Definitions can also be "templatized" whereby Network Slice instantiation is simply a question of selecting the template and specifying its values.

Network resource slicing has been extensively addressed by 3GPP specifications, even if not all aspects have been finalized yet (see [15][11],[56],[57],[58],[59]). Leveraging on existing work, the resources disaggregation concept of 5G-PICTURE goes beyond the network slice model to a more general resource slicing one, especially addressing compute/storage resources slicing or utilizing compute/storage resources to realise network slicing.

Given the different administrative and technology domains present within most networks along with reliance on external infrastructure providers, network slice instances should not be monolithic entities. Furthermore, as networks are dynamic, the problem of optimising/maintaining a set of monolithic network slices that are competing for finite resources across the different network layers is not a trivial problem.

This problem can be simplified by creating a network slice instance interconnecting a number of smaller slice instances, interconnected with each other. In NGMN [13] these are referred to as "Sub-Network instances". A complete network slice instance is created by stitching together one or more of these instances. In 5G-PICTURE we refer to the complete slice as an **end-to-end slice** and to the constituent instances as **sub-slice** instances, in order to include also the compute/storage resource slice instances. With respect to the end-to-end slice, the constituent slices are referred to as sub-slice instances. This also allows sub-slices provided by third-party Infrastructure Providers to be used. For example, a storage service provider could provide a sub-slice which contains functions related to storage (e.g. databases). The storage sub-slice can then be utilized by the Operator to provide services to their Tenants.

In this scenario, each sub-slice instance should have a management component. Composing an end-to-end slice instance from sub-slices also avoids having single points of failure. Sub-slice instances that go down can either be re-provisioned or replaced with another sub-slice. Sub-slice sharing between Slice instances can

also provide an additional level of optimization, especially in parts of the network that are resource-constrained.

3.3.1.3 Physical Network Functions and Network Function Virtualization

A Network slice instance may consist of Nodes and Links that are directly implemented over physical devices. In this case the physical device may be sliced or fully assigned to the Slice Consumer. As an extension to the PNFs, Programmable PNFs behave like specialised devices that provide a programmable interface (for example P4: https://p4.org). This allows custom hardware to provide standard interfaces.

The Network slice instance may also be implemented using virtual functions (fully or partially). Instead it may be implemented using one or more VNFs. Network Function Virtualization (NFV) involves converting physical network functions such as switching and routing into software components that can be run on commodity hardware. NFV is achieved using the following components [11][17].

Infrastructure Resources: Heterogeneous hardware and necessary software for hosting and connecting network functions. They include computing hardware, storage capacity, networking resources (e.g., links and switching/routing devices enabling network connectivity), and physical assets for radio access.

Network Functions Virtualization Infrastructure (NFVI): A collection of infrastructure resources used to host and connect the VNFs.

Virtual Network Functions (VNF): Software-based implementations of NFs that run over the NFVI.

Management and Orchestration (MANO): Performs all the virtualization-specific management, coordination, and automation tasks in the NFV architecture. The MANO framework comprises three functional blocks:

Virtualized infrastructure manager (VIM): responsible for controlling and managing the NFVI resources.

VNF manager (VNFM): performs configuration and life cycle management of the VNF(s) on its domain.

Orchestrator: According to ETSI, it has two set of functions performed by the Resource Orchestrator (RO) and Network Service Orchestrator (NSO), respectively:

Resource Orchestrator (RO): orchestrates the NFVI resources across (potentially different) VIMs.

Network Service Orchestrator (NSO): performs the life cycle management of network services using the capabilities provided by the RO and the (potentially different) VNFMs.

VNFs have the same requirements as their physical counterparts. For example, a VNF OpenFlow Switch (e.g. OpenvSwitch) will need a controller.

3.3.1.4 Multi-Version Service Chains

Different resources of the 5G-PICTURE infrastructure are suitable for different service requirements. For example, a VNF deployed as a VM on a general-purpose hardware has different performance and cost characteristics compared to the same function deployed using special-purpose programmable hardware. A service element (e.g., a VNF or an application component) that can be deployed on different resource types can react efficiently to dynamic load situations and service-level requirements. This requires different (software) versions of the service element to be developed and implemented.

An interesting use case for 5G OS is controlling and orchestrating such multi-version services, consisting of chains of multi-version service elements. Based on the pre-defined objectives for service performance and resource utilization, the best composition of multi-version elements can be selected and mapped to the resources. An important example is deriving the optimal functional splits for the segmented RAN processing, as described in Section 3.2.1.1. Depending on the scenario and service requirements, 5G OS can select, instantiate, monitor, and adapt the functional splits.

Mapping service requirements to such a diverse set of resources and infrastructure capabilities requires awareness of the existing supply of compute, storage and network resources, as well as information on the elasticity of these resources. Elasticity refers to the costs and feasibility of modifying, creating, or re-allocating such resources. Using this information, optimal decisions can be made regarding the level of application split, allocation of compute and storage resources, and connectivity. This is not a trivial problem given that the resource availability requirement for dynamic and new services must not allow to disrupt existing already provisioned services.

3.3.2 Use cases for 5G OS

This section provides an overview of the major use-case categories for Tenants and Operators that are related to the 5G OS operation. These use cases will be refined further in the context of WP5.

3.3.2.1 Use cases for 5G-PICTURE Operator

The 5G-PICTURE Operator is the stakeholder practically operating the 5G-PICTURE solution/framework, and having access to the HW/SW pool of resources so as to enable (instantiate) the dynamic provisioning of infrastructure resources to various Tenants based on their needs and requirements. The role of the 5G-PICTURE Operator can be undertaken either by the infrastructure owner(s), such as by a MNO, a private 5G network owner (e.g. Stadium owner), or by a third party having access to Infrastructure Providers' resources under specific agreement (terms and conditions). Therefore, as shown in Figure 3-24, the 3GPP identified phases of the network slice lifecycle are considered:

- Preparation phase.
- Instantiation, Configuration and Activation phase.
- Run-time phase.
- Decommissioning phase.

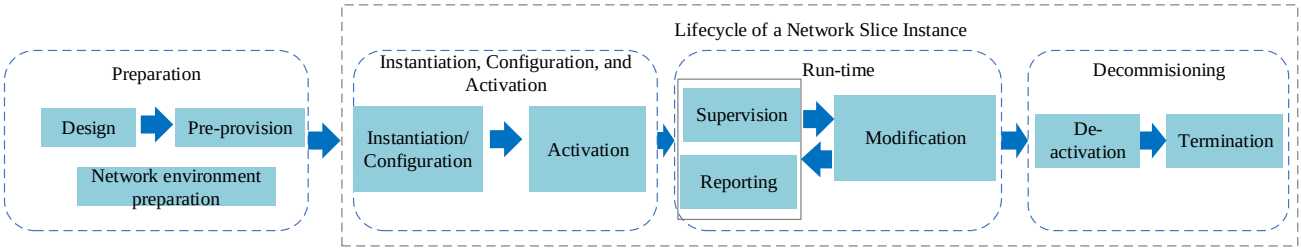

Figure 3-24: Lifecycle phases of a Network Slice.

From another perspective, the use cases for an Operator can be organised into three groups:

1. **Use cases related to slice definition policies:** These use cases refer to the definition and provisioning of slices, where specific policies need to be defined including policies of accepting/satisfying service requests, mapping resource types to tenants (or tenant classes) towards satisfying the requested Service Level Agreements (SLAs), pre-defined Slice categories, etc.
2. **Use cases related to slice deployment.** These use cases refer to the deployment of the slices with regard to function deployment and management, including the deployment of a single or a chain of functions as well as using external Infrastructure Providers. They refer also to the setting up of connectivity between data centers as well as between specific PNFs and to sub-slice connectivity. Connectivity requests also contain constraints related to connecting slices/sub-slices with specific service delivery end-points (e.g. ports and encapsulation virtual interfaces).
3. **Use cases related to SLA maintenance.** These use cases refer to the lifecycle management of slices and the assurance of the QoS delivered over them, so that it complies with the guaranteed SLAs.

3.3.2.2 Use cases for 5G-PICTURE Tenant

Considering the 5G-PICTURE Tenant, the main use cases are related to the (a) Creation, (b) Update and (c) Release of a Slice, depending on the service/business model and privileges that the Tenant has been granted by the 5G-PICTURE Operator. As a degenerate case example, slice creation may just involve instantiating a template with some configuration with the resulting slice not offering any control API to the End User. At the other end slice creation may involve creation of control, management and configuration endpoints along with the virtual network – to provide full control to the requester (e.g. in cases where requestor wants to run their own controller).

3.3.3 5G OS Architecture

Figure 3-25 shows an overview of the 5G OS architecture [73], consisting of different functional components, the high-level interfaces among them, as well as the underlying 5G infrastructure resources. Components shown with a gray background are not of direct relevance to the project and therefore, they are not described in detail in this document.

The components of the 5G OS are organised in a hierarchical manner, propagating service and slice management requests towards the actual infrastructure. A request for instantiating, managing, or modifying a slice or a service enters 5G OS via the following components:

- Service Portal, which is used by 5G-PICTURE tenants for requesting and managing services offered by 5G-PICTURE Operators.
- Business/Operation Support System (OSS/BSS), which are used by 5G-PICTURE operators for managing resources and services on top of the infrastructure offered by Infrastructure Providers. Also, used by Infrastructure Providers for requesting and managing slices they provide to their customers.

Figure 3-26 provides an instance of the 5G OS Architecture mapped to Domains. These components may be under different administrative domains with different business and management policies. They offer different interfaces to the corresponding stakeholders.

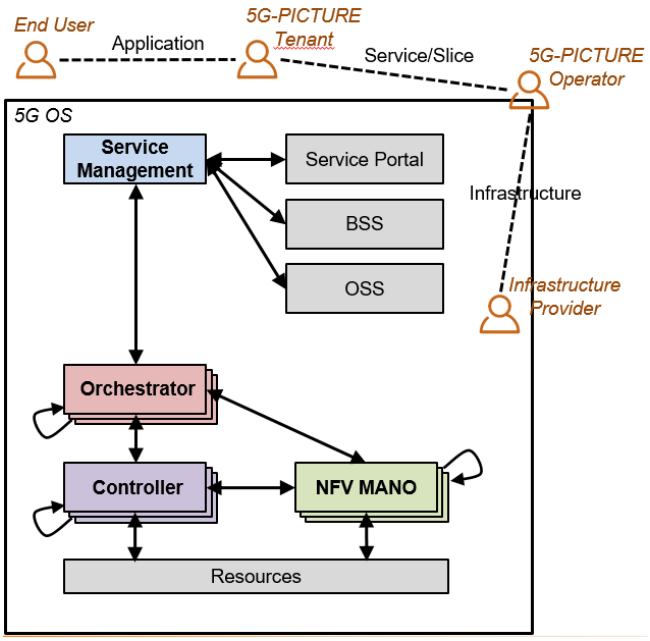

Figure 3-25: 5G OS High-Level Architecture.

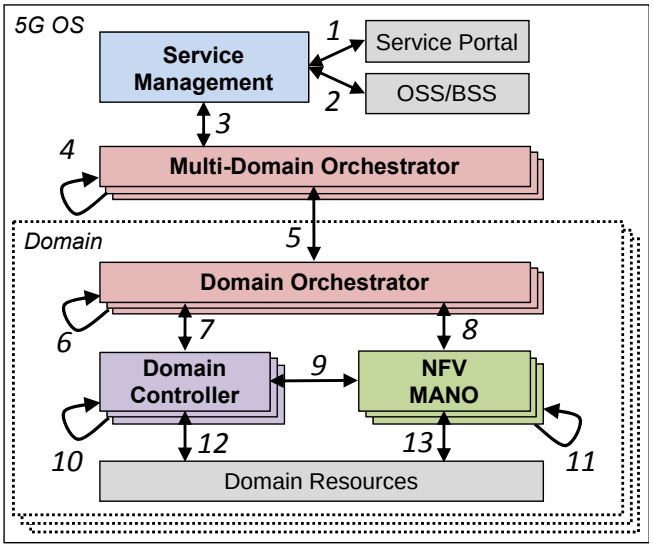

Figure 3-26: 5G OS Interfaces of Interest.

3.3.3.1 Service Management

The interactions between Service Portal or OSS/BSS and the rest of 5G OS happen via the Service Management component, using interfaces labeled as 1 and 2 in Figure 3-26.

The Service Management component converts high-level requests of the aforementioned stakeholders into requirements in terms of resources and slices. For example, by mapping service-level requirements in terms of latency, capacity, functionality to concrete service descriptors, which in turn consist of connectivity and function descriptors. Different versions of the Service Management component can be deployed by different operators, as part of a new 5G OS instance.

Each instance of the Service Management component is responsible for Fault, Configuration, Accounting, Performance and Security (FCAPS) management of slices and maintaining SLAs in its corresponding responsibility area. It converts high-level requests of stakeholders into requirements in terms of resources/slices with embedded functions and connectivity. Additionally, in a domain-based deployment, the Service Management component is responsible for making the initial service placement decisions by interacting with and selecting from the instances of Multi-Domain Orchestrators (MDOs) it is integrated with. The placement calculation takes the current resource availability into account and, ideally, does not degrade the performance and quality of existing services. The information required for solving such a multi-objective optimization problem is provided to the Service Management components via interface 3 from MDO components.

3.3.3.2 Orchestrator

An Orchestrator component (Figure 3-25) links between a Service view and a Resource view. Depending on the deployment scenario, the component can provide different services, but the primary task of the Orchestrator remains to map from a Service to a Resource. The Orchestrator is not responsible for directly accessing the infrastructure. It should make use of a programmatic API defined by the Controller and MANO components that abstract out the resources in terms of Functions (PNF and/or VNF) and Connectivity between them.

If the Service is to be deployed over multiple domains, then

1) each domain must have at least one Domain Orchestrator (DO) (see below), and
2) each Domain Orchestrator must be associated with at least one MDO (see below).

The interfaces of interest are:

1) Service Management <-> Orchestrator (for Domain Model this includes Service Management <-> MDO and MDO <-> DO interfaces) [SM-Or].
2) Orchestrator <-> Controller (for Domain Model this corresponds to DO <-> Domain Controller interface [Or-Co].
3) Orchestrator <-> MANO (for Domain Model this corresponds to DO <-> MANO interface) [Or-MANO].

3.3.3.3 Multi-Domain Orchestrator (MDO)

When a network is divided into multiple domains, MDOs are responsible for lifecycle management decisions of compute, storage, and network resource slices that span across multiple technological and/or administrative domains [53]. Each MDO has information about the set of existing slices and can request instantiation, modification, or termination of slices within the domains it is responsible for. The way a request from a Service Management component is delivered to MDO instances is related to the realisation of the interaction among MDOs, represented by interface 4 in Figure 3-26. This interface can be realised in different ways. For example, MDO instances may have a hierarchical relationship in which the highest MDO in the hierarchy receives the requests and distributes it to other instances [55]. Alternatively, the MDOs may have a peer-to-peer relationship where different MDOs can communicate and cooperate directly, in case a request cannot be fulfilled by them individually [54]. Within the 5G-PICTURE project, we are investigating the best option for realising interface 4.

Via interface 5, each MDO instance can receive information from a group of DOs it is associated with, and can request lifecycle management operations from each DO for the corresponding parts of end-to-end slices that are under the responsibility of that DO.

3.3.3.4 Domain Orchestrator (DO)

Each DO is responsible for compute, storage and network slice lifecycle management decisions within a certain technological or administrative domain. DOs abstract away the differences in these domains and expose a uniform interface to MDOs for requesting and managing the resources from different domains. Similar to the inter-MDO interactions, inter-DO interactions via interface 6 can also be realized in different ways (e.g., hierarchical, peer-to-peer, etc.), which also affects the data and control flow among DOs as well as between DOs and MDOs.

DOs break the slice specification into concrete actions to be performed on top of networking resources and compute and storage resources, by creating connectivity descriptors and (virtual/physical) function descriptors out of the service descriptor that DO has received from upper layers of 5G OS. Via interface 7, DOs interact with the Domain Controller component(s), responsible for controlling the network resources, including (programmable) PNFs. Via interface 8 DOs can interact with NFV MANO component(s), responsible for managing and orchestrating compute and storage resources. DOs are also responsible for maintaining information about existing services and slices within the domain under their control.

3.3.3.5 Controller

The Controller component in Figure 3-25 is responsible for providing programmatic access to the network and to provide resources to the Orchestrator. The interface of interest here is the Controller ↔ Orchestrator and the Controller ↔ Controller (in both peer-to-peer and hierarchical approaches). The specific interfaces and their functions will depend on the specific deployment and the concerned domains. For example, for larger networks or those providing public-safety communications, the Controller ↔ Orchestrator interface may be used to provide robust radio access resources, reliable communication links and a highly available transport network. Moreover, for a deployment with different network technologies, there may be a specific controller per technology (e.g., optical, Layer 2, Layer 3, etc.), and/or per vendor that is connected to each other in a peer-to-peer model in order to jointly control the network. For instance, RAN-domain controllers between different vendors can exchange information for communicating and coordinating spectrum sharing decisions between geographical regions to avoid interference. In contrast, the interface between controllers can follow a hierarchical approach in which one or more controllers are connected to a Master Controller. Considering the RAN and Core Network (CN) domain for instance, a joint control decision can be made to allocate the same amount of maximum capacity for both radio air and BH interfaces, i.e. between user and BS and between BS and gateway (GW). Another example would be two same domain controllers but they operate on different time scales. For example, a centralised controller at the CU can allocate the applied spectrum and bandwidth in a larger time scale (e.g. in second level), while the distributed controller at the DU can schedule the radio resource in a smaller time scale (e.g. at a millisecond level). It is noted that these two relations can be combined into hybrid models. For example, peer-to-peer with certain peers acting as interface nodes with other components such as Controller Applications and master-slave where Slaves have 'local' responsibilities (see European FP7 FLEX[2] and H2020 COHERENT[3] projects).

Note that the Master Controller can provide the required resource view to the Orchestrator. We acknowledge that there is an element of orchestration involved for the Controller ↔ Master Controller interaction for internal co-ordination between the Controllers. However, it should not influence the Orchestrator ↔ Controller interface which is mainly used to request resources in terms of Network Functions, either virtual or physical (VNF/PNF), and their connectivities. Furthermore, the Controller ↔ Controller interface is highly domain-specific and difficult to be standardized as it may be used to exchange a wide variety of information, including but not limited to:

1. State: Controller or module state that can be used for life-cycle management.
2. Status: Specific user or tenant status that can be utilized for monitoring or control.
3. Control: The control decision or delegation to be applied for one or more targets. Such target can belong to: either a particular technical domain, or a specific vendor, or a registered tenant/user.
4. Configuration: Include a set of arrangements in Controller-specific form, which can map generic setting to vendor/technology specific configuration.

[2] http://www.flex-project.eu/

[3] http://www.ict-coherent.eu/

3.3.3.6 Domain Controller

Each domain controller can provide connections and network resources across its specific domain. Different domain controllers might be required inside one domain, e.g., when there are multiple technologies such 4G and Wi-Fi, each requiring their own network controller. Interface 10 in Figure 3-26 among different domain controllers can be implemented in different ways, as discussed for interface 4 and 6. Domain controllers use interface 12 to directly control and manipulate the underlying infrastructure.

3.3.3.7 Network Function Virtualization Management and Orchestration (NFV MANO)

In Figure 3-26 the NFV MANO component provides virtual functions to the Orchestrator component. The MANO <-> MANO interface is required for resilience, high availability as well as for optimisation. The optimisation case is where a set of MANO components can interface with each other to optimally allocate the VNFs or deeper within the stack a NFV MANO stack can talk to multiple VIMs.

3.3.3.8 MANO Domain View Network Function Virtualisation Management and Orchestration (NFV MANO)

NFV MANO manages and orchestrates the virtualized service elements. For example, each NFV MANO instance can calculate the placement for a specific VNF or scale it if necessary within the resources that are available to it. For simplicity, we do not show the details of the MANO system but we assume a model compatible with the architecture defined by the ETSI NFV Industrial Specification Group (ISG) [19]. Multiple instances of the NFV MANO component might be required within one domain, e.g. to cover multiple geographically distributed data centers. Interface 11 is used for the interactions among different NFV MANO instances, which may follow different models. Via interface 13, NFV MANO instances do the actual resource allocation to service elements.

Interface 9 stands for the interactions among the domain controller and the NFV MANO instances. Defining this interface and the relationship among these components is a challenging task we are tackling towards the implementation of the 5G OS. ETSI NFV Industry Specification Group (ISG) has provided recommendations for roles of SDN controllers in an NFV ecosystem [17]. In this document, the resources that can be controlled by an SDN controller are defined as physical/virtual switches and routers, softswitches, as well as switches and routers implemented as VNFs. For example, depending on the scenario, 5G OS may need to deal with one of the following cases, which require different interfaces and control flows between the domain controller and NFV MANO:

1. SDN controller as an underlay network controller [ETSI case 5], controlling the physical or virtual infrastructure that serves the components on top of the virtual infrastructure. This implies that for managing a slice or a service, the domain controller decides about network resource allocation and instructs the NFV MANO to use the compute and storage resources corresponding to this allocation, for instantiating the service entities.
2. SDN controller as a VIM [ETSI case 1 and 3], controlling the internal network of an infrastructure node (e.g. a data center). This means the NFV MANO instructs the domain controller to create the required network paths after the placement of service entities is calculated.

3.3.3.9 Requests/Responses across the Interfaces

Figure 3-27 summarises the high-level requests and replies exchanged among the stakeholder and the major components of 5G OS.

3.3.1 Cross Cutting Concerns

There are multiple cross cutting concerns that are independent of a specific component. These need to be supported by every component for the whole system to work.

3.3.1.1 Logging

Logging is a fundamental requirement both in terms of FCAPS tracking and general serviceability. A standard logging framework should allow for remote storage of logs including the ability to integrate using different methods such as file-based logging, syslog, etc. Given that most of the required components presented in this document will not be developed from scratch, the extent to which logging is supported will vary.

3.3.1.2 Resilience

Each of the proposed component implementations selected may provide resiliency mechanisms. These will have to be utilised or further developed on a case-by-case basis. For this we envisage some form of East-West API that will allow transfer of state from failing components to active ones.

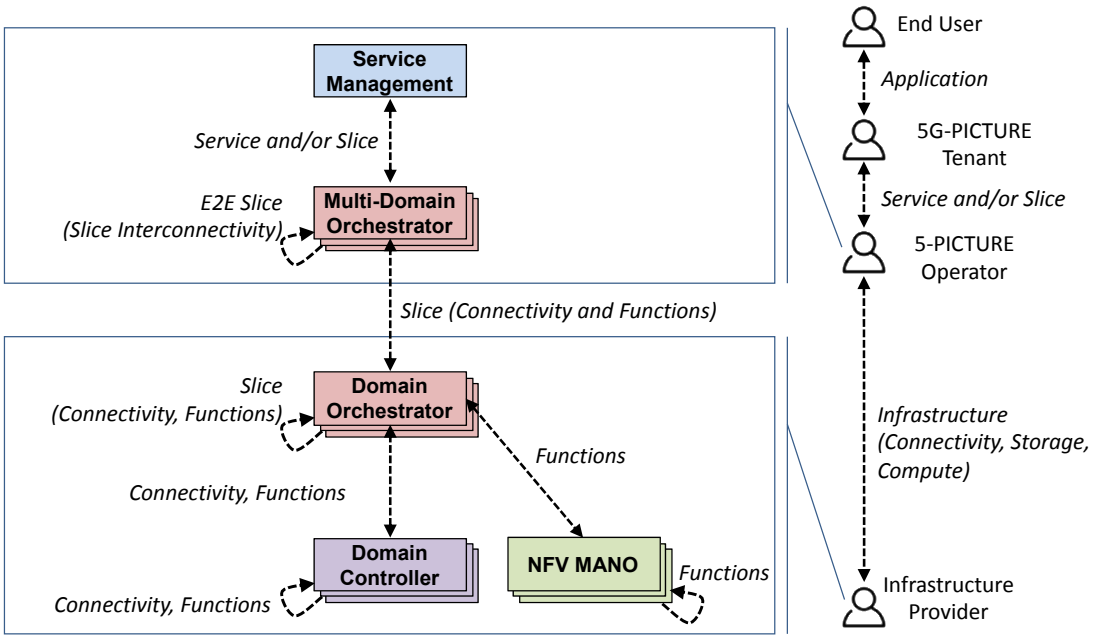

Figure 3-27: Interactions of 5G OS components and stakeholders.

3.3.1.3 Monitoring

Monitoring is a fundamental requirement. This not only includes monitoring the health of resources, slices, sub-slices, but also providing this information in the right format and at the right level of detail for the various actors using/responsible for the system. As an example: a physical link (e.g. an optical fibre) may be sliced at various levels (lambda per slice, using encapsulation, time slots, etc.). A failure at this level may impact one or more sub-slices which, in turn, may affect multiple slice instances and disrupt services for Tenants and End Users. At the level of the Tenants and End Users the failure must be appropriately mapped to their context as the Tenant may not be aware that there is a fibre link involved in the slice. Similarly, to enable tracking of SLA violations, a slice instance must be monitored as a separate entity (as separate SLAs may be involved) even though it may be using shared sub-slice instances.

3.3.1.4 Configuration

Each component will require a configuration mechanism to install and integrate the component with the rest of the system.

3.3.1.5 Resource Availability

Each component will control a set of resources. These may be physical resources such as servers, links, switches, routers or virtual such as CPU, Memory and Flow Space; or abstract such as a generic 'topology' with generalised nodes and links. To enable hierarchy of components and abstraction, there needs to be a well-defined mechanism to list, request, configure and release resources.

4 Preliminary Architecture Evaluation

This section of the deliverable focuses on the evaluation and benchmarking of the proposed 5G PICTURE architecture. To perform this task, different consortium partners have started developing suitable evaluation tools that involve a set of mathematical models, simulation frameworks as well as experimental platforms. These are currently being extended, analysed and tested in order to facilitate a more complete and thorough study of the overall project architecture. In this deliverable we provide our initial evaluation tools as they have been developed in the first year of the project, and a set of scenarios and use cases that have been defined and analysed using these tools.

In view of this, the first part of the architecture evaluation focuses on the scalability analysis of the data and control planes proposed by the generic 5G-PICTURE architecture. In terms of data plane scalability the topics/scenarios considered include: scalability analysis of the BBU processing chain, DA-RAN over elastic optical networks, integration of WDM-PON and mmWave technologies and associated trade-offs, investigation and proposal of suitable approaches to enable scalable service chaining in MEC-assisted 5G Networks, suitable solutions for scalable optimisation exploiting Artificial Intelligence (AI), and finally scalable multi-service placement.

The second part of the evaluation targets some initially defined rail vertical use cases and their evaluation. These use cases focus on the following topics: 5G communications to trains and the adoption of Sub-6 GHz LTE Massive MIMO technologies, multi-technology access network solutions in railway systems and the benefits these can provide, how IoT can be efficiently supported in a rail use case adopting the concept of disaggregated 5G networks and, finally, an initial control plane scalability analysis specifically tailored to a the rail environment.

4.1 Scalability of data and control plane

In the present section, a preliminary evaluation of the 5G-PICTURE solutions in terms of power and resource efficiency is provided. This assessment involves:

- Analysing the processing requirements of the BBU processing chain as a function of the network load. This analysis is used as input in the remaining analysis to determine the computational resources that should be allocated for the provisioning of the FH service chain.
- Quantifying the benefits that are expected in future 5G-RAN deployments by the joint consideration of elastic optical networks and modular DC platform, which are key building blocks in DA-RAN environments. This approach is compared against the traditional RAN and C-RAN approaches showing significant benefits.
- Identifying the coordination, sharing and scalability gains expected in DA-RAN environments where regional compute (MEC) and central cloud cooperate to jointly provide FH and BH services.
- Identifying the optimal selection of wireless and optical transport network technologies that can be deployed in 5G networks for the provisioning of FH services. We show that through the optimal combination of these technologies significant energy savings can be achieved leading to a sustainable 5G solution.
- The development of scalable optimisation techniques for 5G systems based on AI techniques. We show that AI-control and management systems are able to identify the optimal operational parameters of the 5G systems with reduced complexity compared to traditional approaches.

The performance of these schemes is examined over realistic topologies using actual traffic statistics.

4.1.1 Scalability analysis of BBU processing chain

To identify the processing requirements of the BBU chain we used WiBench, an open source suite for benchmarking wireless systems and Intel's VTune Amplifier 2018, a performance profiler for software performance analysis. WiBench provides various signal processing kernels. These kernels are configurable and can be used to build applications to model wireless protocols. The LTE uplink used for the experiments is provided by the WiBench suite and VTune is used to profile the LTE applications. For more details the interested reader is referred to [91]. A summary of the functions that the BBU processing comprises is presented below. This includes:

- The Single Carrier Frequency Diversity Multiple Access (SC-FDMA), which is a precoded Orthogonal Frequency Diversity Multiplexing (OFDM). It is preferred over OFDM for the uplink transmission since it is less susceptible to frequency offsets and has a lower Peak-to-Average Power Ratio. The SC-FDMA Demodulation function removes the Cyclic Prefix (CP) and performs N-point FFT.

- The Sub-carrier Demapper, which extracts the data and the reference symbols from the subframes.
- The Frequency Domain Equalizer, which estimates the CSI by the received pilot signal through the Least Square estimation algorithm. It computes the channel coefficients with the help of CSI, and equalizes the received data using as equalizer a zero forcing MIMO detector in the frequency domain.
- The Transform Decoder that performs M-point Inverse Fast Fourier Transform (IFFT).
- The Constellation Demapper, who receives the signal and extracts the binary stream by generating Logarithmic Likelihood Ratios (LLRs).
- The Descrambler that descrambles the input sequence.
- The Rate Matcher that separates the input stream into R, where R is the Channel Code Rate, de-interleaves each code stream and removes redundant bits. For our experiments R was constantly set to 3.
- The Turbo Decoder that takes soft information for each code, in our case LLR, and it applies iterative the Soft-Input Soft-Output (SISO) algorithm. The Turbo Decoder consists of two SISO decoders that perform the trellis traversal algorithm, and one interleaver/deinterleaver. A higher number of iterations leads to a higher computation cost but achieves improved error correction performance. For all the experiments that were conducted the number of iterations was set to 5.

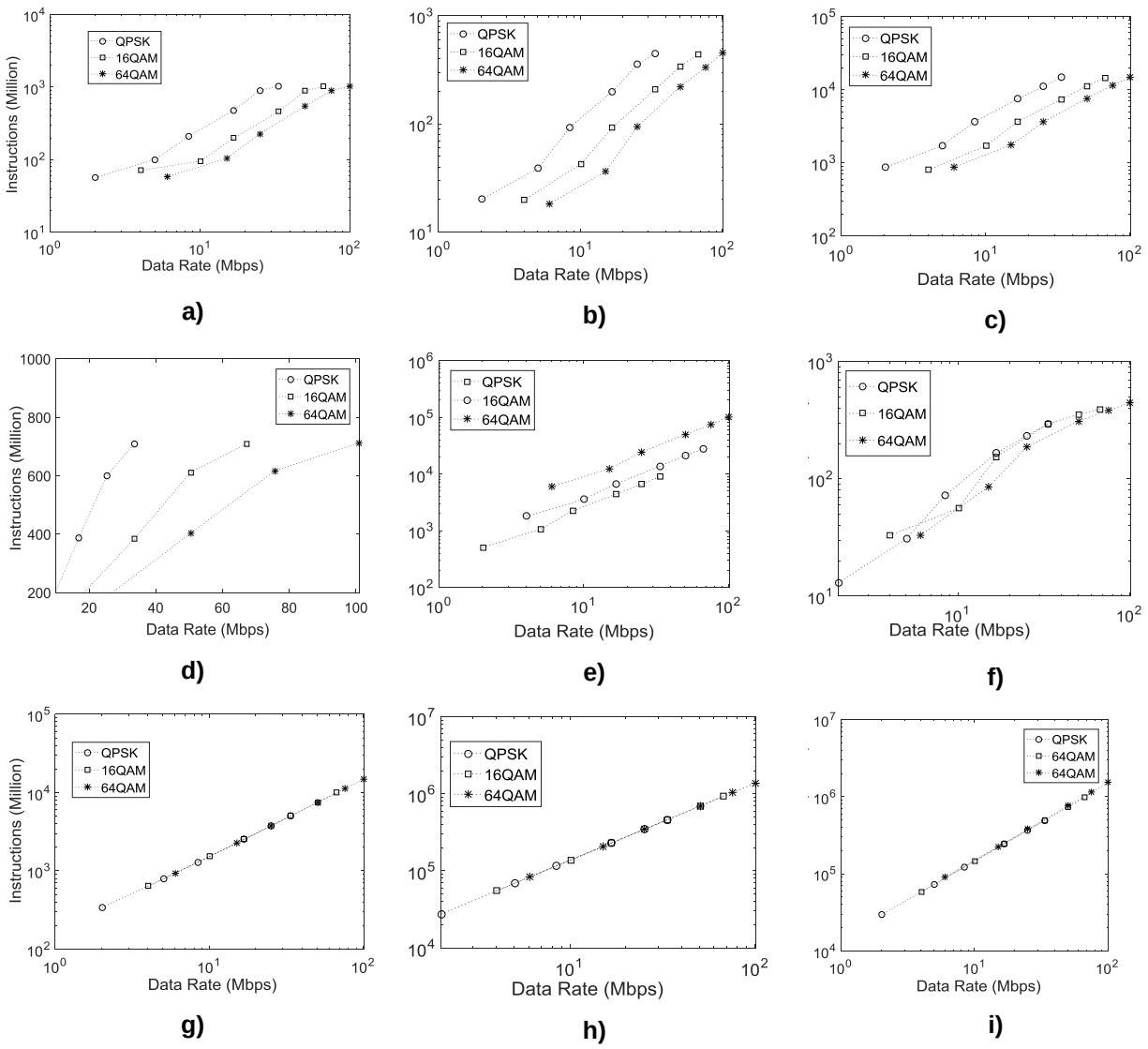

Figure 4-1: Instructions per signal processing function under various data rate for a) SC-FDMA Demodulation, b) Subcarrier Demapper, c) Equalizer, d) Transform Decoder, e) Demodulation, f) Descrambler, g) Rate Matcher, h) Turbo Decoder, and i) Total Instructions.

To increase the statistical validity of the results produced by the profiler, a high number of iterations were performed (1000 subframes). The set of experiments carried out was aiming at exploring the behavior of each processing function for different configurations of the LTE uplink system. In [91] we present the instructions performed to process 1000 subframes by each function as a function of the data rate for different modulation schemes.

Taking into consideration the variance of the measurements we can conclude that all functions present a linear dependence with the data rate. On the other hand, the influence of the modulation scheme on the number of instructions differs for each function. More specifically we observe that the modulation scheme does not affect the instructions number for SC-FDMA Demodulation, Sub-carrier Demapper, Equalizer, and Transform Decoder. For the Constellation Demapper an exponential dependence of the modulation scheme is observed, while the Rate Matcher and the Turbo Decoder exhibit linear dependence.

We observe that the Turbo Decoder performs higher number of instructions, especially as the data rate increases; while the Constellation Demapper, the Rate Matcher and the Equalizer perform fewer instructions. This means that the Turbo Decoder, who requires 1 to 4 orders of magnitude more instructions compared to other functions, determines by large the total number of instructions needed to process a subframe and how this number depends on the data rate and the modulation scheme.

4.1.2 Data plane analysis: DA-RAN over elastic optical networks

We consider an elastic optical network interconnecting RUs with compute resources supporting both BH and FH services. A key design aspect is related with the placement of the BBU functions with respect to the RUs. In addition to this, to relax the stringent delay and synchronisation requirements of existing FH protocol implementations, the concept of functional split processing is adopted. We assume that the remote BBU processing resource pool comprises both GPPs and SPPs hosted at regional or mobile edge DCs supporting processing of the FH functions. Therefore, in addition to the optimal split selection, mapping of FH functions to suitable GPPs/SPPs within the DC is part of the optimisation process. For additional detailed information on this work at the interested reader is referred to [92].

For the optical metro network the TSON is considered, while for the compute/storage (intra-DC) network we consider a standard switch-based topology interconnecting compute/storage resources, where switch layers form a hierarchical networking model. Switches are organised in a simple tree topology, although more sophisticated structures, e.g. fat trees, can be also adopted. A simple hierarchal network interconnecting GPPs and SPPs is shown in Figure 3-3.

To maximise the converged 5G infrastructure energy efficiency, a two-stage optimisation for the wireless/optical and the intra-DC network domains is proposed. In the first stage, the optical transport network provisioning problem is formulated so as to identify the necessary optical network resources for the interconnection of the RUs with the DCs. Then, a second sub-problem linked to the allocation of the FH functions to the disaggregated pool of compute/storage resources is provided. To achieve this, once the FH data reach a DC hosting the candidate pool of resources, a path interconnecting the edge DC node with the GPP/SPP modules (which process the remaining FH functions) is established. The order of FH functions processing is defined by the corresponding SC shown in Figure 3-1. The modelling details are shown in Table 4-1. In the first sub-problem, constraints related to flow (1.1), transport network capacity (1.2), split processing (1.3), RU demand (1.4) and BBU processing (1.5)-(1.8) are introduced. For the intra-DC network we include constraints related to parallel processing of the BBU functions (2.1)-(2.2) and their associated communication requirements (2.3)-(2.4).

The proposed optimisation scheme is evaluated using the optical network shown in Figure 4-2 (a), which covers a 10x10 km^2 area with 50 uniformly distributed BSs. RUs demands are generated according to real datasets [23]. Based on the compute resource type and location the following cases are examined:

i) “Traditional-RAN (T-RAN)”: In this scheme, RUs and BBUs are co-located and FH service processing is carried out exclusively by SPPs. Sharing of BBUs between multiple RUs is not supported and BBUs sizing is performed based on worst case traffic statistics. The power consumption per RU ranges between 600 and 1200 Watts under idle and full load conditions, respectively.

ii) “C-RAN with fixed transport”: This scheme allows BBUs to be instantiated as virtual functions and run on GPPs enabling resource sharing and on-demand compute resource resizing to match the FH service requirements. This approach involves higher per giga operation processing cost (GOPS) at the GPPs compared to SPPs (i.e. 2W/GOPS vs 1.2W/GOPS)). Optical network resources are allocated with the granularity of the wavelength (fixed wavelength grid case) and the optical frame.

iii) “C-RAN with elastic transport”. This scheme offers the flexibility to assign compute resources on

demand exactly as in case (ii) "C-RAN with fixed transport", but enhanced with an elastic optical network solution allowing varying time (optical frames) and elastic spectral allocation capabilities.

iv) "Disaggregated-RAN (DA-RAN)": This novel scheme combines the benefits of D-RAN and C-RAN allowing FH functions to be processed either at SPPs or GPPs based on their specific characteristics. Through this approach, intensive FH functions can be performed at SPPs (ASICS) hosted at the DCs, whereas the remaining functions are instantiated on shared GPPs. An elastic optical transport network solution is also proposed.

Table 4-1: Problem Formulation: DA-RAN over elastic optical networks.

SP 1-Optical Transport Network: Objective: $\min F_1 = \sum_{r\in \mathbf{R}} \mathcal{E}_r \left(\sum_{i\epsilon\Sigma} p_{ri}^{RU}\ \sigma_{ri}\right) + \sum_{e\in \mathbf{E}}\ \mathcal{E}_e\ C_e$			
$\mathbf{R}, \mathbf{D}, \mathbf{E}, \boldsymbol{\Sigma}$	RUs, DCs, Optical Links Split Option Set	P_d, P_r	Total processing capacity of DC $d \in \mathbf{D}$, RU $r \in \mathbf{R}$
$\boldsymbol{p_{rd}}$	Paths interconnecting RU r to DC $d \in \mathbf{D}$	h_r	t network requirements of RU r
$H_{ri}, p_{ri},$	Network, processing requirement of RU r under split option $i \in \boldsymbol{\Sigma}$	δ_{erp}	Binary coefficient taking value 1 if link $e\epsilon\mathbf{E}$ belongs to path p realizing traffic generated at the RU r
p_{ri}^{RU} , p_{ri}^{d} ξ_e , C_e	Local, remote (at DC $d \in \mathbf{D}$) processing requirements of RU $r \in \mathbf{R}$ under split option $i \in \boldsymbol{\Sigma}$. Capacity, cost of link $e\epsilon\mathbf{E}$	σ_{ri} , a_{rd}	Binary variable equal to 1 if split option $i \in \Sigma$ is adopted. Binary variable taking value equal to 1 if $d \in \mathbf{D}$ hosts the BBU SC (or some of its parts) of $r \in \mathbf{R}$
u_{rp}	Binary variable forcing a single flow to be transferred from RU r over a single path $p\epsilon\mathbf{P}_r$, $\mathbf{P}_r = \cup\, \boldsymbol{p}_{rd}$		
Constraints: (1.1). $\sum_{p\in\mathbf{P}_r} u_{rp} = 1,\ r\epsilon\, \mathbf{R}$, (1.2) $\sum_{r\in\mathbf{R}} h_r \sum_{p\in\mathbf{P}_r} \delta_{erp} u_{rp} \le C_e,\ e\epsilon\, \mathbf{E}$, (1.3) $\sum_{i\epsilon\Sigma} \sigma_{ri} = 1,\ r \in \mathbf{R}$ (1.4) $h_r \sum_{i\epsilon\Sigma} H_{ri}\sigma_{ri}$, $r \in \mathbf{R}$, (1.5) $\sum_{i\epsilon\Sigma} p_{ri}^{RU}\sigma_{ri} \le P_r,\ r \in \mathbf{R}$, (1.6) $\sum_{r\in\mathbf{R}} \sum_{i\epsilon\Sigma} p_{ri}^{d}\ \sigma_{ri} \le P_d,\ d \in \mathbf{D}$, (1.7) $\sum_{d\in\mathbf{D}} a_{rd} \le 1,\ r \in \mathbf{R}$, 1 $p_{ri}^{RU} + \sum_{d\in\mathbf{D}} a_{rd}\, p_{ri}^{d} = p_{ri},\ r \in \mathbf{R}, i \in \boldsymbol{\Sigma}$			
SP 2-Optical Transport Network: Objective: $\min F_2 = \sum_{k\in\mathbf{M}^d} \mathcal{E}_k \left(\sum_{r\in\mathbf{R}} \sum_{i\epsilon\Sigma} \sum_{\varphi\in\mathbf{FH}_{ri}^d} p_\varphi\ a_{\varphi\kappa}\right) + \sum_{e\in\mathbf{E}^d} \mathcal{E}_e\ C_e$			
$\mathbf{M}^d$, $\mathbf{E}^d$	Set of processing modules, inter-DC links of DC $d\epsilon\, \mathbf{D}$	$\zeta_{e\varphi p}$	Binary coefficient taking value 1 if link $e\epsilon\mathbf{E}^d$ belongs to $p\epsilon\boldsymbol{p}_{\varphi km}^d$ interconnecting modules k and m
$\mathbf{FH}_{ri}^d$	Ordered set of remaining FH functions for RU $r \in \mathbf{R}$ under split $i \in \Sigma$	$\boldsymbol{p}_{\varphi km}^d$	Set of paths interconnecting module $k\epsilon\, \mathbf{M}$ hosting function $\varphi \in \{1, \dots, FH_{ri}^d - 1\}$ to module $m \in \mathbf{M}$ hosting function $\varphi + 1$ of the FH SC at DC $d \in \mathbf{D}$
Constraints: (2.1)$\sum_{k\in\mathbf{M}^d} \boldsymbol{a_{\varphi\kappa}} = \mathbf{1},\ \varphi \in \mathbf{FH}_{ri}^d,\ r \in \mathbf{R}, \boldsymbol{\Sigma\ i\ \epsilon, d\epsilon}\ \mathbf{D}$, (2.2) $\sum_{r\in\mathbf{R}} \sum_{i\epsilon\Sigma} \sum_{\varphi\in\mathbf{FH}_{ri}^d} \boldsymbol{p_\varphi\ a_{\varphi\kappa}} \le \boldsymbol{P_k}$, (2.3) $\sum_{\boldsymbol{p}\in\mathbf{P}_{\varphi k}^d} \boldsymbol{u_{kp}} = \mathbf{1},\ \ \boldsymbol{\varphi\ \epsilon\ 1}, \dots, \boldsymbol{FH_{ri}^d - 1}, k\epsilon\, \mathbf{M}^d, d\epsilon\, \mathbf{D}$, (2.4) $H_{k\varphi} = H_{ri+1},\ \boldsymbol{k\ \epsilon M^d}, \varphi \in \mathbf{1}, \dots, \boldsymbol{FH_{ri}^d - 1}, r\epsilon\, \mathbf{R}, i \in 1, .., \boldsymbol{\Sigma - 1}$, (2.5) $\sum_{r\in\mathbf{R}, i\in\boldsymbol{\Sigma}, k\in\mathbf{M}^d} \sum_{\varphi\in\mathbf{FH}_{ri}^d} H_{k\varphi} \sum_{p\in\mathbf{P}_{\varphi k}^d} \zeta_{e\varphi p} u_{kp} \le C_e$			

Figure 4-2 (b) illustrates the impact of traffic load on the optimal split option for the cases under consideration. As can be seen, "elastic C-RAN" providing improved network efficiency performs optimally for lower split options (more remote processing) than "C-RAN". This trend is further emphasised in "DA-RAN", offering both improved network and compute resource efficiency through resource disaggregation. Figure 4-2 (c) shows the total infrastructure power consumption with load for the schemes under consideration. The DA-RAN approach outperforms all alternative approaches. The benefits of the DA-RAN is attributed to its sharing gains both in space and time domains due to its flexible and on demand resource allocation capabilities. DA-RAN minimises overprovisioning requirements present in the alternative approaches leading to 10-50% power consumption savings.

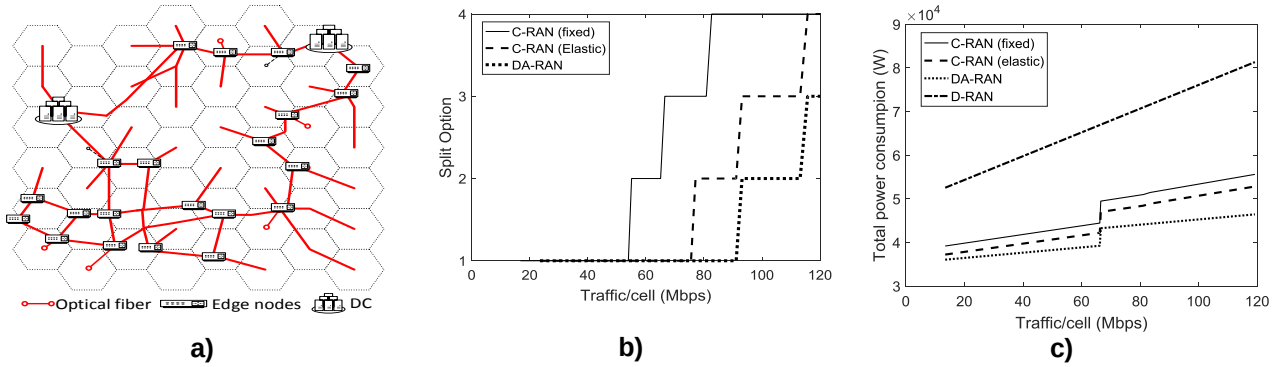

Figure 4-2: a) The Bristol is Open city test bed, b) functional split vs network load, c) infrastructure power consumption.

4.1.3 Data plane analysis: Integration of WDM-PON and mmWave

We consider a multi-technology network infrastructure deploying a set of optical and wireless network technologies to interconnect the RUs with the compute resources. Backhauling of the RUs can be provided either through a set of microwave links or through WDM-PON. In addition, an active optical metro solution is considered aggregating traffic demands generated at the RUs, to provide the necessary capacity for the interconnection of more remote compute resources [92]. Similar to the previous problem set up, the concept of functional split is also adopted. A schematic diagram of the data plane architecture under consideration is illustrated in Figure 4-3.

We consider again a two-stage optimisation problem for which the first stage problem focuses on the joint optimisation of converged 5G infrastructures in terms of CApital Expenditures (CAPEX) and OPerational EXpenditures (OPEX). To minimise CAPEX, initially, the network design problem is formulated to identify the optimal transport network technologies that can be used in support of the operation of the RUs. Once the network design problem has been formulated a second problem linked to the operation design is provided. To keep the analysis tractable, it is assumed that the optical metro network (location of the optical nodes, fibres and RUs) is kept fixed. Thus, the topology design problem is limited to the transport network interconnecting RUs with the aggregation network. The first stage problem is divided into two-subproblems:

(a) Sub-problem 1.1 (SP1.1): Transport Network design.

This subproblem aims at minimizing the total cost for the installation and operation of the transport network capacity from the RUs to the edge nodes. Two options are considered. The first assumes that RUs are interconnected to the metro/optical network using mmWave links while the second relies on the deployment of PONs. For the equipment and installation costs of both technologies (i.e. mmWave tower, optical equipment, fibre trenching costs, etc.), the values reported in [95] have been adopted assuming linear fibre installation costs increase with distance. For microwave links these costs remain almost constant as they primarily depend on initial tower set-up costs. Despite the initial high installation cost of optical technologies their daily operational costs are lower compared to mmWave due to their much lower power consumption.

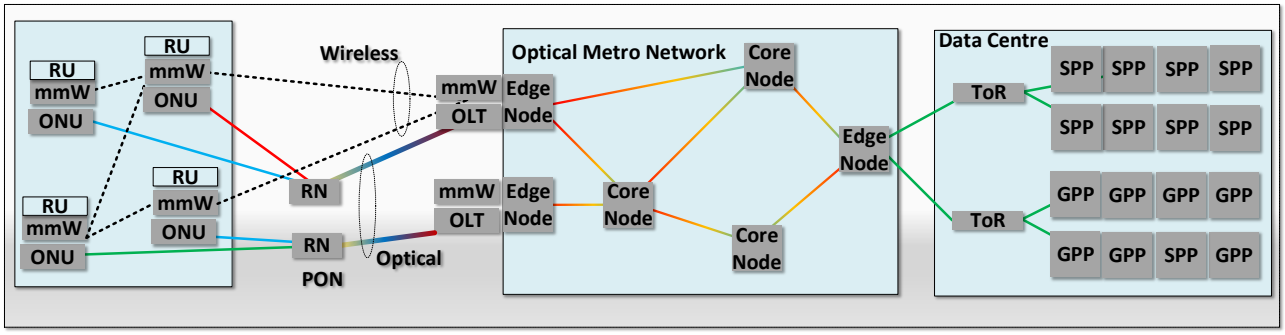

Figure 4-3: Multi-technology network infrastructure.

(b) *Sub-problem 1.2: Operations optimisation.*

The second sub-problem tries to identify the optimal split option and the location of the DCs where the BBUs are processed, so that the total power consumption of the resulting network infrastructure is minimised. The capacity network and processing requirements of each split option are considered in the analysis.

The second stage-problem identifies the optimal processing modules where the remaining parts of the FH service have to be allocated. Once FH data reaches a DC hosting the candidate pool of resources, a path interconnecting the edge DC node with the GPP/SPP modules that will process the remaining FH functions is established. Again, the order of FH functions processing is defined employing the concept of SC. We assume that each function forming the FH SC can be processed either at a single or multiple processing units. The decision to parallelise a function depends on its speed-up factor measuring how much faster a function can be executed when processed in parallel by multiple processing units. The objective of the second stage problem is to identify the optimal degree of parallelisation of each function and the server where each function is hosted to minimise power consumption at the CUs.

The proposed optimisation scheme is evaluated over the Bristol is Open (BIO) topology. In the numerical results, it has been assumed that OPEX is associated with the power consumption and has been converted to monetary values by multiplying with 0.02r.u/ kWh. Our results in Figure 4-4 a) show that, when RUs are fully backhauled through microwave technologies, the total CAPEX and OPEX is high due to the relatively high-power consumption levels of mmWave links, but the increase of WDM-PON penetration reduces the total cost due to its energy efficient operation. However, exceeding a specific number of RUs backhauled by WDM-PON, leads to an increase of the total CAPEX and OPEX due to the significant fibre optical trenching costs. The impact of the WDM-PON penetration of the resulting split option is shown in Figure 4-4 b). It is shown that for low values of WDM-PON penetration, high values of split options (light CPRI flows) are preferable as the operational cost for transporting heavy CPRI flows over microwave is high. On the other hand, an increase in the penetration of WDM-PON results to an increase of the transport network capacity of the converged network infrastructure allowing the selection of bandwidth demanding split options (e.g., split options 1 and 2). Finally, the impact of the BBU function parallelisation on the total power consumption of the converged network in shown in Figure 4-4 c). For high volume of traffic demands, the parallel processing approach that multiple SPPs/GPPs process in a parallel fashion the BBU functions outperform the pipeline case where each function is assigned to a specific SPP/GPP. Parallelisation of BBU functions (i.e. FEC, channel estimation, etc.) results to lower BBU processing times. Smaller processing times at CUs counterbalance the increase of FH flows transmission delays enabling higher degree of consolidation. At the same time, the DA-RAN approach has lower network power consumption compared to the traditional D-RAN approach.

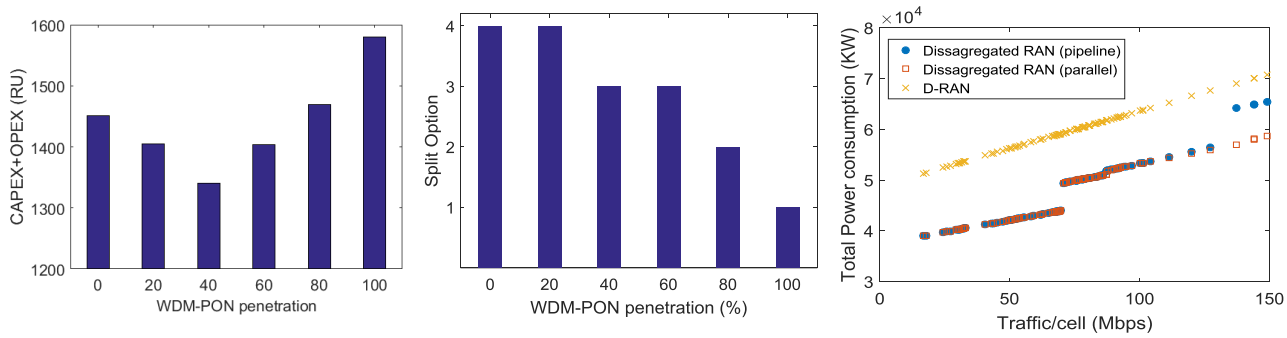

Figure 4-4: a) Total operational cost as a function of the percentage of RUs relying on WDM-PON transport, b) Split option as a function of WDM-PON penetration. b) Impact of processing parallelisation on split option, and c) power consumption.

4.1.4 Scalable Service Chaining in MEC-assisted 5G Networks

MEC has been proposed as an enabling technology to overcome the strict latency and processing requirements of 4G, and more recently, 5G mobile services. The key idea stems from the placement of servers with moderate storage and processing power either within the RAN or close to the mobile edge. This reduces the need for long-haul connectivity between end-devices and the central cloud [44]. This approach allows provisioning of a wide set of delay sensitive services including, location tracking, augmented reality content

delivery, video analytics, RAN-aware content optimisation, caching and application-aware performance optimisation [45].

In addition to these services, MEC can also facilitate the operation of 5G C-RAN networks. We know that C-RAN can be effectively used to manage dynamically changing traffic patterns and orchestrate terminals that vary in their requirements and services. However, it suffers several limitations, being the most notable the need for a high capacity transport network to support its FH requirements. For example, a C-RAN implementation of an LTE system with 100 Mb/s service rate requires a FH connection with 2.5 Gb/s rate. The concept of baseband processing split can address this limitation, at the cost of equipping the RUs with dedicated hardware to process a subset of the BBU functions, which reduces the flexibility of dynamic optimal split option allocation.

To address the relevant limitations we adopt a MEC-assisted 5G network architecture in which MEC servers are used to process low layer functions, while Central Cloud servers for the processing of the upper layer functions of the LTE protocol stack as shown in Figure 3-1.This architectural approach manages to simultaneously i) maximise the traditional C-RAN coordination and resource sharing gains, as processing is still performed by commonly shared compute resources and, ii) minimise the volume of traffic that traverses the metro/core network, releasing resources for other serviced (i.e., fixed).

Adopting this architecture, the problem of optimising the vBBU SC in large scale 5G networks needs to be addressed. In this context, we propose a Multi-Layer Integer Linear Programming (ML-ILP) formulation. However, this type of problems inherently suffers increased computational complexity. To address this issue, we propose the use of the Hierarchical Random Graph (HRG) theory [46]. Taking advantage of the hierarchical structure of the 5G communication and compute infrastructure, the HRG theory can be employed to generate simple tree topologies that reflect the statistical properties of the originally complex 5G infrastructure. Once HRGs have been created, the ML-ILP can be solved with significantly reduced complexity [93].

To this end, we consider a 5G network modelled as an undirected graph $G(n, E)$, with $n \in N, e \in E$ used to denote the set of nodes and links, respectively. In this network, vBBU SCs generated by a set $\mathcal{R}$ of R RUs are supported by a set of heterogeneous compute resources, located both at the edge (MEC) and at the metro/core (Central Cloud).

Let S^1 be the set of MEC and S^2 the set of central cloud servers, with $S^1, S^1 \subset N$. Connectivity between these two end-points is provided through a multi-technology transport network comprising point-to-point microwave links and optical network technologies. For the wireless transport we consider links operating in the Sub-6 GHz and 60 GHz frequency bands while, for the optical transport, we use WDM network platforms [6] combining both active and passive optical elements. Active frame based WDM optical networks offer very low latency, transparent synchronisation and service differentiation at the edge, while WDM-PONs are used for the interconnection of the RUs with the metro/core optical network and the BBUs [6].

Each RU SC assigns its lower BBU functions to the MEC and the remaining ones to the central cloud. Let $\Sigma_{r1}(\Sigma_{r2})$ be the processing requirements of the lower (upper) layer functions of RU $r \in \mathcal{R}$. This process can be optimised through the solution of the following nested ML-ILP problem:

$$\min_{\mathrm{x}_1 \in \mathcal{X}_1} f_1(\mathrm{x}_1) + \mathbb{E}\left[\inf_{\mathrm{x}_2 \in \mathcal{X}_{2(\mathrm{x}_1, \xi_2)}} f_2(\mathrm{x}_2, \xi_2)\right] \tag{4-1}$$

subject to network and capacity constraints, where

$$f_t(\mathbf{x}_t, \xi_t) = \sum_{s \in S^t} \mathcal{E}_{S^t}\left(\sum_{r \in R} x_{rst}\Sigma_{rt}\right) + \sum_{e \in E} \mathcal{E}_e\left(\sum_{r \in \mathcal{R}, s \in S^t, p \in P_{rs}} \delta_{ep} h_{\Sigma_{rt}}\right), t = 1,2 \tag{4-2}$$

is the cost function. The first term of (4-1) reflects the compute, while the second term the network cost for the processing of RU tasks either at the MEC (t=1) or at the central cloud (t=2). x_{rst} is a binary variable indicating whether RU r assigns its procesing tasks to server s or not. Network-related costs capture the costs for creating flows with rate, $h_{\Sigma_{r1}}$, transmitting the lower BBU functions Σ_{r1} from RU r, to the MEC (t=1) and, subsequently, flows with rate $h_{\Sigma_{r2}}$ from the MEC to the central cloud (t=2). P_{rs} denotes the set of candidate paths interconnecting RU r with a server $s \in S^t$ and δ_{ep} is a binary coefficient indicating whether link e belongs to path p or not. Although this formulation can successfully solve the service provisioning problem in MEC-assisted 5G environments, its computational complexity scales exponentially with the size of the network, thus making it

unsuitable for large optimisation scenarios. Addressing this, we propose a decomposition technique based on HRGs that reduces the computational complexity of the SC process.

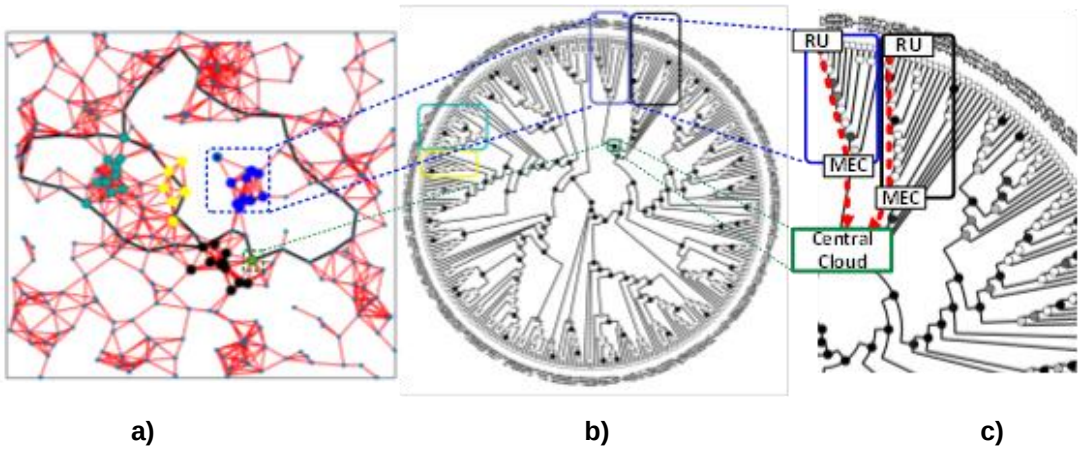

Figure 4-5: a) Network with 300 RUs. Black lines indicate optical ad red lines wireless links, b) HRG graph of the random topology in (a), c) vBBU SC in the HRG domain: RUs forward their low-level BBU functions to the MEC and then to the central cloud.

The rationale behind HRG-based SC is that the computational cost of embedding a SC into the network can be reduced if we manage to detect, in a cost-effective manner, a dendrogram that reflects with high probability the generic topological properties of 5G networks. This hierarchical structure can simplify the SC embedding process as it exposes to the ML-ILP problem a limited set of well-defined candidate paths that can support these flows. To apply HRG-theory in MEC-assisted 5G networks we rely on the following steps:

Step 1: 5G topology decomposition using HRG: 5G networks comprise access networks domains with densely interconnected devices (i.e., V2V, IoT, etc.) and metro/core optical networks with sparsely interconnected switches/routers. HRGs capture these properties through parameter, p_n, indicating the interconnection probability of any two nodes in the network. p_n takes high values in dense network domains (i.e. mmWave networks and PONs) and low values for optical nodes. Assuming that E_n is used to denote the number of ports at node n, C_n the capacity of the node, and R_n, L_n the number of ports of all nodes in the subtrees that are right and left, respectively, of node n, then, the likelihood of an HRG graph *D* is given by [46].

$$L(D, p_n) = \prod_{n \in D} p_n^{E_n/C_n} (1 - p_n)^{L_n R_n - E_n/C_n} \tag{4-3}$$

Equation (4-3) indicates that the connection probability of two nodes in the HRG increases with E_n/C_n (for higher values of E_n, the probability a randomly selected node to be attached to n increases. Similarly, the probability that a randomly selected node is directly attached to a high capacity node is very low, as their number is limited, e.g. the probability that an RU element (that is a very common element in 5G) is directly attached to a core optical node is low and reduces with $L_n R_n$. As $L_n R_n$ increases, the number of elements that are low in the hierarchy increase. It can be easily shown that (4-3) is maximised at $p_n^* = E_n/C_n L_n R_n$ taking values equal to $L(D, p_n) = \prod_{n \in D} p_n^{*\, p_n^*} (1 - p_n^*)^{C_n L_n R_n}$ or in log scale $\log L(D, p_n) = -\sum_{n \in D} C_n L_n R_n \, \mathcal{H}_n(p_n^*)$ where $\mathcal{H}_n(p_n^*)$ is the Shannon entropy function.

Step 2: Optimal Fitting of the HRG to the 5G network: Once the likelihood of the possible HRGs has been determined, a sampling technique based on the Markov Chain Monte Carlo (MCMC) approach can be applied. MCMC samples the candidate HRGs proportionally to their likelihood and identifies the HRG with the maximum $L(D, p_n)$ value [46]. The maximum likelihood HRG fits the real world 5G graph with high accuracy. An example of this process for a 300 node network depicted in Figure 4-5 a), is shown in Figure 4-5 b). Once fitted, the metro/core nodes appear high in the hierarchy of the generated HRG (close to the centre). On the contrary, terminal nodes (i.e., RUs) that are low in the hierarchy are embedded at the edge of the disk.

Step 3: Optimal Service Chaining in the HRG space: Once the 5G network has been decomposed into a hierarchical graph, a solution for the SC problem in MEC-assisted 5G environments can be obtained. The ML-ILP problem can be easily solved in the HRG space as the number of candidate paths that can support the

requested SCs get drastically reduced. At the same time, Central Clouds, which are directly attached to the core, have been placed close to the root of the HRG, whereas MEC servers have been embedded low in the hierarchy providing an intuitive solution to the problem (Figure 4-5 c)).

Step 4: Service re-provisioning: HRGs are updated frequently to better fit the topological changes of the 5G network (i.e. link failures, beam steering, mobility, insufficient capacity, etc.). Given that these topological changes are observed mostly at the edge, the likelihood of the updated 5G graph is very similar to the original one. Therefore, during the re-provisioning phase, MCMC samples only a small subset of graphs with likelihood values close to those of the original graph. Once the updated graph has been determined, Step 3 is executed.

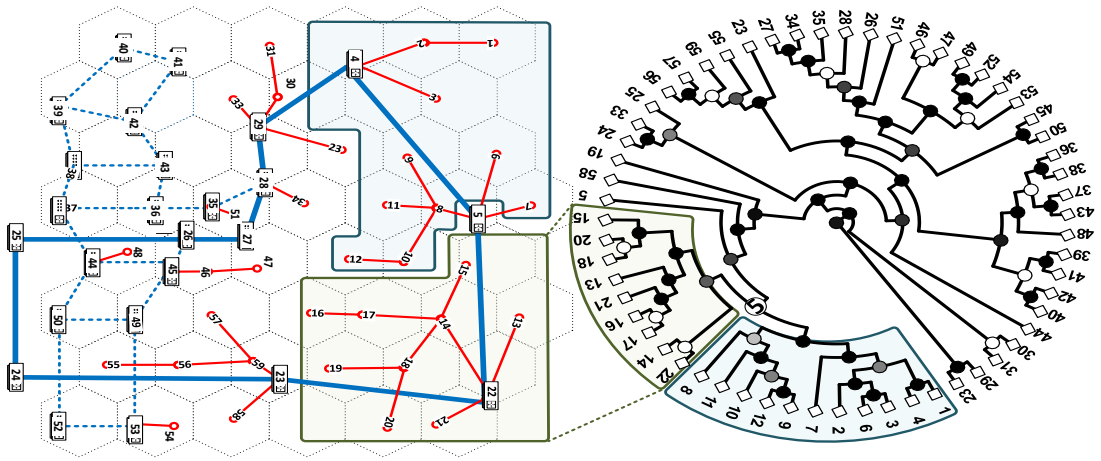

Figure 4-6: a) BIO Converged 5G Network, b) HRG of the BIO Infrastructure.

We evaluate the performance of the proposed HRG-based optimisation framework under various topologies (including the BIO topology shown in Figure 4-6) for the scenario where RUs offload their signal processing functions to the MEC-assisted 5G Network. We assume the realistic traffic statistics reported in [47]. Numerical results indicate that the HRG-based optimisation scheme outperforms the traditional C-RAN approach where all BBU tasks are offloaded to the central cloud and achieves very close performance to the optimal ML-ILP approach (Figure 4-7a). With a very limited number of HRG samples, the optimality gap for the solution obtained is kept below 5% (Figure 4-7b). Using the HRG-based approach, the complexity of the problem under investigation is reduced as the number of candidate paths, and consequently the number of variables, which are used to interconnect the RUs with the compute resources are minimised (Figure 4-7 c).

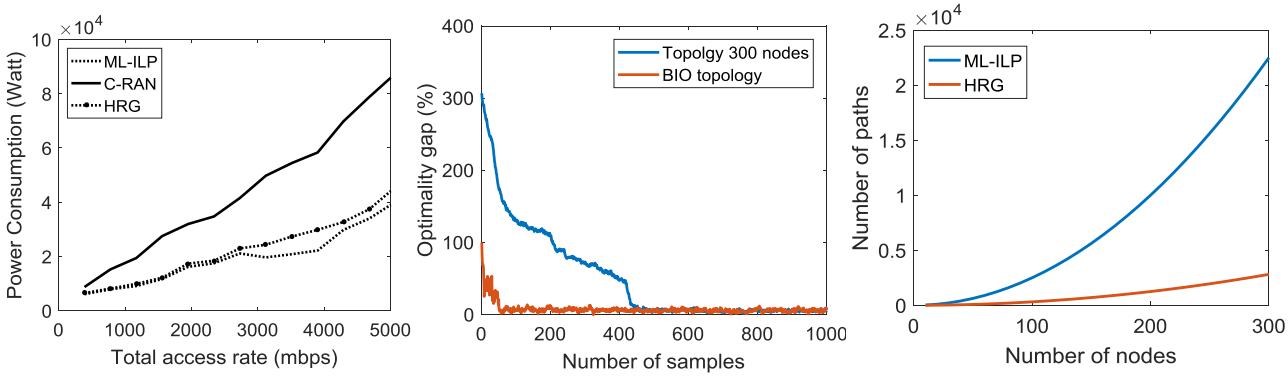

a) b) c)

Figure 4-7: a) Comparison between C-RAN, ML-ILP and the HRG schemes), b) Optimality gap as a function of the number of HRG samples, c) Number of paths used in the ML-ILP and the HRG.

4.1.5 Scalable Optimisation based on Artificial Intelligence (AI)

In the previous subsections, the various architectural aspects of the 5G-PICTURE architecture (DA-RAN, MEC-assisted 5G, integration of heterogeneous networks, elastic optical networks, etc.) have been evaluated adopting optimization frameworks based on linear programming. Although these techniques can effectively identify the optimal operational point of the whole system, their increased computational complexity and their slow convergence time makes them impractical to optimize the operation for real time network deployments. To address this limitation, a two-step Neural Network (NN)-based optimization framework is proposed. This framework allows real time identification of the optimal operational strategies per RU. In the first step, using a specific set of training data, a novel Multilayer Perceptron (MLP) - based NN model is constructed that in-real time can identify the optimal operational policies for the whole 5G infrastructure. A high-level view of this process is shown in Figure 4-8 a) for a specific case where the MLP NN is used to identify the optimal split per RU. To achieve this, the following steps are applied:

1) A training set combining data from history traffic statistics as well as data extracted from the offline – optimisation framework described above is determined. (An algorithmic approach that allows the identification of optimal MLP-NN architecture is provided in the following section).

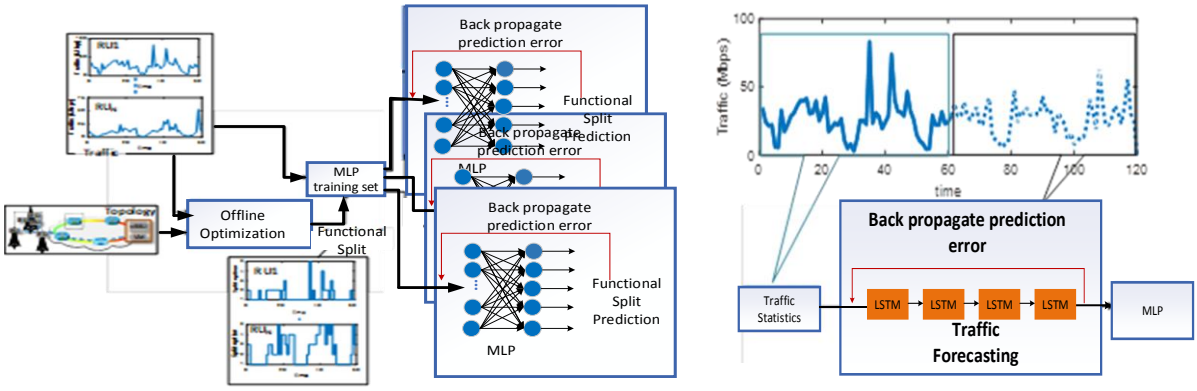

a) b)

Figure 4-8: a) Construction of the training set that will be used for the design of the NN-based 5G optimization framework. In the present example, the training set comprises traffic statistics and optimal baseband splits as they have been obtained by the offline optimisation process. B) NN model-based LSTM and MLP for the optimisation of the 5G network in the upcoming time instants.

2) Once the model has been trained, the MLP-NN model is combined with a Long Short-Term Memory (LSTM) NN model used for traffic forecasting. This aims at identifying the optimal operating conditions for the 5G infrastructure in the upcoming time periods. The flowchart of this process is provided in Figure 4-8 b).

Our objective is to identify an MLP network that maps any input x to the corresponding output, y. Output y is obtained from the solution of the corresponding ILP formulation, while x represents the set of history observations. As an example, consider the scenario for which we apply to the MLP a training set that comprises a set of pairs (x, y), where x represents the traffic statistics for a particular RU at a given point in time, while y represents the functional split. The optimal functional split per RU over time has been obtained through the solution of the ILP model described in the previous sections. This training set is given as input to the MLP neural network in order to learn how to map each input x to the corresponding output, y. Once the system has been trained, the MLP can predict the functional split given any new data without solving the corresponding ILP. The parameters of the MLP model can be derived executing the algorithm of Table 4-1 for different input values (batch size, number of hidden layers, etc.). At the end of the experiments, the combination of parameter value is chosen according to their ability to maximise the prediction accuracy.

The validity of the proposed NN-based optimisation framework is evaluated using the optical transport network topology presented in Figure 4-9 over which 21 RUs are deployed. The coverage area of each RU is shown in Figure 4-9. For this topology, mobile devices served by the corresponding RUs generate demands according to real datasets reported in [63]. Each RU is connected to the optical transport through microwave point-to-point links with 2 Gb/s bandwidth, and 45W power consumption. The optical transport has a single fibre per link, 4 wavelengths of 10 Gb/s each per fibre, and a minimum bandwidth granularity of 100 Mb/s [74] The

processing requirements of the mobiles devices and the RUs are supported through a set of DCs. For this network topology, our objective is to design a NN model that approximates the optimal ILP described in the previous sections. To keep the analysis tractable, the results provided are correspond to the optimal functional split of RU16, however, similar studies have been conducted for all compute/network elements of Figure 4-9 focusing on other parameters of interest such as, network capacity for optical links, compute capacity for DCs, locations where demands are processed for demands, etc.

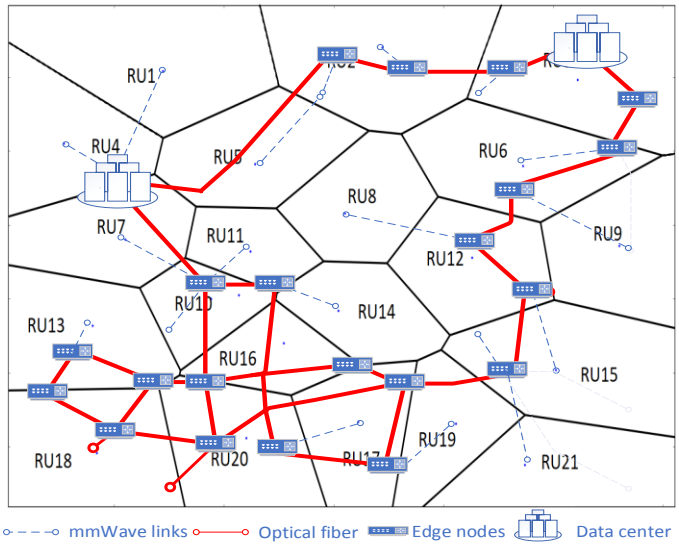

Figure 4-9: 5G network topology under investigation.

To design the two-stage NN model using the LSTM/MLP models, the methodology presented in Section 7 is applied to all network components. For each component, our objective is to design an NN that approximates with very high accuracy the optimal policies obtained through the corresponding ILP model. To identify the optimal NN models, the learning curves showing the Root-Mean-Square Error (RMSE) as a function of the number of epochs, hidden layers, neurons and batch size are first obtained. Based on these curves, the optimal values of the parameters that minimise the corresponding error can be readily determined. A typical set of learning curves for the LSTM model of RU16 is shown in Figure 4-10 and the corresponding optimal values are provided in Table 4-2.

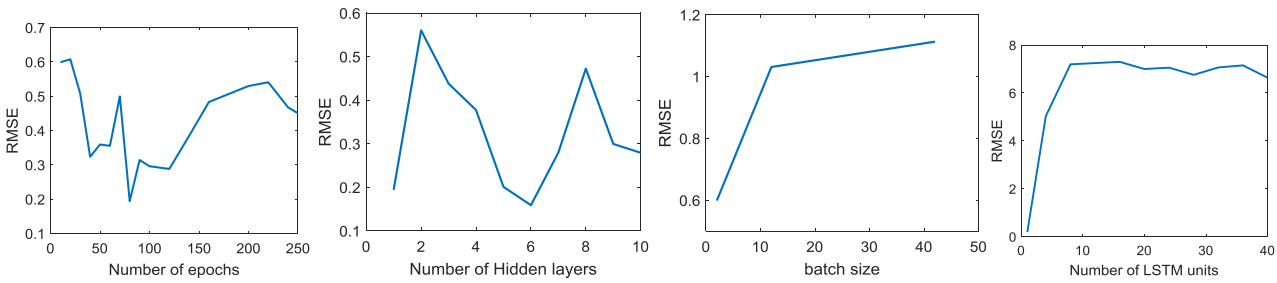

Figure 4-10: Learning curves of the LSTM for RU16.

Table 4-2: Parameter Settings of NNs for the RU16.

	Batch Size	Number of Epochs	Hidden Layers of the Network	Number of Neuron for Output Layer	Activation Function for Hidden Layers	Activation Function for Output Layer
LSTM	2	80	6 hidden layers with 1 neuron each layer	1	Relu	-
MLP	2	600	1 hidden layer with 10 neurons	5	Relu	Softmax

Once the optimal LSTM NN structure has been determined, the model is trained using the history dataset and the corresponding synaptic weights are determined. The test set is applied to the LSTM model to evaluate its forecasting performance. A snapshot showcasing the performance accuracy of the LSTM model for RU16 is illustrated in Figure 4-11 a), where an RMSE of 0.16 is obtained corresponding to a forecasting error in the order of 0.3%.

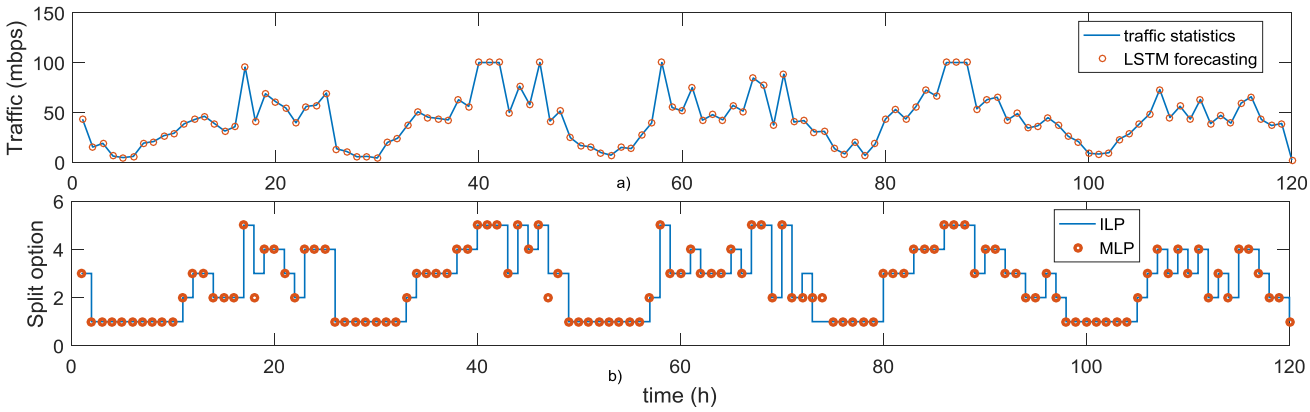

Figure 4-11: a) Traffic forecasting for RU16 using LSTM. b) Optimal functional split prediction for RU16 using the results obtained from the ILP and the MLP.

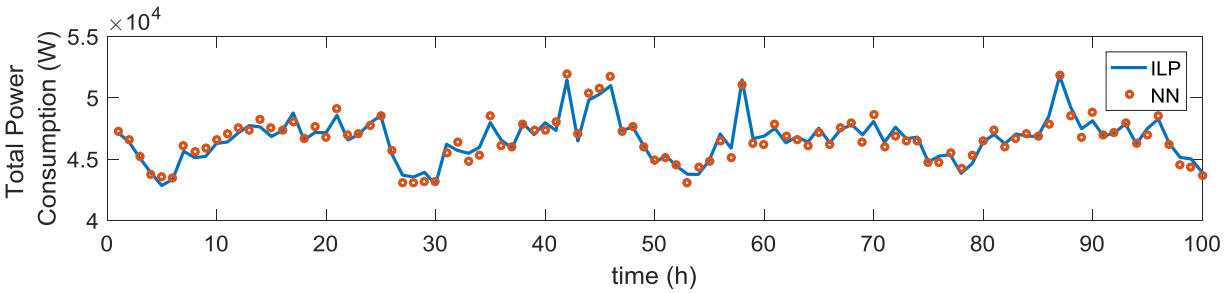

Figure 4-12: Total Power consumption when applying the ILP and the proposed NN scheme.

Following a similar approach to the LSTM problem design, once the MLP network has been defined, the derived model is trained and validated using the training set obtained from the ILP formulation. Figure 4-11 b) shows the performance of the proposed model where it is observed that the MLP is able to identify the optimal functional split with a 95% accuracy.

Finally, the performance of the proposed NN scheme is compared to the ILP-based optimisation in terms of total network power consumption. It is observed in Figure 4-12 that the power consumption over time for both schemes takes very close values, indicating the effectiveness of the proposed NN scheme to identify the optimal operational strategies of every network element. This clearly shows that online optimal service provisioning can be achieved taking a practical low complexity approach adopting machine learning techniques that can be trained to take real time very close to optimal decisions. In this context, the training process plays a key role and can be performed taking advantage of the optimal decisions provided through offline tools based on ILP. For more detail on this analysis the interested reader is referred to [94].

4.1.6 Scalable multi-service placement

According to RAN functional splits discussed in detail in section 3.2.1.1, the RAN functions need to be chained and placed across shared and customised control-plane (CP) and user-plane (UP) processing on a per-slice basis. For instance, as shown in Figure 3-16, the overall RAN service chain can be composed horizontally based on the shared functions provided by the underlying RAN module and/or vertically through the customised CP/UP processing delivered by the slice owner to fulfill its service requirements. Note that the functional split between disaggregated RAN entities is generally determined by the operator based on the aggregated BS KPIs and FH/MH performance, e.g., capacity and latency. However, slice owners can change the functional split through the CP/UP customisation. For instance, a service may request a hardware-based

accelerator for channel decoding and a dedicated radio resource scheduling to enable low-latency communications.

Once RAN service chains are composed, the associated network functions are placed accordingly while respecting the service requirements. Such requirements are described in terms of resources (e.g., compute, memory, and networking) and performance (e.g., average throughput, maximum latency). The placement also considers objectives such as cost/power/resource optimisation imposed by the operator. Here, we propose a two-stage placement algorithm in [105] as the slice service chains are composed both horizontally and vertically. Such algorithm extends the Multi-Objective Placement (MOP) described in [106] and includes the following steps:

Step 1. For each shared function with distinct latency constraint in the chain, determine its eligible regions (ERs) corresponding to the set of RAN nodes that satisfy the latency requirements;

Step 2. Determine the candidate group (CG) comprising the nodes from ERs satisfying the remaining slice requirements;

Step 3. Select the best node (BN) among CG based on the considered operator objective, e.g. load balancing;

Step 4. Repeat the above three steps to place the customised functions based on the results of the shared chains.

An example is shown in Figure 4-13 with 14 nodes (i.e., $\{N_1, \ldots, N_{14}\}$) when placing the function chain of CU ({SDAP, PDCP}) and DU ({RLC, MAC, High-PHY}), which are categorized into 3 levels: $\{N_1, N_2\}$, $\{N_3, \ldots, N_6\}$ and $\{N_7, \ldots, N_{14}\}$. All densely-deployed *M* RUs are grouped into several RU groups, each with *k* RUs that is associated with a pair of (CU, DU). The algorithm firstly selects the ERs based on the latency constraints of service function chains to be placed at CU and DU (cf. Step 1 in Figure 4-13). Then, CGs are formed based on the total processing requirement of a given function chain (cf. Step 2 in Figure 4-13), and BNs are selected to place the shared functions chain (cf. Step 3 in Figure 4-13). Afterwards, the customised processing for each slice is placed based on the results of shared chain following the same algorithm (cf. Step 4 in Figure 4-13). As the input and output endpoints are not slice-customized, an extra round-trip-time (RTT) is included when computing the ER of customised processing to capture the infrastructure-dependent packet processing. Taking the DU in Figure 4-13 as an example, the placement of customised functions of slice 1 (e.g., RLC, MAC) shall preserve the latency constraint with respect to the remaining shared chain (e.g., Input, High-PHY, Output). Thus, the RTT between N_1 and N_5 is considered when placing the customised chain at N_5 (cf. the overall path in Figure 4-13).

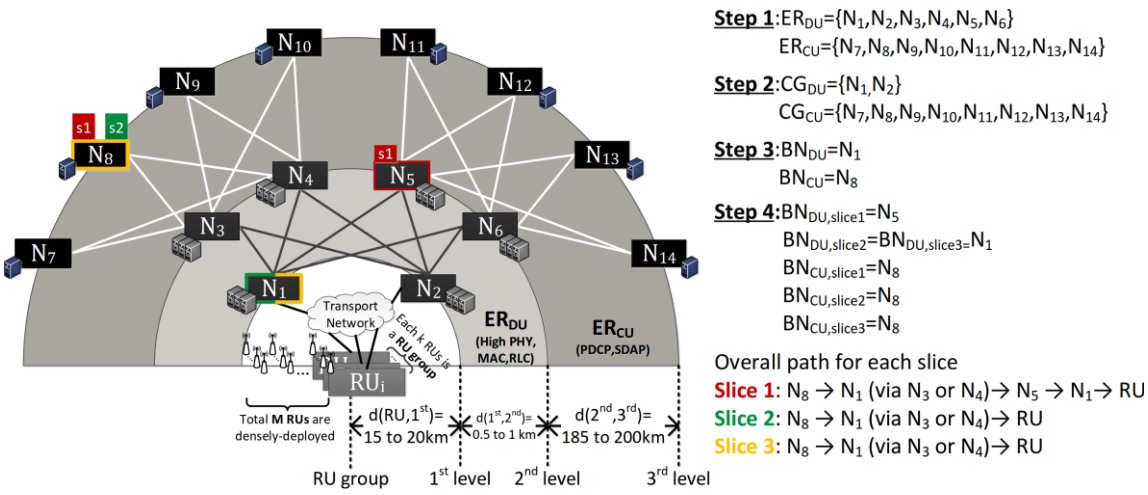

Figure 4-13: Example of a two-stage function placement for multi-service.

In the following we analyse the performance of the proposed multi-service chaining and placement approach based on the processing time data obtained from the OAI platform. We consider the three-level infrastructure topology shown in Figure 4-13 with the following inter-level distances: d(RU,1st)=15 km, d(1st,2nd)=0.5 km, d(2nd,3rd)=185 km. A subset of *M* RUs are grouped together where each group forms the minimum placement granularity for a given chain as depicted in Figure 4-13. For instance, if 6 RUs are grouped together, then 6 function chains are placed simultaneously across DU and CU such that they are physically co-located within the same node. These chains within a group can facilitate real-time control and coordination like joint

processing to enable the CoMP feature. Moreover, we apply the same service chain (i.e., functional split, customised functions) for each slice as in Figure 3-16.

In the top of Figure 4-14, we investigate the acceptance ratio in terms of different numbers of RUs (384 or 480) that are formed in different sizes of RU groups (24 or 6). Note that 5 different resource heterogeneity indexes are investigated as mentioned in Table 4-3. We can see that the acceptance ratios to place 384 chains for two RU group sizes are: 100% when grouping 6 RUs and 75% when grouping 24 RUs for heterogeneous index 1, as shown in the top of Figure 4-14. Such results justify the efficiency of our proposed approach and the higher acceptance ratio benefit when using a smaller RU group. When the node resources become heterogeneous, the orchestrator shall incorporate auto-scaling action to efficiently manage both infrastructure and slice workload dynamics. When grouping 24 RUs, heterogeneity index 4 and 5 provide the largest enhancement as the DU functions (i.e., N_1 to N_6) consume more resources and better exploit the resource heterogeneity, while fewer enhancements are observed when RUs are grouped in 6.

To determine which action shall be taken to further increase the acceptance ratio we compare the number of remaining resources at all DU nodes after the service chain placement (i.e., unused resources) and the number of unsatisfied requested resources (i.e., resources of rejected chains). In the bottom of Figure 4-14, the remaining CPUs are more than the requested ones in the case of 384 RUs grouped in 24, which shall trigger a **scale-up** action to *reallocate the unused resources to a subset of nodes* to increase the acceptance ratio. In contrast, a **scale-out** action shall be triggered to *provision more nodes* in the case of 480 RUs grouped in 6 or 24, as the remaining resources are less than the requested ones.

Table 4-3: Number of CPUs for different nodes among five resource heterogeneity Indexes.

Resource Heterogeneity Index	CPU resource													
	N_1	N_2	N_3	N_4	N_5	N_6	N_7	N_8	N_9	N_{10}	N_{11}	N_{12}	N_{13}	N_{14}
1	32	32	32	32	32	32	2	2	2	2	2	2	2	2
2	48	16	32	32	32	32	1	1	1	1	3	3	3	3
3	32	32	48	48	16	16	1	1	1	1	3	3	3	3
4	48	16	16	16	48	48	2	2	2	2	2	2	2	2
5	48	16	16	16	48	48	3	3	3	3	1	1	1	1

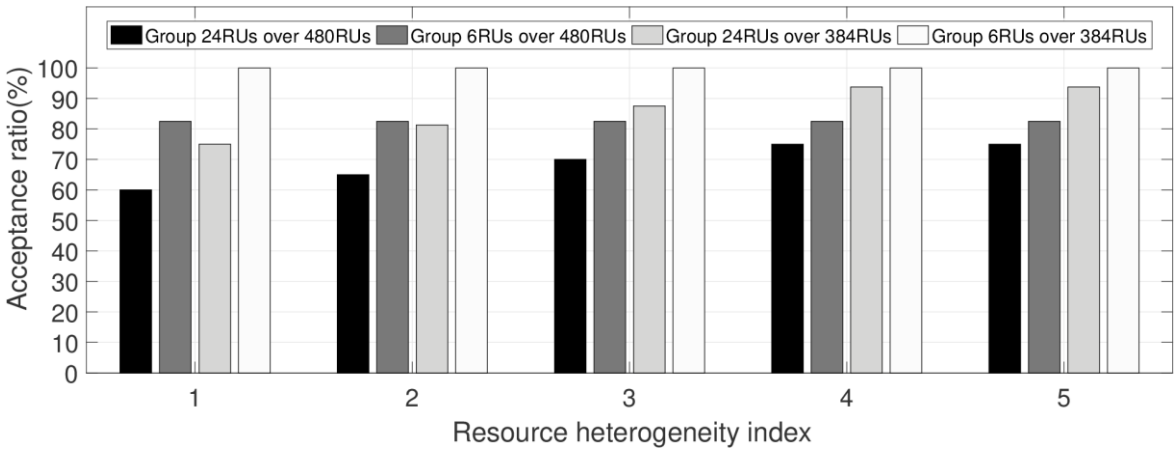

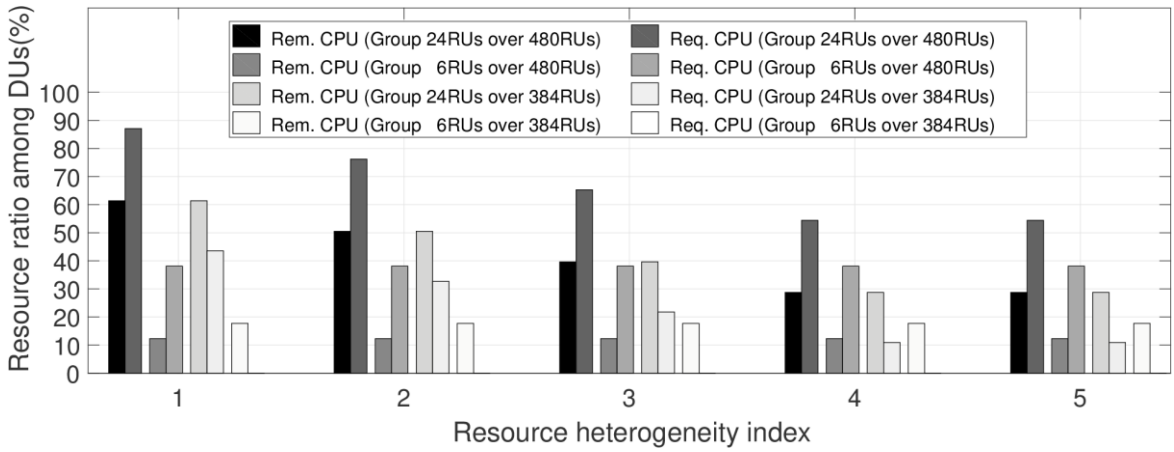

Figure 4-14: Acceptance ratio (top) and remaining/required CPU ratio (bottom) for different resource heterogeneity indexes.

To sum up, two strategies can be applied to enhance the acceptance ratio: (a) utilize a smaller group size of RUs as the minimum placement granularity, or (b) provision heterogeneous resources based on the service requirements to preserve scalability.

4.2 Vertical use case evaluation

4.2.1 Proposed Solutions to 5G communication to trains

5G mobile networks are expected to support higher mobility, higher data rates and lower latency [48]. Recently, we experience the offset of 5G standardization in 3GPP, widely known as New Radio (NR). In the context of NR, the air interface will extend, compared to 4G, to carrier frequencies from 1 GHz up to 100 GHz [49]. Moreover, it will co-exist with the evolved LTE (Release 13 and beyond) [48] and bring together existing and newly emerged technologies.

The solution of placing a massive number of antennas at the BS, i.e. Massive MIMO, has been one of the main candidates. The employment of Massive MIMO technology provides high spectrum efficiency, due to the large multiplexing gain and antenna array gain. Furthermore, high energy efficiency is achieved, because of the concentration of radiated energy.

Another highly researched solution to 5G networks is mmWave. First of all, the consideration of mmWave frequencies resolves the issue of limited spectrum. Moreover, despite the limitation to shorter ranges, compared to Sub-6 GHz, and the existence of penetration loss, research has shown that mmWave systems can support high data rates, reduce the antenna-size and are ideal for small-cell deployments.

At the same time, vehicular communications (i.e. cars, trains) constitute a great part of research towards 5G networks. Based on the above, for the Rail Vertical we will investigate the following two 5G solutions in the rail environment:

4.2.1.1 Cases

<u>a) Sub-6 GHz LTE Massive MIMO coverage cell</u>

In this scenario, 5G connectivity to trains could be achieved by Massive MIMO technology. Access Points (APs) on the train will be served by a Sub-6 GHz LTE Massive MIMO station per cell (Figure 4-15). High data rates are expected due to the multiplexing gain as well as the array gain that a Massive MIMO system offers. Massive MIMO stations could be connected via CPRI to co-ordinate connectivity as the train moves from one cell to another, i.e. hand-over.

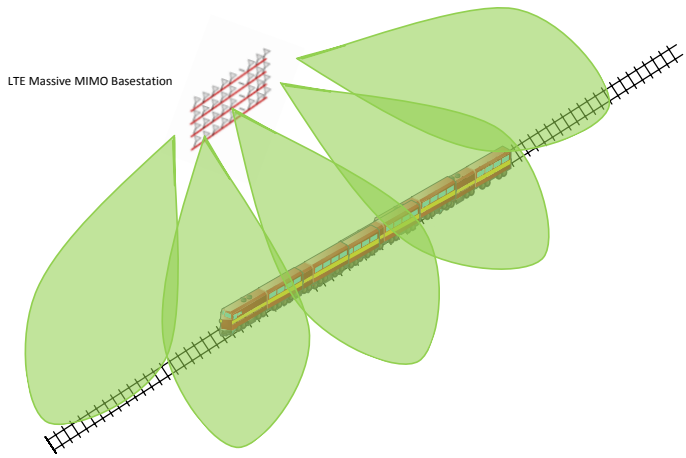

Figure 4-15: Vertical Rail – Sub-6 GHz LTE Massive MIMO cell.

For this scenario, we will consider a BS at a height of 25 m and APs on the train at 2.5 m high. Considering a 2-5 km long railway track, in Bristol (Temple Meads) and London (Paddington), and frequencies 2.6 GHz (MIMO) and 3.5 GHz (Massive MIMO), the channels will be modelled with the ray-tracer simulator, in the University of Bristol (CSN group). Moreover, with the Received Bit mutual Information Rate (RBIR) LTE Matlab simulator, the spectral efficiency will be investigated, in a rail environment, using the ray-tracer acquired channels.

b) mmWave Access Points (APs) along the trackside

For the mmWave scenario, we will consider mmWave APs, at a height of 3 m, placed along the trackside, initially 200 m apart (greater distances, up to 800 m, will be also investigated), and around 3-5 m away from the tracks, and mmWave APs on the train, all at a height of 2.5 m. Thus, FH will be based on mmWave, whereas the BH, i.e. connection between the APs on the trackside, could be connected via CPRI. We will consider both 26 GHz and 60 GHz frequencies.

For the mmWave scenario, we will consider a track 2 km long. Like in the Massive MIMO scenario, the channels will be modelled with the ray-tracer simulator, in the University of Bristol (CSN group). In addition, beamforming will be introduced, selecting beam width in azimuth and elevation. Then, the spectral efficiency will be evaluated, based on the modelled channels, using the RBIR simulator. The same railway environments (Temple Meads, Paddington) will be modelled in this case as well.

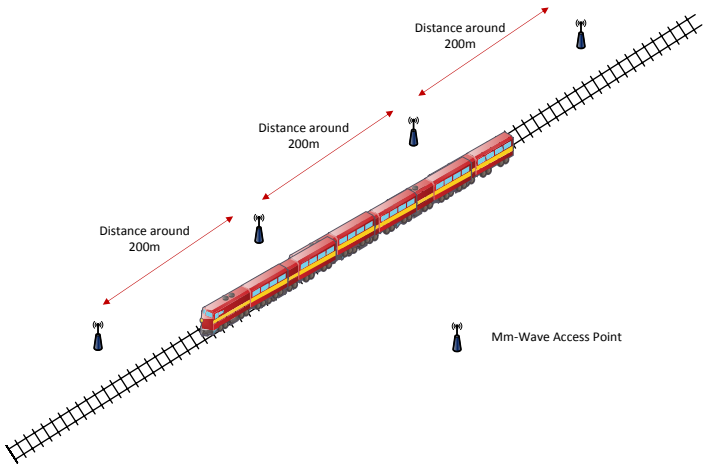

Figure 4-16: Vertical Rail – mmWave APs along trackside.

Technical Challenges

Current standards need to be modified to support rapidly changing channel environments, such as communication to high-speed trains. Location-aware, fast and directional beamforming has shown to improve spectral efficiency [50][51] in Massive MIMO high-mobility cells, however it does increase the computational complexity, especially when CSI cannot be easily obtained. In mmWave vehicular communications, adaptive and highly-directional beamforming has been researched as a mean to deliver high data rates on high-speed trains. Results indicate that in most cases fixed and adaptive beamforming result in the same performance [52].

The second major challenge is the doppler spread, in cases that the antenna beamforming alignment is not precise, i.e. multipaths at different Angle of Arrival (AoA). A high-speed train implies rapid fluctuations on the received signal waveform, and subsequently a relatively small coherence time. For instance, according to [50], when a train moves at 486 km/h, the maximum Doppler shift is estimated at 945 Hz, with carrier frequency 2.35 GHz, and a coherence time of less than 1 ms. A potential solution to address this issue could be the use of highly directive antennas that could eliminate the spread of the received multipath components

Finally, the diversity of train routes could be quite challenging – i.e. different structures of tunnels, mountains that could potentially block Line of Sight (LoS) communication – and this could have an impact on the efficiency of beamforming algorithms. On the other hand, for LoS propagation conditions, these routes are predefined, enabling thus the beam tracking process [50].

4.2.1.2 Initial Results/Evaluation

Sub-6 GHz LTE Cell

Our evaluation on Sub-6 GHz technologies in a rail environment initially targeted SISO configurations and will build up to MIMO and finally Massive MIMO. Thus, our investigation commenced from the consideration and evaluation of point-to-point links along a ~1.5 km rail track, with 1 m resolution, both in Temple Meads (1.4 km) and Paddington (1.6 km), as depicted in Figure 4-17. The LTE BS is shown as a red mark. In Figure 4-17, for the Paddington area, only the route in the red circle was considered at this point.

We considered a transmit power of 51 dBm at 2.6 GHz, placing the BS at 25 m height and the moving AP (considered as an antenna on the train) at 2.5 m height.

Figure 4-17: LTE: Temple Meads (Bristol) route, LTE: Paddington (London) route.

Figure 4-18 and Figure 4-19 depict the average throughput for all modes considered and the maximum throughput over all points on the route for the Temple Meads and Paddington scenarios, respectively. Future results, already obtained but will be presented in following deliverables, will consider an actual train traveling along the track, and MIMO and Massive MIMO configurations.

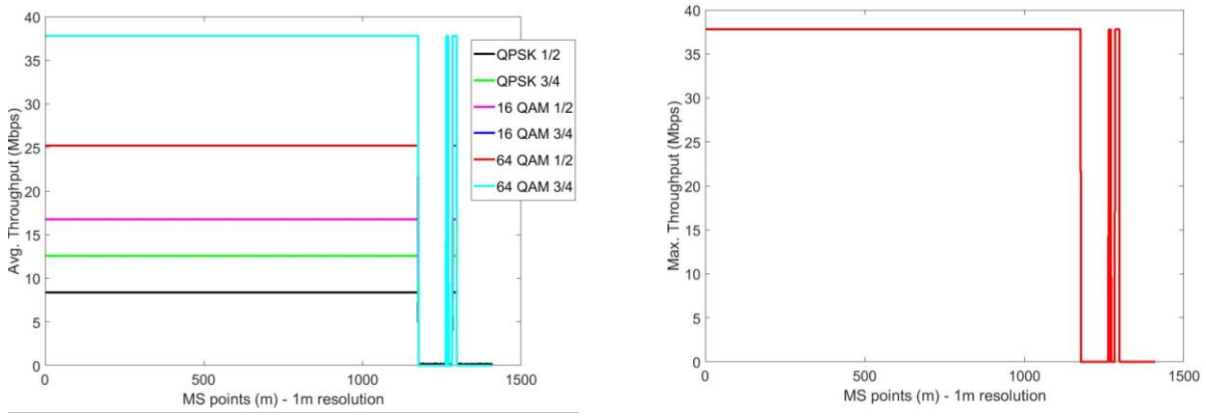

Figure 4-18: Temple Meads: (left) Avg. Throughput for all modes, (right) Max. Throughput.

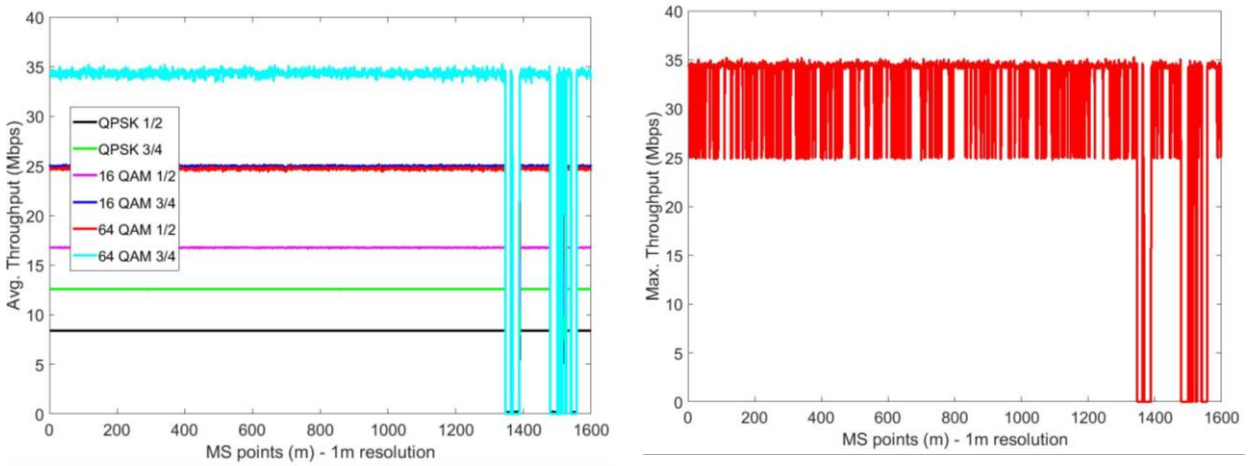

Figure 4-19: Paddington: (left) Avg. Throughput for all modes, (right) Max. Throughput.

mmWave APs along trackside

Our investigation in mmWave technology deployed in a rail environment started by considering point-to-point links on a ~1.5 km track, with a resolution of 1 m, placing the mmWave BSs along the track 200 m apart. The transmit power was 22 dBm, considering both 26 and 60 GHz frequencies. The BSs along the track were placed at a height of 3 m and the APs on the train at a height of 2.5 m. The routes used for our simulations are depicted in Figure 4-18 and Figure 4-19, where every mmWave BS placed along the trackside is shown with a different colour (in Figure 4-19 only the BSs in the red circle were taken into consideration).

As shown in Figures 7-10, both no beamforming and beamforming by selecting the maximum power ray were considered in order to result in the throughput per point along the track. As depicted in the figures, we can also place the BSs 400 m, even 600 m in some cases, since it is obvious that coverage is not lost.

In future deliverables, further investigation will be performed, presenting results with different distances between BSs, considering an actual train moving along the track and other kinds of beamforming, such as exhaustive search.

Figure 4-20: mmWave: Temple Meads (Bristol) route and Paddington (London) route.

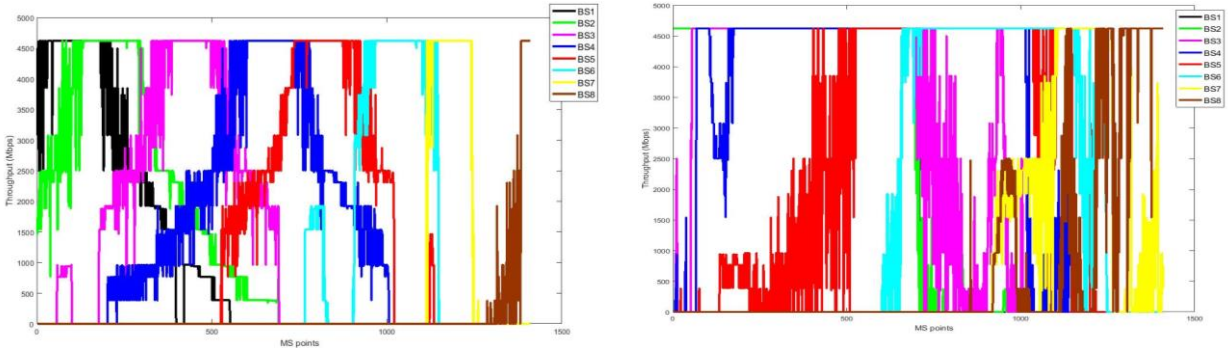

Figure 4-21: Temple Meads 60 GHz: (left) No Beamforming, (right) Selection of Max. Power Ray.

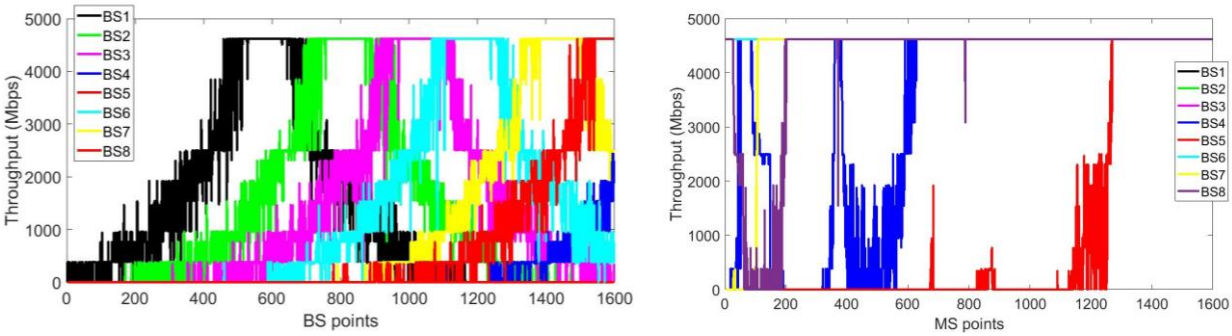

Figure 4-22: Paddington 60 GHz: (left) No Beamforming, (right) Selection of Max. Power Ray.

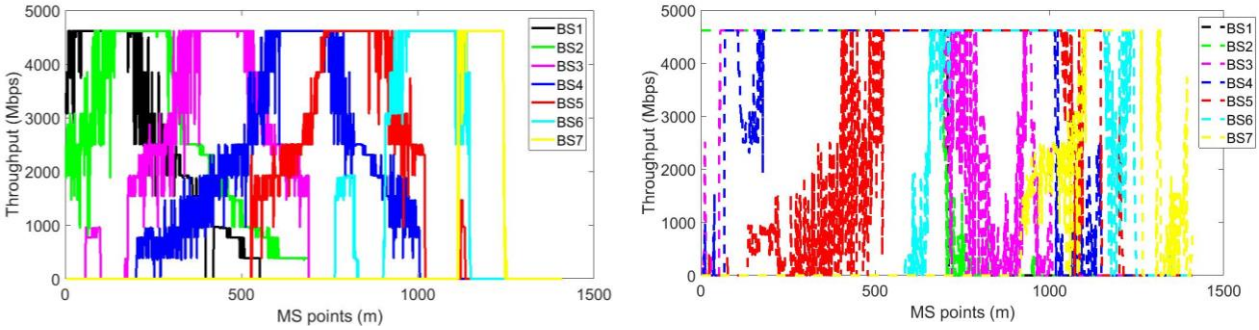

Figure 4-23: Temple Meads 26 GHz: (left) No Beamforming, (right) Selection of Max. Power Ray.

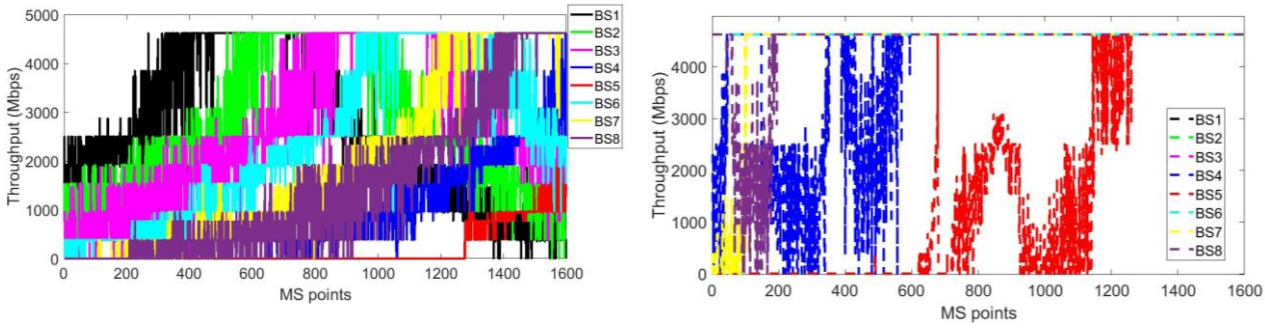

Figure 4-24: Paddington 26 GHz: (left) No Beamforming, (right) Selection of Max. Power Ray.

4.2.2 Multi-technology access in railway systems

We consider a network infrastructure that relies on a set of optical and wireless network technologies to interconnect a variety of end-devices and compute resources as shown in Figure 4-25. Through this approach, data obtained from various sources (monitoring devices, users and social media) can be dynamically and in real-time directed to the operations and control centre (OCC) for processing.

The wireless domain of this infrastructure comprises cellular WiFi, mmWave and LTE technologies for the on-board and on-board to trackside communications. These exhibit a high degree of heterogeneity as they differ both in terms of operational and performance parameters, including spectrum use; antenna characteristics, physical layer encoding, sharing of the available spectrum by multiple users as well as maximum bit rate and reach. LTE is among the prime wireless access cellular technologies in 4G networks as it offers a theoretical net bit-rate capacity of up to 100 Mb/s per macro-cell in the downlink and 50 Mb/s per macro-cell in the uplink if a 20 MHz channel is used. These data rates can be further increased through MIMO technology. At the same time, LTE can provide improved QoS characteristics such as low packet transmission delays, fast and seamless handovers supporting high speed vehicular communications scenarios and operation with different bandwidth allocations.

To quantify the benefits of centralisation in high mobility scenarios, let us consider the case where eNBs are placed 1.2 km apart. For fast moving objects (i.e. trains) with a speed of 300 km/h, handovers will be performed every 7 s, leading to overutilisation of network resources [96][97]. However, by clustering several eNBs together handover frequency can be radically reduced.

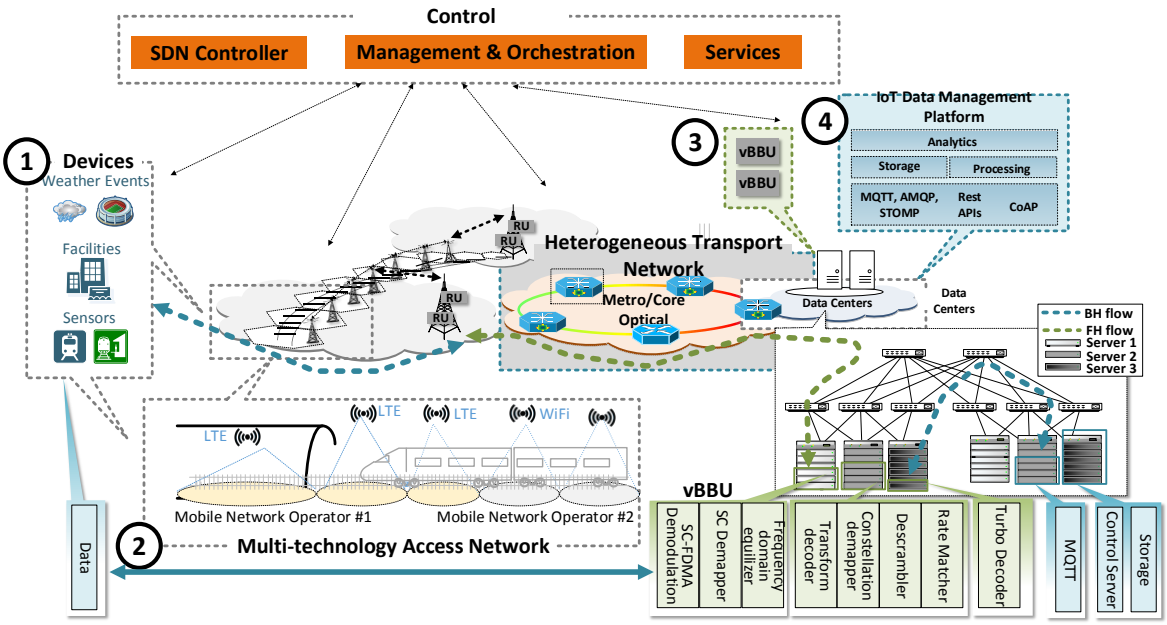

Figure 4-25: Converged Heterogeneous Network and Compute Infrastructures supporting railway services: Use case where data are collected from various devices (1) are transmitted over a 5G network (2) to the cloud based data management platform (3).

To support the transport network requirements associated with C-RAN in a railway environment, we propose the adoption of an optical transport solution offering high capacity and advanced features including dynamic bandwidth allocation both in the time and frequency domain. Given the technology heterogeneity of the proposed infrastructures, a critical function is interfacing between technology domains including isolation of flows, flexible scheduling schemes QoS differentiation mechanisms and mapping of different QoS classes across different domains. This can be achieved adopting flexible hardware functions that allow hardware repurposing through concepts such as hardware programmability. Hardware programmability can potentially enable dynamic and on demand sharing of resources guaranteeing also the required levels of isolation and security. In this context, programmable Network Interface Controllers that are commonly used to bridge different technology domains at the data plane can play a key role. These controllers have a unique ability to provide hardware level performance exploiting software flexibility and can offer not only network processing functions (i.e. packet transactions [98], but also hardware support for a wide variety of communication protocols and mechanisms [99]). To enhance spectral efficiency, macro-cells can be complemented with small cells as they allow higher rates of frequency reuse over carefully designed geographical areas with easy access to the network backbone. In addition to small cells, given that WiFi networks are readily available in almost every public or private area and are easy to install and manage, significant benefits are expected by the joint consideration of WiFi and LTE systems. Additionally, the small cell concept can easily be extended to mmWave to overcome the high interference generated by the close reuse of radio frequency spectrum in heterogeneous networks.

The proposed framework is evaluated using the infrastructure topology, illustrated in Figure 4-26. This infrastructure covers a 10x10 km^2 area over which 50 RUs are uniformly distributed and comprises a set of optical edge nodes in the optical segment, and optical point-to-point links for fronthauling the RRHs. The optical network technology adopted deploys a single fibre per link, 4 wavelengths per fibre, wavelength channels of 10 Gb/s each, minimum bandwidth granularity of 100 Mb/s and maximum link capacity of 40 Gb/s. The power consumption model for the optical nodes is provided in [6]. Furthermore, a 2×2 MIMO transmission with adaptive rank 10 MHz bandwidth adjustment has been considered, while background network traffic over the serviced area according to real datasets reported in [100].

The railway-related network traffic is generated by a set of sensing devices installed both on-board and at the trackside. This traffic needs to be transferred at the servers where the Operational Data Management (ODM) platform is located and processed by a specific set of computing resources. The whole area is also covered by a set of WiFi access points offering 135 Mb/s capacity having power consumption 1.28 W during data transmission, 0.94 W during data reception, 0.82 W under idle mode and 64 mW under sleep mode. In addition to this, a set of mmWave access points is considered. Finally, each DC has a processing capacity of 80 Giga IPS and its power consumption follows the step-size power consumption model.

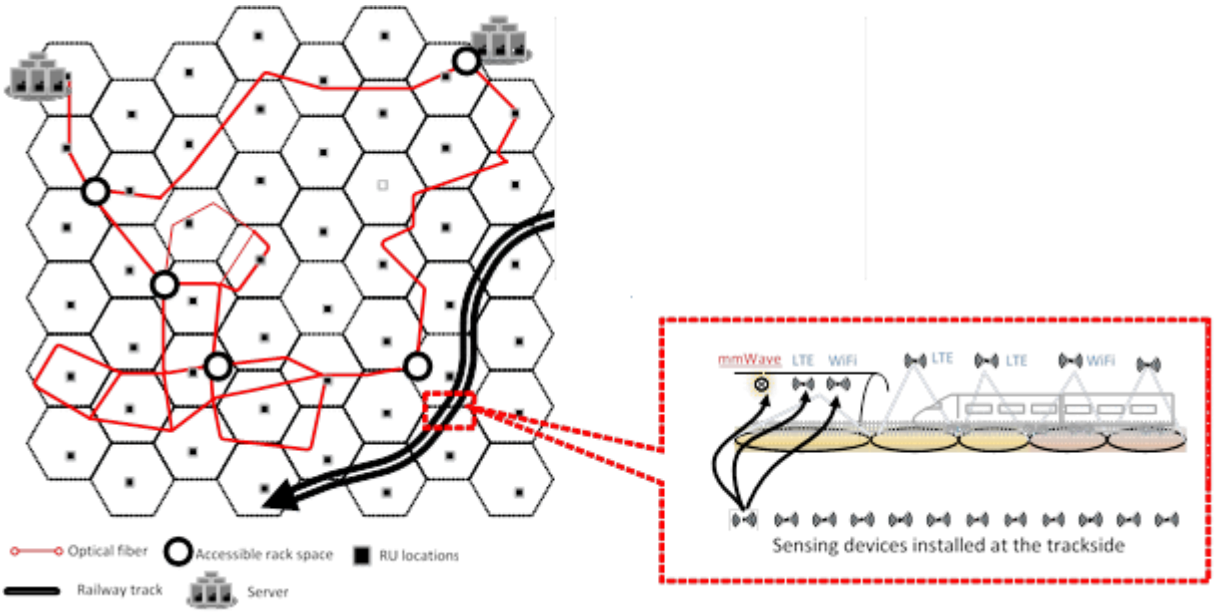

Figure 4-26: Railway track at Bristol.

The objective of the optimisation framework is to identify the optimal SCs in order to jointly optimise the performance of converged network and computation infrastructure as well as the battery lifetime of the sensing devices. The former can be achieved by identifying the optimal routing paths and the location of the DCs where demands need to be processed, whereas the latter by ensuring that all sensing devices will forward their traffic through the optimal wireless access network technology. Through the appropriate selection of the optimal wireless access technology (WiFi, mmWave, LTE), sensing devices will try to prolong their battery lifetime without violating QoS specifications.

Figure 4-27 illustrates the impact of service requirements in terms of network traffic and mobility on the end-to-end service delay and the average power consumption per sensing device.

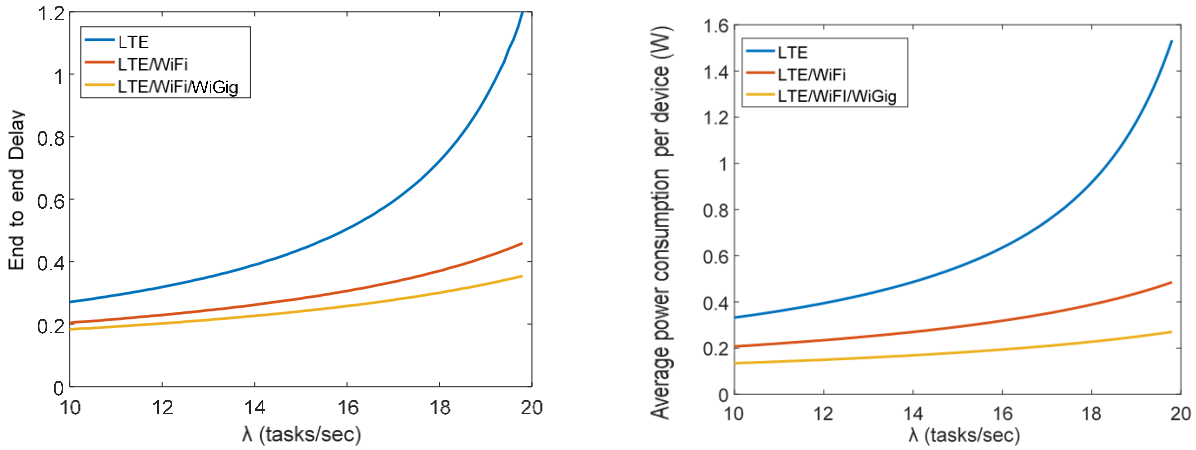

Figure 4-27: Impact of network integration on end-to-end service delay and sensing device power consumption (compute-to-network ratio= 0.03).

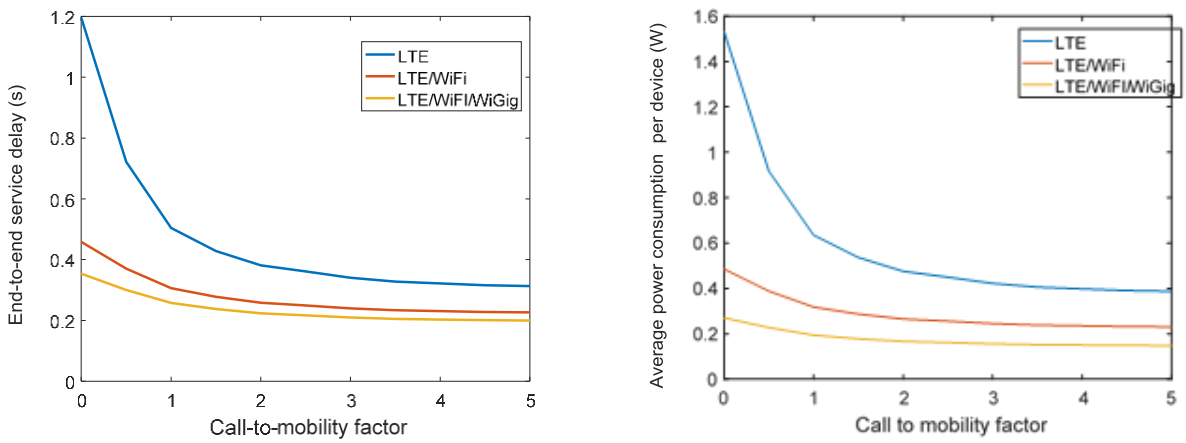

Figure 4-28: Impact of mobility on end-to-end service delay and device power consumption for Wireless Access Technologies (λ=10).

To achieve this, the Network-to-compute resources and the Call-to-mobility ratios are introduced to capture the communication cost and the average speed of the sensing devices, respectively. The former is used to capture the relation between computational and network bandwidth requirements, while the latter is defined as the fraction of the service holding time over the cell residence time. From Figure 4-28 it is observed that, with the increase of the network load, both the end-to-end service delay and the power consumption of the mobile devices increases. However, for higher degree of network convergence we are able to drastically reduce the service delay and the power consumed by the mobile devices.

As also discussed in [6], when mobility is high (lower call-to-mobility factor), additional resources are required to support the seamless handovers in the wireless access domain. This additional resource requirement also propagates in the optical railway network and the DC domain in order to ensure availability of resources in all domains involved (wireless access and backhauling, optical railway network, and DCs) to support the requested services and enable effectively seamless and transparent end-to-end connectivity between sensors

and the computing resources. This leads to underutilisation of network resources and, therefore, increased delays. The present approach, through the higher degree of consolidation and the better utilisation of the network resources it offers, can handle high degrees of mobility and also support services with significant communication requirements in a very efficient manner.

4.2.3 Internet of Things in Disaggregated 5G Networks: A Rail Use Case

Machine to Machine (M2M) communications and IoT have resulted in tremendous growth of globally generated data which according to the International Data Corporation is expected to exceed 163 zettabytes/year by 2025 [81]. Once analysed, this massive amount of data generated by billions of connected devices ranging from smart devices and autonomous vehicles to remote sensors, can assist infrastructure providers, a variety of vertical industries, policy makers and the public to derive new insights and improve society's quality of life. 5G systems with their ability to offer high-speed/low-latency internet connectivity as well as easy access to storage and processing resources, can enable massive IoT to a broad spectrum of vertical industries [82].

To achieve this, 5G networks rely on a set of hardware, software and architectural innovations. These include: *i)* the concept of C-RAN, *ii)* a high capacity transport network to offer connectivity between the RUs and the CU for the support of the FH services required by C-RAN, integrating advanced wireless and optical network elements, *iii*) a set of compute resources responsible for the processing of operational data and the provisioning of real-time data analytics, and iv) an intelligent control plane enabling precise network resource allocation and data forwarding to the appropriate processing platforms.

A typical example of a 5G network exploiting a flexible optical transport solution to provide IoT services for vertical industries is the use case of railway systems. As an example, Figure 4-31 illustrates a specific use case developed in the context of the IN2RAIL project [83]. In this rail use case, data collected from various devices installed on-board and at the track side of the rolling stock (1) are transmitted over a multi-technology network (2) operating in accordance to the C-RAN paradigm (3) to the cloud-based data management platform (DMP) (4) that is responsible to perform data collection, storage and processing.

In this environment it is very important to identify the optimal assignment of each task to the appropriate processing platform as this decision is expected to give significant efficiency gains. In the case of IoT over 5G, this decision is linked to the placement of BBU's and DMP's construction elements (i.e., message broker, control server and database manager) to suitable processing units. In current deployments, this is performed without taking into consideration the details and specificities of the individual processing functions of BBUs and IoT services [84], [85] which can provide significant efficiency gains [86]. To take advantage of the appropriate mapping of processing functions to suitable available compute resources that can be hosted at DCs, we rely on the concept of compute resource disaggregation. This approach allows individual allocation of processing functions, associated with a specific FH and IoT-BH services, to different servers depending on the nature and volume of their processing requirements. To quantify the benefits of the proposed approach we have performed experiments analysing the processing requirements of an IoT platform using an actual DMP system support the experimental smart metering campaign of the In2Rail project [83].

In addition, a Multistage Integer Linear Programming (ILP) modelling framework has been developed to assign the construction elements of the nested FH/IOT-BH chain to suitable servers available at the DC. The output of our experiments was used as a realistic input to our ILP model to evaluate the energy consumption requirements of the compute resources for the proposed approach where softwarised BBUs [87] and IoT DMPs are placed within the DCs (referred to as SW-IOT). As the proposed approach is based on the concept of disaggregation we refer to it as the disaggregated SW-IOT (DSW-IOT).

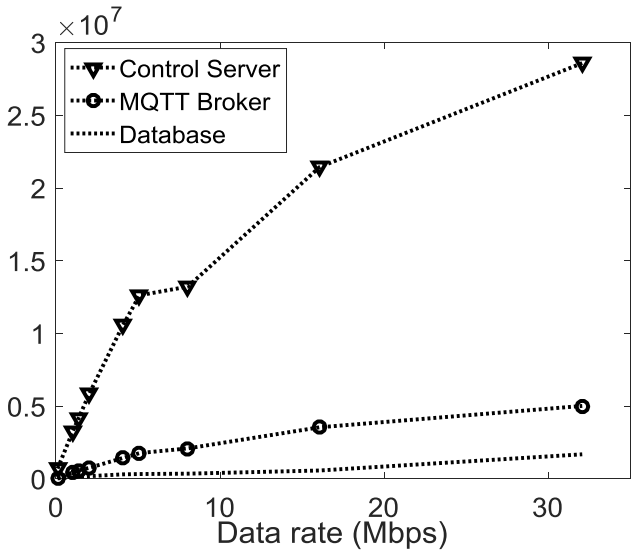

Figure 4-29: Instructions per second under various data rate for DMP components of Figure 4-25.

Similar to the previously discussed use cases, in this section we consider the case where IoT services are provided over a generic 5G C-RAN infrastructure. For C-RAN, the RU processing requirements are supported by a set of compute resources located at the DCs. The compute requirements for BBU processing for each RU is calculated by the sum of all contributing computing elements responsible to perform the required functions including, SC-FDMA demodulation, SC demapper, frequency domain equalizer, transform decoder, constellation demapper, descrambler, rate matcher and turdo decoder. The DMP comprises three main components including the Message Queuing Telemetry Transport (MQTT) broker, the central server and the time series database (Figure 4-25). Our objective is to identify the optimal GPP where each function can be allocated so the total power consumption at the DC is minimised satisfying, at the same time, QoS constraints imposed by the C-RAN and the IoT services.

To achieve this, we initially calculate the actual processing requirements of each BBU function and of each DMP component service through the WiBench and the DMP platform for smart metering railway services reported in [83] respectively, under various wireless access system configurations and different IoT loads (Figure 4-29). The processing requirements of each function are then used as input to the multistage ILP-based optimisation framework that creates nested service chains that assign each function to a suitable GPP in an energy efficient manner.

Table 4-4: Technical specifications of the servers used in the numerical evaluations.

CPU Description	MHz	Chips	Cores	Total	RAM (GB)	Max IPS	Max Power (Watt)	Idle (Watt)	(IPS/ watt)
Intel E3-1260L v5	2900	1	4	8	16	31802689	47.9	14.4	529836
Intel Xeon E5-2699 v4	2200	2	44	88	64	226542946	247	46.6	775056
Intel Xeon Platinum 8180	2500	2	56	112	192	378651974	426	39.5	833346
Intel Xeon Platinum 8176	2100	8	224	448	768	1304763025	1478	206	766748

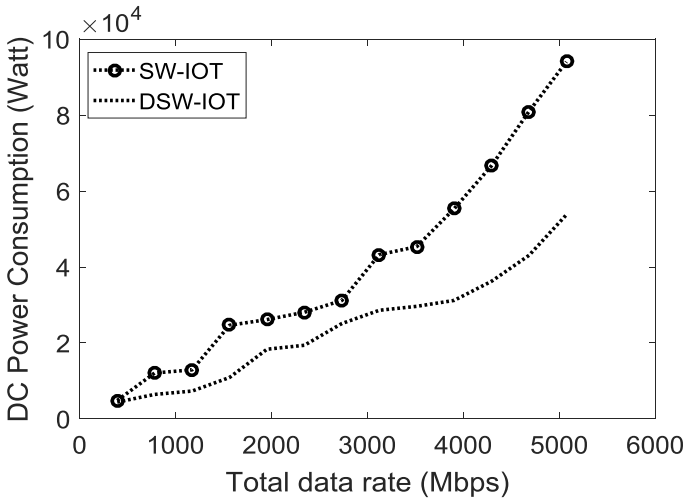

Figure 4-30: DC power consumption for the traditional softwarised IoT (SW-IOT) and the disaggregated SW-IOT (DSW-IOT) as a function of the total wireless access traffic.

Experiments were conducted using WiBench, an open source implementation of the LTE protocol stack. Intel's VTune Amplifier 2018 was used to provide the performance analysis. For the DMP, we analysed the processing requirements of the message brokering servers (MQTT), ii) the Control Server that receives the data either from the MQTT broker or HTTP requests and forwards them for storage and iii) the time series database used for storage. The investigation of each BBU function, for various configurations of the LTE uplink system, was conducted through a series of experiments. Results show a linear dependence, for every function, between the number of instructions performed and the data rate. Instructions increase exponentially with the IOT data rate for the Constellation De-mapper, and linear for the Rate Matcher and the Turbo Decoder, while for all other functions are independent. The total number of instructions, for the BBU processing, is mainly determined by the Turbo Decoder, which involves 1 to 4 orders of magnitude higher instruction number compared to the other functions, depending on the data rate. The processing requirements of the DMP were derived by calculating the instructions per second required by its components as a function of the total IoT load (Figure 4-29).

To quantify the benefits of the proposed approach, the simple DC network topology of Figure 4-25 is considered. This topology comprises 6 racks each comprising 48 servers. Connectivity between racks is provided assuming the intra-DC optical network solution described in [89]. In the numerical calculations we consider four types of servers, randomly placed within the racks. The technical specifications of these servers are provided in Table 4-4, while their power consumption follows the linear stepwise function described in [6]. For the wireless access, we consider the topology described in [83] in which the served area is covered by a set of RUs providing connectivity for the IoT devices installed on-board and at the track side of the rolling stock. RUs forward their FH flows to the DCs for processing. Figure 4-30, compares the performance of the proposed optimization DSW-IoT scheme in terms of power consumption with the conventional SW-IoT as a function of the served IoT traffic. As expected, the power consumption at the DCs increases with the IoT load. However, the DSW-IOT offers much better performance due to its increased ability to mix and match compute and network resources, leading to improved utilisation of the servers and to higher energy efficiency.

4.2.4 Initial Control Plane Scalability Analysis

As already discussed the SDN main concept relies on the separation of the control from the data forwarding by providing a centralised control over the network through the controller. A key problem with the nature of the SDN architecture is the centralised approach for the placement of the controllers. Network topologies with a large number of devices and long distances between them (introducing delays in communication between the switch and the central controller) require the creation of a more distributed architecture that allow the continuous operation of time sensitive applications. The ultimate goal is to create SDNs that are easily expandable and cover large geographical areas.

In the following, an approach for measuring the control plane latency is being discussed. The main idea is the creation of a northbound application over the OpenDayLight (ODL) platform – as a network administrator – that communicates externally with the controller, using the REpresentational State Transfer (REST) APIs. The application implements at first step a mechanism for collecting data associated with the network topology and

at second step a mechanism for sending echo messages to all switches simultaneously, in order to measure the time response of the ODL controller [54].

TOOLS: All the information needed by ODL were exported in the form of json files (alternatively xml could have been used). The formatting of large files, the editing and the mass export of specific data, the jq command was used, which is basically a filter for json files. The jq library contributed to the practical aspect of the application and to its optimisation in terms of time and space.

ODL REQUIREMENTS: The version of ODL that was used for this problem was Nitrogen S2. To run the controller, some features must be installed to support the l2switch function, the mdsal model, the restconf protocol, the connectivity capability, and the support for the graphical display and network configuration of ODL (DLUX). Thus, the following features were installed:

- ✓ odl-restconf: Allows access to RESTCONF API
- ✓ odl-l2switch-switch: Provides network functionality similar to an Ethernet switch
- ✓ odl-mdsal-apidocs: Allows access to Yang API
- ✓ odl-dlux-all: ODL graphical user interface

NETWORK TOPOLOGY: A linear topology was chosen to be used for the implementation, in order to simulate the line connection of two train stations (Redhill-Tonbridge) shown in Figure 4-31. The controller communicates with the switches through a dedicated control network (Out-of-band Controller). Transmission delay was not emulated in the Out-of-band network, hence the extracted results regard the processing time of the controller. The number of the APs range from 4 to 256, to quantify how the number of switches affects the control plane latency.

Figure 4-31: Railway network topology considered in the analysis.

APPLICATION'S ARCHITECTURE: The application takes advantage of the ODL's REST architecture by using the REST API at http: // <odl-IP>: 8181 / restconf /. In general, modifications are only made in the config state, which automatically updates the operational state of the controller. From the operational state, the network manager receives the desired information.

Python was chosen as the programming language because of its ability of executing bash commands. Python was combined with bash shell scripting to take advantage of the ODL REST API with the usage of the curl command.

In the beginning, through REST API we extract the topology of the network. Specifically, using the curl (bash command), with the appropriate headings and the GET method in the following URL:

```
curl -u <USERNAME>:<PASSWORD> -X GET -s
```

we obtain in json (or xml) format, information about the network. In particular, the obtained json file includes the id of every link in the network, as well as the source and destination node and port of each link. From the above, the number of switches is exported.

For measuring the control plane delay, the application sends simultaneously echo messages to all the switches of the network through the NB REST interface and records the time elapsed for receiving a reply. Thus, curl commands with the POST method are employed in the following URL:

```
curl -u <USERNAME>:<PASSWORD> -X POST -s
```

The REST API above requires an input in json format that specifies the destination AP of the echo message. The curl commands are executed in parallel and their number is equal to the number of the APs in the network, in order to see how the number of APs affects the time responsiveness of ODL controller. For higher accuracy the above procedure is repeated 100 times, and the delay is considered as the average delay of each repetition. The results for linear topologies with different number of APs is shown in Figure 4-32 where as expected an exponential increase of the processing delay as a function of the controlled APs is observed.

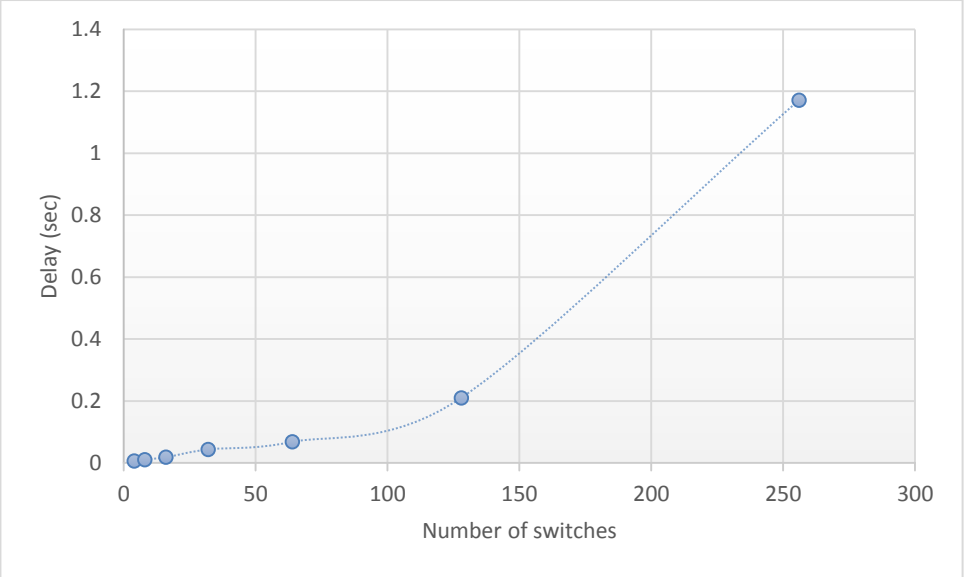

Figure 4-32: Processing time of ODL as a function of the number of switches.

5 Conclusions

5G-PICTURE focuses on designing and developing a converged fronthaul and backhaul infrastructure integrating advanced wireless and novel optical network solutions. To address the limitations of the current D-RAN and C-RAN approaches, 5G-PICTURE adopts the concept of flexible functional selected based on factors such as the transport network and service characteristics for resource and energy efficiency.

5G-PICTURE proposes a paradigm shift, from the RAN and C-RAN to the “DA-RAN approach. DA-RAN is a novel concept adopting the notion of “disaggregation” of HW and SW components across the wireless, optical and compute/storage domains. “Resource disaggregation” allows decoupling of these components creating a common “pool of resources” that can be independently selected and allocated on demand to compose any infrastructure service. In DA-RAN key enables are i) hardware programmability: enabling dynamic on demand resource sharing and ii) network softwarisation: enabling migration from the traditional closed networking model to an open reference platform instantiating various network functions. This will enable provisioning of any service by flexibly and efficiently mixing-and-matching network, compute and storage resources.

This deliverable summarises the 5G KPIs the 5G-PICTURE solution needs to support and describes in more detail some Verticals that the project is concentrating on. These Verticals include the Rail, the Smart City and a Stadium use case that the project is planning to also demonstrate as part of the activities of WP6. In addition to these, Industry 4.0 is included in the discussion although no relevant demonstration activities are planned. However, this Vertical is considered relevant enough to be supported by 5G solutions. In view of this 5G-PICTURE aims to address its requirements from an architectural perspective.

In addition, to the requirements definition, this document also provides a high-level view of the 5G-PICTURE architecture, in terms of its functionality, capabilities and features. The project’s layered architecture is described, and the details of the proposed structure and individual layers are analysed involving detailed discussion on the Programmable Data Plane, the Physical and Virtual Functions, as well as the 5G Operating System that the project proposes.

Finally, this deliverable reports on the evaluation studies aiming to analyse and benchmark the performance of the proposed architecture. In view of this mathematical models and simulation tools have been purposely developed and are currently being extended, analysed and tested. A set of modelling/simulation results have been presented and described in this document aiming to provide some preliminary evaluation of the 5G-PICTURE architecture. The first part of the architecture evaluation has focused on the scalability analysis of the data and control planes proposed as part of the generic 5G-PICTURE architecture. This analysis concentrated on the following topics: scalability analysis of the BBU processing chain, data plane analysis: DA-RAN over elastic optical networks, data plane analysis: integration of WDM-PON and mmWave, Scalable Service Chaining in MEC-assisted 5G Networks, Scalable Optimization based on Artificial Intelligence and scalable multi-service placement. The second part of the evaluation focused on some initially defined rail vertical use cases and their evaluation. These include: 5G communications to trains and the adoption of Sub-6 GHz LTE Massive MIMO technologies, analysis of the benefits of multi-technology access network solutions in railway systems, Internet of Things in Disaggregated 5G Networks for a rail use case and an initial control plane scalability analysis for the rail environment. Our preliminary modelling and simulation results are also presented and discussed identifying the benefits of the proposed approach as well as some relevant trade-offs.

6 References

[1] 5G-XHaul, "Dynamically Reconfigurable Optical-Wireless Backhaul/Fronthaul with Cognitive Control Plane for Small Cells and Cloud-RAN", https://www.5g-xhaul-project.eu/

[2] SONATA: Service Programming and Orchestration for Virtualized Software Networks, www.sonata-nfv.eu

[3] 5G-PICTURE deliverable D2.1: "5G and Vertical Services, use cases and requirements", January 2018.

[4] A. Tzanakaki *et al*., "5G infrastructures supporting end-user and operational services: The 5G-XHaul architectural perspective," *2016 IEEE International Conference on Communications Workshops (ICC)*, Kuala Lumpur, 2016, pp. 57-62.

[5] Recommendation ITU-R M.2083-0 (09/2015) IMT Vision – Framework and overall objectives of the future development of IMT for 2020 and beyond M Series, https://www.itu.int/dms_pubrec/itu-r/rec/m/R-REC-M.2083-0-201509-I!!PDF-E.pdf

[6] A. Tzanakaki et al., "Wireless-Optical Network Convergence: Enabling the 5G Architecture to Support Operational and End-User Services," IEEE Comm. Mag., vol. 55, no. 10, pp. 184-192, Oct. 2017.

[7] U. Dötsch et al., Quantitative Analysis of Split Base Station Processing and Determination of Advantageous Architectures for LTE, Bell Tech. J, 18 (1), 2013.

[8] Common Public Radio Interface: eCPRI Interface Specificatione, CPRI Specification V1.1, 1/2018

[9] Common Public Radio Interface: Requirements for the eCPRI Transport Network, v1.1, 1/2018

[10] W. Stallings and M. M. Manna, Operating systems: internals and design principles. Pearson, 2015.

[11] 3GPP: Service requirements for next generation new services and markets, https://portal.3gpp.org/desktopmodules/Specifications/SpecificationDetails.aspx?specificationId=3107

[12] I. A. Dhotre, Operating systems. Technical Publications, 2009.

[13] NGMN, Description of Network Slicing Concept, 2016, Available at: https://www.ngmn.org/fileadmin/user_upload/161010_NGMN_Network_Slicing_framework_v1.0.8.pdf, Last Accessed: April 2018.

[14] eCPRI Specification 12 V1.1 (2018-01-10) p. 12

[15] 3GPP: Telecommunication management; Study on management and orchestration of network slicing for next generation network (TR28.801), 2018, Available at: https://portal.3gpp.org/desktopmodules/Specifications/SpecificationDetails.aspx?specificationId=3091.

[16] 3GPP Specification 22.261 "Service requirements for next generation new services and markets", release 15, July 2017

[17] ETSI, "Network Functions Virtualisation (NFV); Ecosystem; Report on SDN Usage in NFV Architectural Framework (Version: ETSI GS NFV-EVE 005 V1.1.1)", Report, 2015, Available at: http://www.etsi.org/deliver/etsi_gs/NFV-EVE/001_099/005/01.01.01_60/gs_NFV-EVE005v010101p.pdf, Last Accessed: April 2018.

[18] Ordonez-Lucena et. al., 'Network slicing for 5G with SDN/NFV: Concepts, Architectures, and Challenges', IEEE Communications Magazine, 2017.

[19] ETSI NFV ISG, "GS NFV-MAN 001 V1.1.1 Network Function Virtualisation (NFV); Management and Orchestration," Dec. 2014.

[20] 5G-PICTURE deliverable D3.1, "Initial report on Data Plane Programmability and infrastructure components", March 2018.

[21] 5G-XHaul, D2.2 System Architecture Definition, June 2016.

[22] S. Han et al., "Network support for resource disaggregation in next-generation datacenters", In Proceedings of HotNets-XII. ACM, 10, 2013.

[23] X. Chen et al., "Analyzing and modeling spatio-temporal dependence of cellular traffic at city scale," IEEE ICC, pp.3585-3591, 2015.

[24] S. Rangan, T. S. Rappaport and E. Erkip, "Millimeter-Wave Cellular Wireless Networks: Potentials and Challenges," in Proceedings of the IEEE, vol. 102, no. 3, pp. 366-385, March 2014.

[25] 5G-PICTURE, Deliverable D4.1: "State of the art and initial function design", February 2018.

[26] TR 38.801 Study on new radio access technology: Radio access architecture and interfaces (Release 14), 3GPP, Mar. 2017.

[27] eCPRI Specification V1.0, Common Public Radio Interface: eCPRI Interface Specification, 2017.

[28] https://www.electronicsweekly.com/news/design/communications/5g-difference-will-make-2017-07/, July 2017.

[29] 3GPP, "TR 38.801, Study on new radio access technology: Radio access architecture and interfaces", Technical Report, 2017.

[30] xRAN Fronthaul Working Group, "XRAN-FH.WP.0-v01.00", White Paper, 2018. Available: Online: www.xran.org.

[31] xRAN Forum, "XRAN Forum Merges with C-RAN Alliance to Form ORAN Alliance", Press Release, February 27, 2018. Available: Online: www.xran.org.

[32] ETSI TS 136 101 V14.3.0, "User Equipment (UE) radio transmission and reception", 2017.

[33] TS 38.470 NG-RAN; F1 general aspects and principles (Release 15), 3GPP, Jan. 2018.

[34] TS 38.473 NG-RAN; F1 Application Protocol (F1AP) (Release 15), 3GPP, Apr. 2018.

[35] F. Musumeci et al., "Optimal BBU Placement for 5G C-RAN Deployment Over WDM Aggregation Networks," J. Lightwave Technol. 34, 2016.

[36] Metro Ethernet Forum, www.mef.net.

[37] S. Ruffini, P. Iovanna, M. Forsman and T. Thyni, "A Novel SDN-Based Architecture to Provide Synchronization as a Service in 5G Scenarios," IEEE Communications Magazine, vol. 55, no. 3, pp. 210-216, March 2017.

[38] J. Gutiérrez, et al., 5G-XHaul: a converged optical and wireless solution for 5G transport networks. Trans. Emerging Tel. Tech., 27: 1187-1195. 2016.

[39] M. Sauer et al., "Radio over fibre for picocellular network architectures," IEEE J. Lightwave Tech., vol. 25, no. 11, 2007.

[40] RFC 3720, http://tools.ietf.org/html/rfc3720.

[41] American NIST for IT Standards Technical Group T11. June 4, 2009 http://www.t11.org/ftp/t11/pub/fc/bb-5/09-056v5.pdf

[42] www.infinibandta.org/

[43] U. Dötsch et al., Quantitative Analysis of Split Base Station Processing and Determination of advantageous architectures for LTE," in Bell Labs Technical Journal, vol. 18, no. 1, pp. 105-128, June 2013.

[44] G. Brown, "Mobile Edge Computing Use Cases & Deployment options," Juniper White paper, July 2016.

[45] ETSI White paper, MEC Deployments in 4G and Evolution Towards 5G, No. 24, Feb. 2018.

[46] A. Clauset et al., Hierarchical structure and the prediction of missing links in networks, Nature 453, 98-101, 2008.

[47] X. Chen et al., "Analyzing and modeling spatio-temporal dependence of cellular traffic at city scale," ICC, 2015.

[48] S.-Y. Lien, S.-L. Shieh, Y. Huang, B. Su, Y.-L. Hsu, H-Y. Wei, "5G New Radio: Waveform, Frame Structure, Multiple Access, and Initial Access", *IEEE Communications Magazine*, vol. 55, no. 6, pp. 64-71, June 2017.

[49] C. Kilinc, J.F. Monserrat, M.C. Filippou, N. Kuruvatti, A.A. Zaidi, I. Da Silva, M. Mezzavilla, "New Radio 5G User Plane Design Alternatives: One 5G Air Interface framework supporting multiple services and bands", *IEEE Globecom Workshop*, Washington DC, Feb. 2017.

[50] X. Chen, J. Lu, T. Li, P. Fan, K.B. Letaief, "Directivity-Beamwidth Tradeoff of Massive MIMO Uplink Beamforming for High Speed Train Communication", *IEEE Access*, vol. 5, pp. 5936-5946, April 2017.

[51] X. Chen, J. Lu, P. Fan, "Massive MIMO Beam-forming for high Speed Train Communication: Directivity vs Beamwidth", [available online arXiv: 1702.02121v1], Feb. 2017.

[52] J. Kim, H.-S. Chung, I. G. Kim, H. Lee, M.S. Lee, “A Study on Millimeter-Wave Beamforming for High-Speed Train Communication”, *IEEE Conference on Information and Communication Technology*, Jeju, Oct. 2015.

[53] R. Guerzoni, D. Perez Caparros, P. Monti, G. Giuliani, J. Melian, R. Figueiredo, A. Ramos, C. J. Bernardos, G. Biczók, B. Sonkoly, F. Tusa, A. Galis, I. Vaishnavi, F. Ubaldi, A. Sgambelluri, C. Santana, R. Szabo, “Multi-domain Orchestration and Management of Software Defined Infrastructures: a Bottom-Up Approach”, EuCNC 2016.

[54] OpenDaylight Clustering [Online]. Available: http://docs.opendaylight.org/en/stable-carbon/getting-started-guide/common-features/clustering.html

[55] 5G-XHaul Project, Deliverable D2.4, “Network Topology Definition”, January 2017. [Online]. Available: http://www.5g-xhaul-project.eu/download/5G-XHaul_D2_4.pdf

[56] 5G Americas, “Network Slicing for 5G networks and Services”, November 2016. Available: http://www.5gamericas.org/files/3214/7975/0104/5G_Americas_Network_Slicing_11.21_Final.pdf

[57] 3GPP, TR 22.891, Feasibility Study on New Services and Markets Technology Enablers; Stage 1 (Release 14)

[58] 3GPP TR 23.799, Study on Architecture for Next Generation System (Release 14)

[59] 3GPP TS 28.530 V0.5.1 (2018-03), Telecommunication management; Management of 5G networks and network slicing; Concepts, use cases and requirements (Release 15)

[60] 3GPP TS 28.531 V0.3.1 (2018-03), Management and orchestration of networks and network slicing; Provisioning; Stage 1 (Release 15).

[61] M. Fiorani, S. Tombaz, J. Martensson, B. Skubic, L. Wosinska and P. Monti, "Modeling energy performance of C-RAN with optical transport in 5G network scenarios," in *IEEE/OSA Journal of Optical Communications and Networking*, vol. 8, no. 11, pp. B21-B34, Nov. 2016.

[62] M. Anastasopoulos, A. Tzanakaki and D. Simeonidou, "Stochastic Energy Efficient Cloud Service Provisioning Deploying Renewable Energy Sources," in *IEEE Journal on Selected Areas in Communications*, vol. 34, no. 12, pp. 3927-3940, Dec. 2016.

[63] X. Chen et al., “Analyzing and modeling spatio-temporal dependence of cellular traffic at city scale,” in proc. of IEEE ICC, pp.3585-3591, 2015.

[64] S. Haykin, Neural Networks and Learning Machines, New Jersey: Pearson, 2009.

[65] V. K. Tumuluru, P. Wang and D. Niyato, "A Neural Network Based Spectrum Prediction Scheme for Cognitive Radio," IEEE, 2010.

[66] Z. D. Zaharis, C. Skeberis, T. D. Xenos, P. I. Lazaridis and J. Cosmas, "Design of a Novel Antenna Array Beamformer Using Neural Networks Trained by Modified Adaptive Dispersion Invasive Weed Oprimization Based Data," IEEE, 2013.

[67] A. Omri, R. Bouallegue, R. Hamila and M. Hasna, "Channel Estimation for LTE Uplink System by Perceptron Neural Network," International Journal of Wireless & Mobile Networks (IJWMN), 2010.

[68] M. Baradas, G. Boanea and V. Dobrota, "Multipath Routing Management using Neural Networks-Based Traffic Prediction," The Third International Conference on Emerging Network Intelligence, 2011.

[69] C. Rottondi, L. Barletta, A. Giusti, and M. Tornatore, "Machine-Learning Method for Quality of Transmission Prediction of Unestablished Lightpaths," J. Opt. Commun. Netw. 10, A286-A297 (2018).

[70] S. Yan et al., “Field trial of Machine-Learning-assisted and SDN-based Optical Network Planning with Network-Scale Monitoring Database” ECOC 2017.

[71] A. Farhadi-Beldachi et al., Experimental Demonstration of 5G Fronthaul and Backhaul Convergence based on FPGA-based Active Optical Transport, ECOC 2018.

[72] A. Tzanakaki *et al*., "5G infrastructures supporting end-user and operational services: The 5G-XHaul architectural perspective," *2016 IEEE International Conference on Communications Workshops (ICC)*, Kuala Lumpur, 2016, pp. 57-62.

[73] Sevil Dräxler, Holger Karl, Hadi Razzaghi Kouchaksaraei, Azahar Machwe, Crispin Dent-Young, Kostas Katsalis, Konstantinos Samdanis, “5G OS: Control and Orchestration of Services on Multi-

Domain Heterogeneous 5G Infrastructures," accepted in Eur0pean Conference on Networks and Communication (EuCNC2018), 2018.
[74] Y. Yan, G. S. Zervas, Y. Qin, B. R. Rofoee, and D. Simeonidou, "High Performance and Flexible FPGA-Based Time Shared Optical Network (TSON) Metro Node" in European Conference and Exhibition on Optical Communication (ECOC) (We.3.D), 2012.
[75] Common Public Radio Interface, http://www.cpri.info/
[76] 1588-2008 - IEEE Standard for a Precision Clock Synchronization Protocol for Networked Measurement and Control Systems.
[77] Cisco Systems, "Data Center Design – IP Network Infrastructure," http://www.cisco.com/en/US/docs/solutions/Enterprise/Data Center/DC 3 0/DC-3 0 IPInfra.pdf, Oct. 2009
[78] "Data Center Architecture Overview". [Online].Available: http://www.cisco.com/c/en/us/td/docs/solutions/Enterprise/Data_Center/DC_Infra2_5/DCInfra_1.html
[79] M. Al-Fares et al., "A scalable, commodity data center network architecture," in proc. of SIGCOMM, pp. 63–74, 2008.
[80] A. Greenberg et al., VL2: a Scalable and Flexible Data Center Network," in proc. of SIGCOMM, pp. 51–62, 2009.
[81] Data Age 2025, www.seagate.com/gb/en/our-story/data-age-2025/
[82] D. M West, "How 5G technology enables the health Internet of Things", Brookings, 2016.
[83] M. Anastasopoulos et al., "ICT platforms in support of future railway systems", in Proc. of TRA 2018.
[84] F. Musumeci et al., "Optimal BBU Placement for 5G C-RAN Deployment Over WDM Aggregation Networks," in Journal of Lightwave Technology, vol. 34, no. 8, pp. 1963-1970, April15, 15 2016.
[85] G. Paulraj et al., "Resource-aware virtual machine migration in IOT cloud", Future Gen. Comp. Sys., 2018.
[86] A. Tzanakaki, Optical networking: An important enabler for 5G (invited), ECOC 2017.
[87] Q. Zheng et al, "WiBench: An Open Source Kernel Suite for Benchmarking Wireless Systems", IEEE ISWC 2013.
[88] C. Y. Chang, N. Nikaein and T. Spyropoulos, "Impact of Packetization and Scheduling on C-RAN Fronthaul Performance," 2016 IEEE Global Communications Conference (GLOBECOM), pp. 1-7.
[89] J. Perelló et al., "All-optical packet/circuit switching-based data center network for enhanced scalability, latency, and throughput," in IEEE Network, 2013.
[90] A. Tzanakaki et al., "Wireless-Optical Network Convergence: Enabling the 5G Architecture to Support Operational and End-User Services," IEEE Comm. Mag., vol. 55, no. 10, pp. 184-192, Oct. 2017.
[91] N. Gkatzios, M.P. Anastasopoulos, A. Tzanakaki, D. Simeonidou, Compute Resource Disaggregation: An Enabler for Efficient 5G RAN Softwarisation, in proc. EUCNC 2018, RAS, 2018.
[92] A. Tzanakaki, M. Anastasopoulos, and D. Simeonidou, "Converged Access/Metro Infastructures for 5G services," in Optical Fiber Communication Conference, OSA Technical Digest (online) (Optical Society of America, 2018), paper M2A.3.
[93] M.P. Anastasopoulos, A. Tzanakaki, D. Simeonidou, Service Chaining in MEC -- Assisted Large Scale 5G Networks, ECOC 2018.
[94] A. Pelekanou, M. Anastasopoulos, A. Tzanakaki and D. Simeonidou, "Provisioning of 5G services employing machine learning techniques," *2018 International Conference on Optical Network Design and Modeling (ONDM)*, Dublin, Ireland, 2018, pp. 200-205.
[95] Economics of Backhaul, http://www.exaltcom.com/Economics-of-Backhaul.aspx
[96] CHINA mobile White paper, C-RAN: The Road Towards Green RAN, [Online]: http://labs.chinamobile.com/cran/
[97] Huawei, Building 4G on High-Speed Railways, [Online]: http://www1.huawei.com/en/static/HW-371912.pdf

[98] Sivaraman, A., et al., Packet Transactions: High-Level Programming for Line-Rate Switches. ACM SIGCOMM 2016, pp. 15-28.

[99] G. Brebner, "Programmable hardware for high performance SDN," Optical Fiber Communications Conference and Exhibition (OFC), 2015, Los Angeles, CA, 2015, pp. 1-3.

[100] X. Chen et al., “Analyzing and modeling spatio-temporal dependence of cellular traffic at city scale,” in proc. of IEEE ICC, pp.3585-3591, 2015.

[101] D. M West, “How 5G technology enables the health Internet of Things”, Brookings, 2016.

[102] M. Anastasopoulos et al., "ICT platforms in support of future railway systems", in Proc. of TRA 2018.

[103] F. Musumeci et al., "Optimal BBU Placement for 5G C-RAN Deployment Over WDM Aggregation Networks," J. Lightwave Technol. 34, 1963-1970 (2016).

[104] G. Paulraj et al., Resource-aware virtual machine migration in IOT cloud, Future Gen. Comp. Sys., 2018.

[105] C.-Y. Chang, N. Nikaein, O. Arouk, K. Katsalis, A. Ksentini, T. Turletti, K. Samdanis, “Slice Orchestration for Multi-Service Disaggregated Ultra Dense RANs”, *IEEE Communications Magazine*, August 2018.

[106] O. Arouk, N. Nikaein, and T. Turletti, “Multi-Objective Placement of Virtual Network Function Chains in 5G,” in Proceedings of Cloud Networking (CloudNet), 2017 IEEE 6th International Conference on. IEEE, 2017, pp. 1–6.

7 Appendix

7.1 Artificial Neural Network Preliminaries

Artificial NNs are defined as systems of interconnected computational units, known as neurons, which interact with the environment. Each neuron has a non-linear, differentiable function, known as activation function, used to compute a weighted sum of the outputs of the previous-layer. In NNs, knowledge is stored in interneuron connection strengths, known as synaptic weights using a learning algorithm. The learning algorithm is a function that updates the value of synaptic weights during the learning operation. The Backpropagation algorithm is the most popular learning algorithm for training NNs and comprises two phases, the forward phase and the backward phase. Through the first phase, the signal is transmitted from the input to the output on a layer by layer basis, keeping the synaptic weights' unaltered. In the second phase, the comparison between the network's output and the desired response leads to an error signal. The error signal is propagated backwards through the network, starting from the output, and then the synaptic weights are re-evaluated to minimize the loss function. The loss function is a function that calculates the divergence between predicted and expected network's response values [64]. Figure 7-1 shows a typical MLP neural network with J hidden layers over which the backpropagation algorithm is applied.

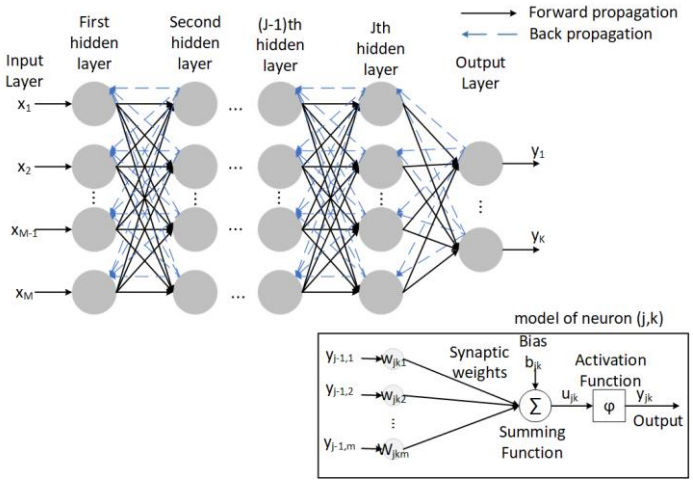

Figure 7-1: Graphic illustration of an MLP NN structure with backpropagation algorithm.

The modelling details of the backpropagation algorithm for the MLP network are summarized in Table 7-1. Specifically, if neuron k is an output neuron, then the linear combiner output $v_k(n)$ is calculated by the weighted sum of the inputs· $y_{Jm}(n)$ with the respective synaptic weights $w_{km}(n)$ using equation (3.1) (see lower part of Table 7-1). $v_k(n)$ is then applied to an activation function φ, which limits the amplitude of the output of neuron k (3.2) resulting to the final output of neuron k at the n iteration, namely $y_k(n)$**.** The estimation error at the output of neuron k is calculated through (3.3), while the total instantaneous error $E(n)$ of the whole network is calculated using (3.4). The error is propagated backward and the correction Δw_{ki} is applied to the synaptic weight w_{ki} (3.5)-(3.9). A similar set of equations is applied for the hidden neurons (3.10)-(3.17).

Table 7-1: Overview of the Backpropagation Algorithm applied to the MLP-NN.

Parameters:
M = dimensionality of the input space and number of neurons in hidden layers, *m = 1,2, …, M*
J = number of hidden layers, j = 1,2, …, J
K = number of neurons in output layer, k = 1,2, …, K
N = number of epochs, n = 1,2, …, N
$\boldsymbol{w_m}$*=synaptic weight vector of neuron m*
d = desired response vector
y = neuron output

$\boldsymbol{\delta_k}$ =local gradient at neuron k

η = learning rate

$\boldsymbol{e_k}$ = error

Initializations:

Set the synaptic weights of the algorithm to small values selected from uniform distribution.

Computations:

- **If neuron *k* is an output neuron then**:

(3.1) $\boldsymbol{u_k(n)} = \sum_{m=1}^{M} \boldsymbol{w_{km}(n)} \cdot \boldsymbol{y_{Jm}(n)} + \boldsymbol{b_k}$

(3.2) $\boldsymbol{y_k(n)} = \boldsymbol{\varphi(u_k(n))}$

(3.3) $\boldsymbol{e_k(n)} = \boldsymbol{d_k(n)} - \boldsymbol{y_k(n)}$

(3.4) $\boldsymbol{E(n)} = \sum_{k\epsilon C} \boldsymbol{e_k{}^2(n)/2}$

(3.5) $\boldsymbol{\Delta w_{ki}(n)} = -\boldsymbol{\eta} \frac{\partial E(n)}{\partial w_{ki}(n)}$

(3.6) $\frac{\partial E(n)}{\partial w_{ki}(n)} = -\boldsymbol{e_k(n)\varphi'_k(u_k(n))} \cdot \boldsymbol{y_{ji}(n)}$

(3.7) $\boldsymbol{\delta_k(n)} = \boldsymbol{e_k(n)\varphi'_k(u_k(n))}$

(3.8) $\boldsymbol{\Delta w_{ki}(n)} = -\boldsymbol{\eta}\, \boldsymbol{\delta_k(n)} \cdot \boldsymbol{y_{ji}(n)}$

(3.9) $\boldsymbol{w'_{ki}(n)} = \boldsymbol{w_{ki}(n)} + \boldsymbol{\Delta w_{ki}(n)}$

else if it is a hidden neuron at layer j:

(3.10) $\boldsymbol{u_{jm}(n)} = \sum_{m=1}^{M} \boldsymbol{w_{jm}(n)} \cdot \boldsymbol{y_{j-1,m}(n)} + \boldsymbol{b_{jm}}$

(3.11) $\boldsymbol{y_{jm}(n)} = \boldsymbol{\varphi(u_{jm}(n))}$

(3.12) $\boldsymbol{e_k(n)} = \boldsymbol{d_k(n)} - \boldsymbol{y_k(n)}$

(3.13) $\boldsymbol{E(n)} = \sum_{k\epsilon C} \boldsymbol{e_k{}^2(n)/2}$

(3.14) $\boldsymbol{\Delta w_{ji}(n)} = -\boldsymbol{\eta} \frac{\partial E(n)}{\partial w_{jm}(n)}$

(3.15) $\boldsymbol{\delta_{jm}(n)} = \boldsymbol{\varphi'_{jm}\left(u_{jm}(n)\right)} \cdot \sum_{k=1}^{K} \boldsymbol{\delta_{jk}(n)} \cdot \boldsymbol{w_{jk}(n)}$

(3.16) $\boldsymbol{\Delta w_{jm}(n)} = -\boldsymbol{\eta}\, \boldsymbol{\delta_{jm}(n) y_{j-1,m}(n)}$

(3.17) $\boldsymbol{w'_{jm}(n)} = \boldsymbol{w_{jm}(n)} + \boldsymbol{\Delta w_{jm}(n)}$

7.2 Traffic forecasting using Long Short-Term Memory Neural Networks

Long Short-Term Memory (LSTM) is a special case of Recurrent Neural Network (RNN) capable to learn long-term dependencies, since it can remember information that was acquired in previous steps of the learning process. LSTM contains a set of recurrent blocks, known as memory blocks, each of which has one or more memory cells. Each cell is composed of three basic units, the input, output and forget gate that are responsible to decide whether to forget, keep, update or output information that has been acquired previously. LSTM is the most successful model for predicting long-term time series.

In the present study, the LSTMs are optimally designed to forecast the traffic load of each RU based on history traffic data available. To train the LSTMs, the dataset containing history measurements of each RU is split into two parts, the training set and the test set. The training set contains 70% of the total dataset while the remaining 30% comprises the test set. The test set is used to validate the effectiveness of each LSTM designed. To identify the optimal LSTM architecture for each RU, an extensive set of experimentations is performed. Given that the LSTM architecture can be fully characterized by the number of hidden layers, neurons, epochs and the batch size, our objective is to the identify how these parameters can be optimally combined to minimise the forecasting error. This process is summarised as follows:

Step 1- Batch size. The batch size is the number of training instances used in each iteration. The weights are updated after each batch propagation. We choose the value for the batch size that minimises forecasting error keeping all other parameters constant.

Step 2- Number of epochs: The number of epochs determine the maximum number of passes over the training dataset. Various values for the number of epochs are tested in order to identify the optimal one that minimises the forecasting error.

Step 3- Number of neurons. In this step, our objective is to identify the optimal number of neurons that achieves optimal traffic forecasting accuracy.

Step 4- Number of hidden layers. The last parameter that we study is the number of hidden layers. As before, after extensive experimentations we choose the number of hidden layers that minimises the forecasting error calculated through the root-mean-squared-error RMSE formula.

8 Acronyms

Acronym	Description
5G OS	5G Operating System
AGV	Automated guided vehicles
AI	Artificial Intelligence
AoA	Angle of Arrival
API	Application Programming Interface
APs	Access Points
ATC	Automatic Train Control
BBU	Baseband Unit
BIO	Bristol Is Open
BN	Best Node
BS	Base Station
BSS	Business Support System
BVT	Bandwidth Variable Transponder
CAPEX	CApital Expenditures
CBR	Constant Bit Rate
CG	Candidate Group
CO	Central Office
CoMP	Coordinated Multi-Point
CP	Cyclic Prefix
C-RAN	Cloud-RAN
CSI	Channel State Information
CU	Central Unit
DAC	Digital-to-Analogue Converter
DA-RAN	Dis-Aggregated RAN
DC	Domain Controller
DL	Downlink
DMP	Data Management Platform
DO	Domain Orchestrator
D-RAN	Distributed-Radio Access Network
DU	Distributed Unit
EDFA	Erbium Doped Fibre Amplifiers
eMBB	enhanced Mobile Broadband
EoMPLS	Ethernet over Multi-Protocol Label Switching
ER	Eligible Region
ETB	Ethernet Train Backbone
ETB	Ethernet Train Backbone level
F1AP	F1 Application Protocol
FCAPS	Fault, Configuration, Accounting, Performance and Security
FCS	Frame Check Sequence

FEC	Forward Error Correction
FFT	Fast Fourier Transform
FPGA	Field Programmable Gate Array
GOPS	giga operation per second
GPP	general-purpose processors
GST	Guaranteed Service Transport
GTP	GPRS Tunnelling Protocol
HRG	Hierarchical Random Graph
HW	hardware
IAB	integrated Access and Backhaul
IFFT	Inverse Fast Fourier Transform
IML	Infrastructure Management Layer
IoT	Internet of Things
IPS	instructions per second
ISG	Industrial Specification Group
ITU	International Telecommunications Union
KPI	Key Performance Indicators
LLR	Logarithmic Likelihood Ratios
LoS	Line of Sight
LSTM	Long Short-Term Memory
LTE	Long Term Evolution
LUT	Look up table
M2M	Machine to Machine
MAC	Medium Access Control
MCM	Markov Chain Monte Carlo
MDO	Multi-Domain Orchestrator
MEC	Mobile Edge Computing
MEF	Metro Ethernet Forum
MIMO	Multiple-Input Multiple-Output
MLP	Multilayer Perceptron
mMTC	massive Machine Type Communications
MNO	Mobile Network Operator
MPI	Multi-protocol interfaces
MQTT	Message Queuing Telemetry Transport
NAT	Network Address Translation
NFV	Network Function Virtualization
NIC	Network Interface Card
NMS	Network Management System
NN	Neural Network
NR	New Radio
NSO	Network Service Orchestrator
OAI	OpenAirInterface

OCC	Operations and Control Centre
ODM	Operational Data Management
OLT	Optical Line Terminal
ONU	Optical Network Unit
OPEX	OPerational EXpenditure
OPP	Open Packet Processor
OS	Operating System
OSS	Operations Support System
OSS/BSS	Business/Operation Support System
PCS	Physical Coding Sublayer
PDCP	Packet Data Convergence Protocol
PDU	Protocol Data Unit
PDV	Packet Delay Variation
PLZT	Lead Lanthanum Zirconate Titanate
PMA	Physical Medium Attachment
PNF	Physical Network Function
PRB	Physical Resource Block
PTP	Precision Time Protocol
QoS	Quality of Service
RBIR	Received Bit mutual Information Rate
REC	Radio Equipment Control
REST	REpresentational State Transfer
RLC	Radio Link Control
RMSE	Root-Mean-Square Error
RN	Remote Node
RO	Resource Orchestrator
RoE	Radio over Ethernet
RRC	Radio Resource Control
RTT	Round-Trip-Time
RU	Remote Unit
SC	service chaining
SC-FDMA	Single Carrier Frequency Diversity Multiple Access
SDAP	Service Data Adaptation Protocol
SDR	software-defined radio
SLA	Service Level Agreements
SPP	specific-purpose processors
SW	software
TCN	Train Communication Network
TSN	Time Sensitive Networking
TSON	Time Shared Optical Network
UHD	ultra-high definition
UL	Uplink

URLLC	Ultra-Reliable and Low Latency Communications
VLIW	Very Long Instruction Word
VNF	Virtual Network Function
VOQ	Virtual Output Queues
VR	Virtual Reality